



UNIVERSITEIT VAN PRETORIA  
UNIVERSITY OF PRETORIA  
YUNIBESITHI YA PRETORIA

# Synthesis of a manganese oxide catalyst for reduction of domestic fuel burning emissions

by

Marilize Steyn

20046708

Submitted in partial fulfillment of the requirements for the degree  
Master of Science in Environmental Management

in the

Department of Geography, Geoinformatics and Meteorology  
Faculty of Natural and Agricultural Sciences

at the

University of Pretoria

Supervisor:

Prof PBC Forbes

Date of submission:

September 2022

## DECLARATION

I, Marilize Steyn, declare that the dissertation, which I hereby submit for the degree Master of Science at the University of Pretoria, is my own work and has not previously been submitted by me for a degree at this or any other tertiary institution.

Signature: Ma

Date: 30 September 2022

## SUMMARY

The negative health and socio-economic impacts of emissions associated with domestic fuel burning are widely recognized. Studies in South Africa have found that domestic fuel burning accounted for approximately 75% of all air quality related premature mortalities and approximately 70% of respiratory hospital admissions over selected metropolitan areas and the Highveld and Vaal Triangle areas (FRIDGE, 2004). The negative impacts of household emissions are exacerbated by the fact that they are released in the breathing zone of individuals (DEA, 2019).

Various studies have been conducted in South Africa to investigate interventions to reduce domestic fuel use and emissions from burning, such as the electrification of households, the use of top down ignition techniques and improvements in the energy efficiency of housing (Scorgie, 2012; Matandirotya et al., 2019). While various investigations have been done on reducing household emissions by reducing the use of polluting fuels and improvements in combustion efficiency, comparatively fewer studies have been conducted on the reduction of emissions through secondary emission reduction using abatement technology (Amann et al., 2018; Lim et al., 2015; Li et al., 2007; Messerer et al., 2004, Yamamoto et al., 2013; Hukkanen et al., 2012; Ozil et al., 2009; Paulsen et al., 2019).

The study aimed to investigate the potential of abatement technologies such as catalytic conversion to reduce particulate matter from locally available domestic stoves. The study focused on the reduction of particulate matter emissions which is expected to be comprised mainly of organic particles, soot and inorganic fly ash. Although catalytic methods have not been effectively utilized widely in practical domestic applications, studies have shown effective soot reduction during laboratory testing (Paulsen et al., 2019; Gao et al., 2020).

To prevent the formation of organic particulate matter, organic compounds and soot formed during the combustion process can be oxidized to CO<sub>2</sub> using supported noble metal catalysts and metal oxide catalysts. Noble metal catalysts generally are more active than metal oxide catalysts, but metal oxide catalysts are more resistant to certain catalyst poisons such as halogens, As and Pb. Metal oxide catalysts importantly have a lower cost and can be sufficiently reactive for some applications (Huang et al., 2015). Manganese was selected for

this study due to the promising results achieved with laboratory testing (Gao et al., 2020). Furthermore, Mn oxide catalysts have low toxicity, low raw material cost and have a diversity of crystalline structures which determines the catalytic activity (Huang et al., 2015).

Three catalyst preparation techniques were tested namely precipitation, wet deposition and dry deposition. The catalyst was synthesized onto a stainless steel mesh support for direct use in domestic flues. The catalysts were examined using scanning electron microscopy (SEM) to determine the catalyst morphology, catalyst coverage and particle size. The catalysts were further analysed using Energy Dispersive X-Ray (EDX) analysis to determine the semi-quantitative composition of the catalysts.

The application of the synthesized catalyst was tested in a commercially available stove without a catalyst (referred to as baseline runs) and with the catalyst in place at the bottom of the flue (four catalyst runs in series using the catalyst prepared by precipitation followed by a comparative run using the catalyst prepared using wet deposition). The test runs were conducted under similar ambient conditions at the same time each day to improve reproducibility. The soft wood used as fuel was sized, weighed and bagged to reduce fuel variability and to ensure consistent fuel moisture content. The particulate concentrations were measured gravimetrically by active collection onto polytetrafluoroethylene (PTFE) filters using a Gilian (GilAir Plus) Personal Sampling pump at a flowrate of 600 cm<sup>3</sup>/min over a period of 10 min.

Contrary to expectation, the collected particle mass concentrations of the catalyst runs were found to be higher than the baseline runs. Scanning Electron Microscopy (SEM) analysis showed that the catalyst run filters had particulate clusters comprised of spherical particles in the pores of the filters. The baseline runs had very few, if any, of these particle clusters. Electron Dispersive X-Ray Spectroscopy (EDX) analysis indicated that the increased particulate concentration on the catalyst runs was not likely to solely be attributed to the catalyst being dislodged from the support, as no manganese was detected in the particulate matter. The increased particulate matter could result from the dislodgement of very small metal particles from the catalyst which served as nucleation nodes for particle growth. The metallic nuclei could potentially have a carbonaceous, non-metal coating which may lead to non-detection by EDX. The increase in particulate matter could also be caused by the impinge-

ment of particulate matter precursors on the catalyst followed by particle growth and dislodgement from the catalyst substrate by the flue gas. If the catalyst does not oxidize the impinged pollutant efficiently, particle growth can occur with the increased residence time in the concentrated flue gas stream, resulting in chain-like aggregates.

Even though laboratory testwork has indicated that manganese based catalysts are able to oxidize CO, soot and VOCs, the practical application of the catalyst differs significantly in terms of residence time and contact between pollutants, which can have a significant impact on the efficiency of the catalyst. It is recommended that a range of optimized, potentially active catalysts be tested to improve the oxidation of particulate matter precursors to CO<sub>2</sub>. Should a suitable catalyst be identified and synthesized, design optimization of the catalyst can be pursued which may include parameters such as the mesh configuration and type used as catalyst support and the number of catalyst layers used. It is recommended that an optimised catalyst be tested on a variety of fuels.

It is further recommended that the catalyst be tested over a prolonged period to determine whether the catalyst remains self-cleaning or clogs over time. Continuous particulate matter monitoring should be conducted in future testwork to provide information on the performance of the catalyst during the different stages of combustion and the monitoring of gaseous components such as CO, VOCs and CO<sub>2</sub> should be included to determine the extent of oxidation of the particulate matter precursors.

The testwork has shown that an active catalyst can be synthesized onto a mesh catalyst support in a facile manner and utilized in domestic fuel burning devices. The catalyst is easy to install and can be customised to fit non-standard domestic combustion units. The manganese based catalyst is heat resistant and does not release detectable particles or toxic materials. The catalyst is light in weight and requires no electricity to operate. During the limited test runs conducted, the catalyst did not clog, the airflow was not restricted and the stove vented as per the baseline runs. It is therefore recommended that a range of optimized, potentially active catalysts be tested to improve the oxidation of particulate matter precursors to CO<sub>2</sub>.

## **ACKNOWLEDGEMENTS**

It is with immense gratitude that I acknowledge the support and help of my Supervisor, Prof PBC Forbes, without whose support this study would not have been possible. I would like to thank Prof Liezel van der Merwe for assistance with the calcining of the catalyst samples. I would further like to express my gratitude to Mr Coenraad Snyman and Ms Charity Maepa for their assistance with the SEM-EDX analysis. I appreciate the advice and assistance from Mr Nico Van Vuuren in designing the catalyst and Ms Alette Devega for assistance with the initial flue gas measurement instruments. Lastly, my sincere gratitude to Dr Nicolaas Claassen for his assistance in the preparation and analysis of the filter samples. Finally, my appreciations go to everyone who has contributed, in one way or another, to the completion of this study.

# TABLE OF CONTENTS

<b>DECLARATION</b> .....	II
<b>SUMMARY</b> .....	III
<b>ACKNOWLEDGEMENTS</b> .....	VI
<b>CHAPTER 1: INTRODUCTION</b> .....	1
1.1. BACKGROUND .....	1
1.2. PROBLEM STATEMENT .....	2
1.3. RESEARCH OBJECTIVE .....	2
1.4. DISSERTATION OUTLINE .....	3
<b>CHAPTER 2: LITERATURE REVIEW</b> .....	4
2.1. EMISSIONS FROM DOMESTIC FUEL BURNING.....	4
2.1.1. Fuel usage.....	4
2.1.2. Health impacts from domestic fuel burning.....	6
2.1.3. Domestic burning devices utilized in South Africa .....	9
2.2. COMBUSTION PROCESSES AND EMISSION QUANTIFICATION AND ANALYSIS .....	10
2.2.1. Emission factors .....	10
2.2.2. Combustion theory .....	12
2.2.3. Characterisation of emissions.....	16
2.2.4. Atmospheric reactions and impacts of emissions .....	18
2.3. ADDRESSING DOMESTIC FUEL BURNING .....	20
2.3.1. Electrification of households.....	22
2.3.2. Top down fire making .....	23
2.3.3. Offsetting Projects .....	24
2.3.4. Fuel switching.....	25
2.3.5. Provision of new stoves.....	26
2.3.6. Energy efficient housing .....	27
2.3.7. Addressing domestic fuel burning.....	28
2.4. POTENTIAL FOR THE USE OF ABATEMENT TECHNOLOGY.....	28
2.4.1. Background review .....	28
2.4.2. Abatement methods.....	31
2.4.3. Abatement design .....	41
<b>CHAPTER 3: EXPERIMENTAL METHODS</b> .....	43
3.1. PROTOTYPE ABATEMENT PRODUCTION .....	43
3.2. EXPERIMENTAL.....	44
3.2.1. Catalyst development testwork.....	46

3.2.2.	Bulk catalyst synthesis .....	50
3.3.	Catalyst testwork .....	51
3.4.	Measurement methodology.....	54
3.5.	Characterization methodology .....	56
3.6.	QUALITY CONTROL AND ASSURANCE .....	57
	CHAPTER 4: RESULTS AND DISCUSSION .....	58
4.1.	CATALYST DEVELOPMENT TESTWORK.....	58
4.1.1.	Synthesis using precipitation.....	58
4.1.2.	Synthesis using wet and dry impregnation .....	68
4.2.	BULK CATALYST PREPARATION .....	71
4.2.1.	Bulk synthesis using precipitation .....	71
4.2.2.	Bulk synthesis using wet impregnation .....	74
4.3.	CATALYST TESTING .....	74
	CHAPTER 5: CONCLUSIONS AND RECOMMENDATIONS.....	84
	REFERENCES .....	86
	APPENDIX A: Method for preparing cassettes.....	97
	APPENDIX B: Method for weighing gravimetric samples .....	100
	APPENDIX C: Filter Masses (Raw data) .....	101
	APPENDIX D: Journal Article .....	102



## LIST OF FIGURES

Figure 2.1 The combustion process and products typically formed (based on Nystrom (2016) and Seinfeld and Pandis (2016)) .....	13
Figure 2.2. Particle formation mechanisms (Adapted from: Nystrom (2016)). .....	155
Figure 2.3. Comparing access to electricity between South Africa and Sub Saharan Africa (Source: World Bank Group).....	233
Figure 3.1. 0.5 mm thick steel mesh used as catalyst support.....	433
Figure 3.2. Experimental design .....	444
Figure 3.3. Overview of the experimental design.....	455
Figure 3.4. Catalyst preparation setup for precipitation tests a) side view and b) top view	47
Figure 3.5. Samples were calcined in a Lenton muffle furnace.....	488
Figure 3.6. Reagent mixture at a measured temperature of 170 °C. Precipitate can clearly be seen at the base of the beaker.....	51
Figure 3.7. Experimental setup showing the stove and positioning of catalyst .....	52
Figure 3.8. Catalyst secured at flue inlet to optimise the reaction temperature.....	544
Figure 3.9. Three Piece 37 mm styrene cassette .....	555
Figure 3.10. Measurement of PTFE filters using a Mettler Toledo microgram analytical balance .....	555
Figure 3.11. Flue gas measurement in the plume above the flue gas exit point .....	566
Figure 4.1. Mesh with precipitate before (a) and after (b) transfer to the muffle furnace ...	58
Figure 4.2. SEM micrographs of Run 1 of the precipitation synthesis showing the precipitate formed on the wire mesh sample (20 0 X and 100 0 X magnification) .....	599
Figure 4.3. SEM micrograph showing spherical particle clusters at 1000 0 X magnification during Run 1 of the precipitation synthesis .....	59
Figure 4.4. EDX results showing manganese oxide precipitate on the mesh (precipitation synthesis Test Run 1).....	60
Figure 4.5. EDX results showing manganese oxide precipitate on the mesh (bulk synthesis reparation sample).....	60
Figure 4.6. SEM micrograph showing clusters of precipitate at 10 0 X magnification formed from Run 3 of the precipitation synthesis .....	61
Figure 4.7. SEM micrographs of the catalyst synthesized in Test Run 3 showing amorphous clusters of precipitate at 500 x and 100 0 X magnification .....	61
Figure 4.8. SEM micrographs at 5000 x magnification comparing the precipitate exposed to air prior to calcination (a) and sample transferred directly to the muffle furnace once rinsed and dried (b)	
Figure 4.9. SEM micrographs of the catalyst synthesized from Test Run 4 showing precipitate on the mesh at 10 0 X magnification .....	63

Figure 4.10. SEM micrographs of the catalyst synthesized from Test Run 4 showing precipitate coverage at 50 0 X magnification .....	63
Figure 4.11. SEM micrographs showing clusters made up of spherical particles at 100 0 X and 500 0 X magnification produced from Test Run 4 .....	64
Figure 4.12. SEM micrograph showing the precipitate comprising of spherical particles shown at 1000 0 X magnification produced from Test Run 4.....	64
Figure 4.13. SEM micrograph showing the precipitate coverage at 10 0 X magnification for the catalyst produced from Test Run 5 .....	65
Figure 4.14. SEM micrographs showing the precipitate coverage at 50 0 X magnification for the catalyst produced from Test Run 5 .....	65
Figure 4.15. SEM micrographs showing precipitate comprised of spherical particles at 100 0 X and 500 0 X magnification for the catalyst produced from Test Run 5 .....	66
Figure 4.16. SEM micrographs showing spherical particles of various sizes at 3000 0 X magnification for the catalyst produced from Test Run 5 .....	67
Figure 4.17. SEM micrographs at 5000 x magnification comparing the samples prepared with the addition of TEG (a) and samples prepared without TEG (b)	
Figure 4.18. SEM micrographs showing the catalyst prepared on a sandblasted mesh surface at 10 0 X and 50 0 X magnification produced from Test Run 5 .....	67
Figure 4.19. SEM micrograph showing the catalyst clusters at 100 0 X magnification produced from Test Run 6 .....	68
Figure 4.20. SEM micrographs showing the catalyst synthesized using wet impregnation at 10 0 X (a) and 50 0 X (b) magnification.....	69
Figure 4.21. SEM micrographs showing the plate like coverage of the catalyst prepared using wet impregnation at 500 0 X and 1000 0 X magnification.....	69
Figure 4.22. SEM micrographs comparing the catalysts synthesized using wet impregnation (left) and precipitation (right) techniques at 100 x magnification.....	70
Figure 4.23. SEM micrographs comparing the surface of samples prepared using wet impregnation (a) and precipitation (b) at 500 0 X magnification.....	70
Figure 4.24. SEM micrographs showing the catalyst prepared using dry impregnation on a sandblasted mesh at 10 0 X and 50 0 X magnification .....	71
Figure 4.25. Mesh after synthesis and calcination from the bulk catalyst synthesis using precipitation.....	72
Figure 4.26. SEM micrographs showing the coverage of the precipitate on the mesh at 10 0 X magnification produced from the bulk catalyst synthesis using precipitation. ....	72
Figure 4.27. SEM micrographs showing the precipitate coverage at 50 0 X and 100 0 X magnification produced from the bulk catalyst synthesis using precipitation. ...	73

Figure 4.28. SEM micrographs showing spherical particles with agglomeration at 500 0 X and 1000 0 X magnification produced from the bulk catalyst synthesis using precipitation.....	73
Figure 4.29. SEM micrographs at 500 x magnification comparing the catalyst synthesized from Test Run 5 (a) and synthesis of the bulk sample (b).....	74
Figure 4.30. Substrate after wet impregnation and calcination.....	74
Figure 4.31. PTFE filters with their numbered filter support after the testwork.....	75
Figure 4.32. Measured PM mass concentrations for the Baseline and Catalyst Runs.....	75
Figure 4.33. SEM micrograph of the field blank filter showing the structure of the filter and the pores (Filter 2) at 400 x magnification.....	76
Figure 4.34. SEM micrograph of the Baseline Run 1 filter (Filter 3) at 417 x magnification .....	77
Figure 4.35. SEM micrograph of the Baseline Run 3 filter (Filter 10) at 400 x magnification .....	77
Figure 4.36. SEM micrograph of a chain-like structure found in one of the pores for Baseline Run 3 (Filter 10) .....	78
Figure 4.37. SEM micrograph showing particulate clusters in the pores of the filter from Catalyst Run 3 (Filter 9) at 20 0 X magnification.....	79
Figure 4.38. SEM micrograph (at 20 0 X magnification) of the Catalyst Hot Run Filter 6 showing fewer particulate clusters due to the shorter sampling time than the catalyst run.....	79
Figure 4.39. SEM micrograph (at 1150 x magnification) of Catalyst Run 3 (Filter 9) showing the particulate clusters .....	80
Figure 4.40. SEM micrograph (at 5000 x magnification) of Catalyst Run 3 (Filter 9) showing the spherical particulates and a fly ash particle. ....	81
Figure 4.41. SEM micrograph at 1000 x (a) and 3000 x (b) magnification showing spherical particles smaller than 1 $\mu$ m in size for the Catalyst Hot Run (Filter 6).....	81
Figure 4.42. SEM micrographs comparing the filters from catalyst Run 3 (Filter 9) (a) to baseline Run 3 (Filter 10) (b).....	82

## LIST OF TABLES

Table 3.1. Test Runs conducted .....	53
--------------------------------------	----

## LIST OF ABBREVIATIONS

DALY	Disability adjusted life year
DEA	Department of Environmental Affairs
DFFE	Department of Fisheries, Forestry and Environment
DOE	Department of Energy
EC	Elemental carbon
EDX	Energy dispersive X-Ray spectroscopy
EG	Ethylene glycol
E-R	Eley-Rideal reaction mechanism
ESP	Electrostatic Precipitation
FBE	Free basic electricity
HACA	Hydrogen abstraction and carbon addition
L-H	Langmuir-Hinshelwood reaction mechanism
LPG	Liquified petroleum gas
MVK	Mars-Van Krevelen reaction mechanism
NEP	National Electrification Programme
OC	Organic carbon
PAC	Poly aromatic compounds
PM	Particulate matter
PM <sub>2.5</sub>	Particulate matter with an aerodynamic diameter of less than 2.5 µm
PM <sub>10</sub>	Particulate matter with an aerodynamic diameter of less than 10 µm
PTFE	Polytetrafluoroethylene
SEM	Scanning Electron Microscopy
TPR	Temperature Programmed Reduction
VOC	Volatile Organic Compounds
WHO	World Health Organization

# CHAPTER 1: INTRODUCTION

## 1.1. BACKGROUND

Although there has been much progress in the provision of electricity to households in South Africa, many still rely on traditional fuel sources such as wood and coal (Israel-Akinbo, Snowball & Fraser, 2018). A study conducted by the Department of Energy came to a similar conclusion as their results indicated that poorer households relied on multiple sources of energy regardless of electrification status (DOE 2012, 19).

The negative health and socio-economic impacts of emissions associated with domestic fuel burning are widely recognized. In a synthesis of the available information on air quality in South Africa, the emissions from domestic fuel burning was shown to have the highest health impact of all air pollution sources (Friedl et al., 2008). The South African comparative risk report analyses the risk associated with 17 risk factors, including indoor air pollution and urban air pollution (MRC, 2008). The report estimated that 20% of South African households are exposed to indoor pollution from the burning of solid fuels. Areas that experience the highest impact of domestic fuel burning would be densely populated with a high density of emission sources. The negative impacts of household emissions are exacerbated by the fact that they are released in the breathing zone of individuals (DEA, 2019). Globally, the greatest negative health impact of domestic energy use is from incomplete combustion of fuels in low efficiency stoves and lighting devices (WHO, 2014).

A South African study analyzing the economic impact of various air quality initiatives found that technology interventions in the domestic sector would be the most efficient way to reduce healthcare costs associated with urban air pollution (Leiman et al., 2007). The interventions that have been investigated in South Africa include the electrification of households, the use of alternative fuels, improved household energy efficiency and encouraging the use of top down fire ignition methods, amongst others (Scorgie, 2012; Matandirotya et al., 2019).

## **1.2. PROBLEM STATEMENT**

While various investigations have been done on reducing household emissions by reducing the use of polluting fuels and improvements in combustion efficiency, comparatively fewer studies have been conducted on the reduction of emissions through secondary emission reduction using abatement technology. The emissions from domestic, fixed bed devices differ from that of larger sources such as solid fuel boilers and abatement technologies typically used on such installations are not necessarily appropriate due to the size of the installations and the physical and chemical properties of the emissions.

The particulate matter emissions comprise mainly of organic particles, soot and inorganic fly ash (Torvela et al., 2014). Various technologies have been developed to capture particulate matter (non-catalytic methods) such as cyclones, scrubbers and air filters, but due to the expected size distribution of the emissions, non-catalytic methods are unlikely to achieve the desired emission reduction (Perry et al., 1994). Catalytic oxidation could be utilized to oxidize particulate matter precursors such as volatile organic compounds and soot particles to reduce secondary particulate formation. Although catalytic methods have not been effectively utilized in practical domestic applications, studies have shown effective soot reduction during laboratory testing (Gao et al., 2020).

## **1.3. RESEARCH OBJECTIVE**

The study investigated the potential of abatement technologies in reducing particulate matter emissions from a locally available domestic cast iron stove. An assessment of the literature was first conducted to inform the study by identifying the emissions that are likely to arise from the burning of domestic solid fuel such as wood and coal and identifying the available catalytic and non-catalytic abatement technologies for the reduction of the particulate emissions reported in the literature. The objectives of the study were thus to:

1. Synthesise a prototype emission control device suitable for use in a domestic cast iron stove and to characterise the synthesised products using scanning electron microscopy.
2. Perform a screening test on the effectiveness of the prototype to reduce particulate matter emissions from a locally available, wood fired, domestic cast iron stove.

#### **1.4. DISSERTATION OUTLINE**

The dissertation is outlined as follows: Chapter 2 presents a literature review which gives an overview of the characteristics and impacts of emissions from domestic fuel burning and how domestic fuel burning emissions have been addressed previously in South Africa. Furthermore, the chapter outlines the catalytic and non-catalytic methods for reducing domestic fuel burning emissions. It concludes with a discussion of the abatement technologies that could be appropriate to reduce these emissions. Chapter 3 presents the methods and procedures that the study employed, and the results thereof are presented and discussed in Chapter 4. Lastly, Chapter 5 presents the conclusions of the study and recommendations for future testwork.

## **CHAPTER 2: LITERATURE REVIEW**

This chapter presents an overview of relevant literature related to the study. As previously stated, this study aims to investigate whether emissions from domestic fuel burning can be reduced using end-of-pipe abatement. The chapter, therefore, discusses the characterisation and impacts of domestic fuel burning and how it has been addressed in South Africa. Furthermore, it investigates the catalytic and non-catalytic abatement technologies that are available to reduce PM emissions. The last section concludes with a discussion on which abatement technologies could be applicable to the reduction of domestic fuel burning emissions.

### **2.1. EMISSIONS FROM DOMESTIC FUEL BURNING**

#### **2.1.1. Fuel usage**

Although there has been much progress in the provision of electricity to households in South Africa, many still rely on traditional fuel sources such as wood and coal (Israel-Akinbo, Snowball & Fraser, 2018). Households were found to utilize predominantly wood and coal in areas of South Africa close to coal mines for space heating purposes and electricity and paraffin for cooking (Friedl et al., 2008). Coal usage was found to be more prevalent in the Mpumalanga Province due to the proximity of coal mines, with 21% of households reporting using wood and coal (StatsSA, 2022).

In a study conducted in Zenzele, a non-electrified, low income settlement in the Gauteng Province, household fuel usage was investigated by means of surveys and hanging scales to quantify the fuel use of 15 households (Naidoo, 2014). The study found that there were significant seasonal variations in fuel use. Coal and wood were not frequently utilized during the summer months and that in winter, wood was burnt in the morning, if needed, and wood together with coal were utilized in the evenings. While cost of fuels played a role, the choice of fuel also has cultural aspects associated with it.



A study conducted in Kwadela, Mpumalanga Province found that 90% of the residents made use of solid fuels for cooking and heating purposes during the winter. During the summer, the use of these fuels continued, albeit at reduced rates (Nkosi et al., 2017).

In a study conducted in Doornkop in the Gauteng Province and Kwaguqa in the Mpumalanga Province, it was found that 80% of electrified households utilized coal for space heating and cooking (Mdluli & Vogel, 2010). The study found that coal was utilized to save electricity and that households that did not use coal mainly did so because their stoves were broken or they did not have a stove. A very small percentage did not utilize coal as they reported negative health impacts. The study suggested that continued coal use could be partly attributed to functioning coal supply networks as relatively cheap coal was delivered to households.

The Department of Energy (DOE), now the Department of Mineral Resources and Energy (DMRE) conducted a survey of energy-related behaviour and perceptions in South Africa in 2012 (DOE, 2012). The survey gathered information on fuel usage and electricity usage for various applications such as lighting, cooking and space heating. The survey results indicated that poorer households tended to rely more heavily on multiple energy sources. A study conducted by Friedl et al. (2008) indicated that households use a mix of fuel sources and switch between fuel sources to suit their particular needs.

The survey by the Department of Energy further indicated that households made use of a substitution strategy when there are electricity interruptions or the household budget for prepaid electricity is exhausted (DOE, 2012). In terms of geographical differences, rural households were found to be more reliant on firewood as an energy source than household residing in urban areas and small towns. The study found that a complex set of factors, including cultural inertia and the perceived high cost of electricity, exist that explains the usage of dirty fuels for cooking, despite electrification.

A study by Israel-Akinbo et al. (2018) examined how poor households transition from traditional energy carriers such as wood to modern energy carriers such as electricity, biofuels and liquefied petroleum gas. The transition could follow an 'energy ladder' model whereby households move from traditional energy carriers to transitional and then to modern

energy careers as their income improves. The 'energy stacking' model indicates that households will utilize a combination of energy carriers on the upper and lower stages of the energy ladder, depending on their needs. The study found that for cooking, households will transition from traditional fuels to modern fuels as income rises in accordance with the energy ladder approach. In the case of energy usage for heating purposes, income was not a statistically significant determinant of energy usage, which means households will not necessarily switch to modern fuels as income rises, in line with the energy stacking model. A study conducted by the Department of Energy came to a similar conclusion as their results indicated that poorer households relied on multiple sources of energy regardless of electrification status, which further points to an energy stacking model rather than the energy ladder theory (DOE 2012).

A study conducted by Madubansi and Shackleton (2006) investigated the change in energy use in five rural settlements in South Africa. The study found that, despite electrification, households continued to use wood for their thermal needs and viewed electricity as an additional energy source and not necessarily as an alternative.

Even though it is recognized that a mixture of fuels is used in the domestic sector, the actual volumes utilized are not well researched and estimates for wood use in urban areas are scarce (Pauw et al. 2006). In rural areas the estimated annual use of wood used per household was estimated at an average of 4.5 tons/household/annum (Damm & Triebel, 2008). The number of households using solid fuels is included in the National Census as well as the General Household Survey and respondents are required to provide their main energy carrier used for different purposes (cooking, heating, lighting), which does not provide a full picture of energy usage due to the use of multiple energy carriers or fuel stacking. It is thus expected that significantly more households use solid fuels than is reported in these surveys (Pauw et al., 2022).

### **2.1.2. Health impacts from domestic fuel burning**

The Global Burden of Diseases Study estimated that household air pollution was responsible for 2.8 million deaths and 85.6 million disability adjusted life years (DALYs) globally in 2015 (Cohen et al., 2017). The study concluded that household fuel burning contributed significantly to mortality in low and middle income countries. The study further described

household fuel burning along with ambient air pollution as a 'substantial health challenge' and concluded that reductions in ambient PM<sub>2.5</sub> can be expected to increase life expectancy over a short period of time.

In analyzing the data for the Global Burden of Disease project, it was noted that the use of solid cooking fuels does not only contribute to poor indoor air quality, but affects ambient air quality and thus outdoor air pollution as well (Smith et al., 2014). Therefore, interventions such as improved stoves with chimneys does not solve the problem of the use of dirty fuels. The study noted that the risk should be framed as the risk associated with the use of solid fuels for domestic purposes or 'household air pollution', rather than drawing the distinction between indoor and outdoor impacts of this type of fuel use. In South Africa low-income areas experience between 51 and 78% higher PM<sub>10</sub> concentrations than urban/suburban residential and industrial areas respectively (Hersey et al., 2015). In the Gauteng Province, both PM<sub>10</sub> and PM<sub>2.5</sub> display diurnal patterns that are most distinct during winter in low-income areas (Hersey et al., 2015).

In the South African context, while studies have shown an association between air pollution and negative health impacts, the quantification of these health impacts is limited by the availability of appropriate data (Wright et al., 2017). Various studies have attempted to estimate the health impacts of emissions resulting from domestic fuel burning. A study assessing the socioeconomic consequences of different pollution sources found that domestic fuel burning accounted for approximately 75% of all air quality related premature mortalities and approximately 70% of respiratory hospital admissions over the study area which comprised of selected metropolitan areas and the Highveld and Vaal Triangle areas (FRIDGE, 2004). In the City of Johannesburg and Ekurhuleni, Gauteng Province domestic fuel burning was calculated to be the most significant cause of premature mortalities and respiratory hospital admissions of all the emission sources considered.

In a synthesis of the available information on air quality in South Africa, the emissions from domestic fuel burning was shown to have the highest health impact of all air pollution sources (Friedl et al., 2008). Areas that experience the highest impact of domestic fuel burning would be densely populated with a high density of emission sources. The South African comparative risk report analyses the risk associated with 17 risk factors, including indoor air

pollution and urban air pollution (MRC, 2008). The report estimated that 20% of South African households are exposed to indoor pollution from the burning of solid fuels and proposed interventions to reduce this risk including behavioral change to reduce exposure and technologies to improve cooking and heating devices. The report further concludes that the health impacts associated with urban air pollution have been under recognized.

Shezi and Wright (2018) reviewed studies that provided evidence on hazardous air pollutant exposure and respiratory health outcomes in South African between 2005 and 2017, and it was found that there were no studies available that provide local relative risk data or exposure response functions that could be used in calculating the burden of disease attributable to hazardous air pollutants. The study further highlighted the need for local epidemiological studies to provide evidence of the association between pollutant exposure and negative health outcomes to motivate for policy making and to contribute to the international body of knowledge.

A study conducted in two towns in the Mpumalanga Province, South Africa found that the prevalence of respiratory illness amongst children was significantly elevated for households that utilize non-electrical fuels for cooking and heating (Albers et al., 2015).

In the study conducted by Mdluli et al. (2010), respondents reported that although there have been campaigns to raise awareness on the negative health impacts of coal usage, respondents did not believe that coal usage would have long term health impacts.

Various local and international studies have highlighted the negative health impacts of domestic solid fuel use, which highlights the need to address these emissions to improve community health. Residential burning of solid fuels is a major source of particulate matter emissions, which degrade air quality particularly in low-income settlements (Nkosi et al., 2018). Furthermore, literature has indicated that there is a strong positive association between fine and ultrafine particulate exposure and negative health outcomes such as cardiovascular impacts, cancer risk and premature mortality, amongst others (Alemayehu et al., 2020). The study therefore focused on the reduction of particulate matter and conducted particulate matter measurements to assess the potential use of abatement technology on domestic solid fuel stoves.

### **2.1.3. Domestic burning devices utilized in South Africa**

Various studies have investigated the types of fuel burning devices utilized in electrified and non-electrified areas of South Africa. In a study conducted to determine fuel use in Zenzele, a non-electrified, low income settlement in the Gauteng Province, it was found that where coal stoves were available, households preferred using these for cooking and heating purposes (Naidoo, 2014). In that settlement seven out of the 15 study participants utilized coal stoves and the remaining eight utilized smaller, handmade coal stoves. It was further found that electrified households with elderly women residing preferred using coal stoves for heating and cooking. The study indicated that there was widespread use of coal fired brazier stoves (imbaulas), constructed out of a perforated drum, but that these were utilized outdoors due to the emissions generated.

A study conducted in a non-electrified area of Alexandra in the Gauteng Province found that residents collected firewood which was used in inefficient imbaula stoves (Kimemia et al., 2010). Of the 103 households interviewed, a total of 40 imbaulas were found and characterized. Even though the devices were manufactured from similar containers, the study found that the devices varied in design and that there was no standard configuration.

A study in Kwadela located in the Mpumalanga Province revealed that the most common burning appliance in the study area was cast iron coal stoves fed primarily with coal, supplemented by wood and dung to start the fire (Nkosi et al., 2017). The traditional stoves used were old with combustion emissions leaking from the stoves, leading to poor indoor air quality. The stove consists of burning chamber, cooking plates and a baking area. The stoves were equipped with chimneys that varied in height. The chimney heights were found to extend between 150 cm and 287 cm from the roof level, which does not allow for adequate dispersion as emissions are not transported from the breathing zone. The study found that ash was removed from the stoves before lighting the stove and that the stove parts, including the chimney, would be cleaned once to twice a week.

While conducting a study in two township areas in Gauteng and Mpumalanga Provinces, Mdluli et al. (2010) found that 44% of coal burning households in Doornkop and 2% of coal

burning households in Kwaguqa burned coal in coal stoves, while imbaulas were utilized by 15% and 6% of households respectively.

Households utilize solid fuels in a variety of cooking and heating devices, ranging from traditional coal stoves to brazier stoves or imbaulas. The study will focus on devices that have a means of capturing emissions such as flues. Due to the variability in stove design and flue arrangements, the catalyst design should be customizable to fit different configurations.

## **2.2. COMBUSTION PROCESSES AND EMISSION QUANTIFICATION AND ANALYSIS**

### **2.2.1. Emission factors**

Various laboratory and field measurement studies have been conducted globally to derive emission factors for different stove/fuel combinations. Average emission factors for wood, dung, crop residue and charcoal were developed for household stoves in a laboratory or simulated kitchen using the water boiling test (WHO, 2014). The study noted that further research into in-field measurements were required to improve the quality of data on emission factors. The WHO guidelines on indoor air quality notes that there are limited measurements of emissions from stoves in the field and during the actual process of cooking and space heating. The guidelines further state that there is not a good understanding of the variability and causes of variability in emissions over geographical scales.

In explaining the differences between derived emission factors, the WHO notes that operator behavior affects the emissions and that emission factor derivation is complicated by the variability in fuel use and fuel characteristics and seasonality of fuel use (WHO, 2014). It was noted that household combustion is fundamentally not a steady state process. The evidence collected, however, indicated that laboratory tests were not representative of actual household activities, which highlights the need for in-field testing.

In assessing emissions from wood fired stoves in Europe, Fachinger et al. (2017) found that while many studies have examined the emissions of PM, CO and NO<sub>x</sub>, few studies have measured in real time the chemical compositions of the pollutants emitted from wood stoves. Their assessment divided the measurements into three phases - cold/warm startup, stable burning conditions and the burnout phase. The study analyzed emissions from various types of wood as well as non-wood sources such as paper and concluded that although there

were some differences in particle composition when different types of wood was used, the impact thereof on the emission factors was comparatively low. The use of fuel other than wood was found to increase emissions significantly and influenced the chemical composition of the particles emitted. The study further concluded that emissions are operator dependent and that the user can minimize emissions from a stove by controlling the burning conditions therein. The study highlighted that, due to the impact of burning conditions on emissions, direct comparison between the emission factors derived in other studies would be complicated.

Nkosi et al. (2018) conducted field measurements on traditional cast iron coal stoves in South Africa and concluded that residential fuel burning was a major source of fine particulate matter. The study highlighted the need for local emission factors and conducted in-field measurements of PM emissions from two households in kwaDela, Mpumalanga Province utilizing a mixture of coal and wood as fuel to calculate emission factors for coal stoves. The stoves were fed with coal and wood purchased from local stores. The study again showed that PM emissions vary with operator behavior and that there was a negative correlation between fuel mass used and emissions due to insufficient mixing of flue gas and combustion air. The study did not differentiate between the different stages of combustion. PM emissions varied between 6.8 g/kg and 13.5 g/kg of fuel.

Makonese et al. (2017) calculated emission factors for coal fired brazier stoves (imbaulas) from stoves collected from user communities as well as stoves manufactured in a laboratory. The study calculated emission factors for two methods of lighting the fire, the bottom lit updraft method as well as the top lift updraft method. The study found that emission factors for PM<sub>2.5</sub> and PM<sub>10</sub> were reduced by up to 80% when using a top lift updraft method when compared to emission factors for the bottom lit updraft method. To collect the exhaust gas, the imbaulas were placed under a collection hood and the gas diluted to allow for online measurement as concentration exceeded the measurement range of the instruments during the initial phases of combustion. The study found that PM<sub>2.5</sub> constituted more than 90% of the PM<sub>10</sub> fraction. The results further indicated that the method of lighting did not affect the emission of CO, CO<sub>2</sub> and NO<sub>x</sub>. The combined PM<sub>10</sub> emission rates were calculated to be in the range of 0.0008 - 0.0012 g/s.

In a study by Nkosi et al (2018), isokinetic and direct stack sampling was conducted on traditional cast iron coal stoves to determine how particulate matter emission profiles changed with stove operating behaviour. The study obtained an emission factor range of between 6.8 g/kg and 13.5 g/kg of fuel used, where coal was used as a fuel with wood and paper to ignite the fire. It was found that operating behaviour, such as poking or re-fueling the fire produced higher emissions. The study conducted a limited number of field tests due to equipment failure and the need to consider the impact (inconvenience) of sampling on the households and highlighted the need to conduct field studies using a larger sample size due to the variability of the emissions measured.

### **2.2.2. Combustion theory**

Section 2.2.1 reviewed the emission factors derived for various combustion device/fuel combinations. These emission factors provide the overall particulate matter mass emitted, but do not provide information on the composition of the particulate matter or the species that are formed during combustion. To provide insight into the species that are formed and the role of combustion conditions on the species formed, a brief review of combustion theory is provided in this section.

The composition of flue gas and fly ash formed varies considerably depending on fuel type, combustion conditions and combustion characteristics. The fuel type used influences combustion in a number of ways through the moisture content of the fuel, the level of contaminants, the size of the fuel and the peak temperatures that are achieved. Moisture in fuel leads to lower combustion temperatures, which can lead to low efficiency combustion zones. Mineral contaminants partition between the solid and vapor phase, with volatile minerals forming fly ash (WHO, 2014).

During the combustion process, solid fuel is first volatilized and then oxidizes (Nystrom, 2016). In the case of biomass, a partially burned pyrolysis product or char is formed once most of the fuel has volatilized. The char is then further combusted. Under complete combustion, the fuel is fully oxidized. For complete combustion to occur sufficient air, sufficiently high temperatures, long enough residence time and sufficient fuel and air mixing are required. Products of incomplete combustion such as CO, VOCs and soot particles are formed when these requirements are not met. When the combustion process is interrupted, mainly



by quenching or poor mixing in the case of household devices, incomplete combustion products such as hydrocarbons and CO enter the flue gas or escape the combustion chamber (WHO, 2014). When poor mixing occurs, pockets of pyrolysis gasses can form which react chemically within these pockets, and can either be chemically rearranged in the combustion chamber or be emitted via the flue gas (Fitzpatrick, 2009).

Emissions from combustion can be classified into four main categories:

1. complete combustion products such as CO<sub>2</sub> and H<sub>2</sub>O
2. incomplete combustion products such as CO and many other carbon containing organic compounds
3. thermal NO<sub>x</sub>, which is limited at lower temperatures in household burning devices (WHO, 2014)
4. combustion products formed from the contaminants in fuel such as fuel NO<sub>x</sub>, sulfur compounds and fly ash.

Secondary pollutants such as ozone, sulfates, organic aerosols and poly aromatic compounds (PACs) can also be produced downwind of the combustion device. The combustion process is shown in Figure 2.1.

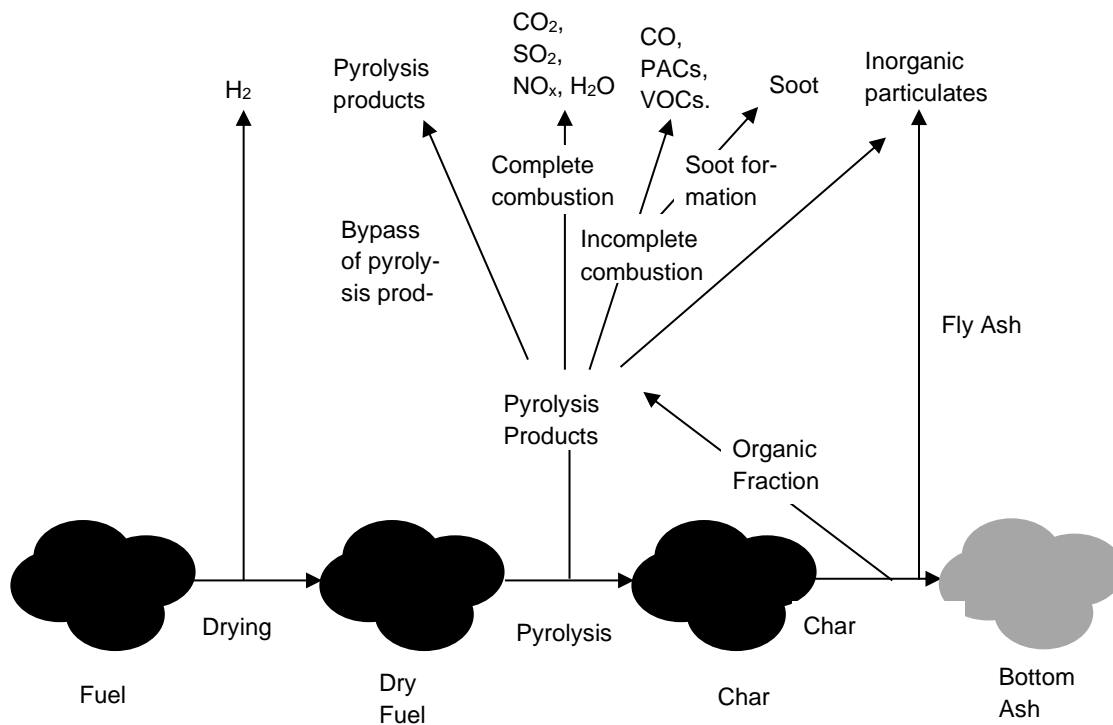


Figure 2.1. The combustion process and products typically formed (based on Nystrom (2016))

Particulate matter emissions can be classified into an inorganic fraction and an organic fraction. The organic fraction comprising of carbonaceous material results from incomplete combustion. The inorganic fraction is formed from the release of inorganic fuel contaminants during volatilisation and then are formed as the gas cools and condenses. The ash particulates that are too large and dense to be carried with the flue gas form the bottom ash (Nystrom, 2016).

The carbonaceous particles can be further classified into elemental carbon (EC) and organic carbon (OC), where EC is the optically absorptive fraction and OC is the non-absorptive fraction of the organic aerosol. Studies have indicated that the organic fraction can exceed the inorganic fraction in wood stoves or similar appliances. Soot can be described as fine particulate agglomerates consisting mainly of carbon. The formation of these particulates is dependent on the fuel utilized as well as combustion conditions (Nystrom 2016, 22).

The organic carbon fraction consists of many compounds in the gas and particle phase at ambient temperature and the composition is very temperature dependent. Polycyclic aromatic compounds (PAC) consist of fused benzene rings and although they make up a minor fraction of the organic fraction, they are of concern as they are known to be toxic, mutagenic and carcinogenic. The fuel properties affect the combustion conditions which in turn influence the particulate and PAC emissions (Munyeza et al., 2019). PACs exist in both the gas phase and particulate phase depending on their size and are often emitted alongside soot particulates. The formation of PACs is not fully understood, but studies have suggested they form by pyrolysis and pyrosynthesis (Nystrom, 2016). Nystrom (2016) found elevated levels of carbonaceous emissions including soot and organics as well as a higher fraction of larger particles under high burn rates from biomass combustion.

Particulate matter can be classified into size fractions corresponding to their formation mechanism (Seinfeld and Pandis, 2016):

- Nucleation mode - particles with diameters up to 10 nm
- Aitken mode – particles with diameters between 10 to 100 nm in size
- Accumulation mode – particles with diameters between 0.1  $\mu\text{m}$  and 2.5  $\mu\text{m}$
- Coarse fraction - particles with a diameter above 2.5  $\mu\text{m}$

Nucleation occurs when particles are formed as a result of the collision of supersaturated vapors of low volatility gas phase species. When the particle clusters grow faster than they dissociate, a stable particle nucleus forms. Homogenous nucleation occurs when gas phase particulates form directly from the gas phase and heterogeneous nucleation occurs when gas particles condense onto already existing particulates. Particles can grow larger by way of condensation which occurs when gases are converted to liquids or solids on the surface of a particle not in the gas phase. Particles can also grow by way of coagulation, where particles collide and fuse into larger particles. Particle collision can be due to Brownian motion or by other phenomenon such as electrical or gravitational forces. After primary formation, particles grow further by secondary coagulation and condensation processes. Particle formation is illustrated in 2.2.



Figure 2.2. Particle formation mechanisms (Adapted from: Nystrom (2016) and Seinfeld and Pandis (2016))

Soot is comprised of agglomerations of carbonaceous particles impregnated with tar and is formed when the gasses are sufficiently fuel rich for nucleation and condensation to occur (Seinfeld and Pandis 2016). These initial soot particles can then grow to form large spherical particles or agglomerate or aggregate to form chains (Fitzpatrick, 2009).

Two mechanisms have been proposed for the formation of soot. The first route is via hydrogen abstraction and carbon addition (HACA) and the second is the reaction and transformation of wood pyrolysis fragments. A third mechanism proposed by Fitzpatrick et al. (2008) involves PAC formation through the cracking of lignin monomers through a cyclopentadiene intermediate in addition to the HACA mechanism. In comparing the pyrolysis products from coal and biomass, Fitzpartick et al. (2009) found that coal pyrolysis products contained more aromatics and alkyl aromatics and long chain alkenes while biomass pyrolysis produces oxygen containing products from cellulose and lignin. The study suggested that HACA

mechanisms of soot formation are less important for coal combustion compared with biomass combustion and that the aromatic nature of coal results in an aromatic route of soot formation through either the formation of cyclopentadiene followed by naphthalene or through o-cyclic compounds and oxygenated PACs.

The PM emissions are therefore expected to consist of various organic species as well as inorganic particulates. The organic emission products react within the flue gas to aggregate and form chain-like structures. The combustion products further coagulate and condense to form fine particulate matter.

### **2.2.3. Characterization of emissions**

The most suitable method for reducing particulate matter depends on the physical and chemical properties of the particulates. These characteristics are determined by the morphologies, size and composition of the particles. Measuring total particulate matter mass concentrations do not provide sufficient information on the morphology, surface chemistry and composition. This information is crucial in determining the most efficient collection or treatment method.

Zhang et al. (2018) sampled primary PM particles from various sources using ultrafine polyamide nanofiber filters and the individual particles were analysed. The 'smoke' sources sampled, such as barbecue, cigarette, incense and biomass emissions, were found to have a narrow size distribution with more than 95% PM<sub>2.5</sub> particles and more than 80% were smaller than 0.5 µm. Particulates from wood smoke sources were found to have a higher concentration of larger particles, attributed to incomplete combustion. The combustion smoke particles were found to contain a large amount of oil-like particles which gradually solidified under atmospheric conditions. The capture mechanisms of the smoke particulates were found to be different to the capture mechanisms of solid particles such as 'dust' or fly ash emissions with strong adhesion of soot particles to the filter fibers.

The combustion of wood resulted in many soot particles forming from the aggregation of ultrafine particulates to form smaller groups of chain structures. Fly ash made up of mainly inorganic material also resulted from biomass burning. The surfaces of the collected particles were analysed and it was found that the PM<sub>2.5</sub> particles were mainly organic aerosols.

The PM<sub>10</sub> fraction of the barbecue smoke contained mainly soot aggregates with smaller quantities of fly ash and minerals (Zhang et al., 2018).

The study by Makonese et al. (2019) analysed emissions from a coal brazier during the different phases of combustion. The study found that during the ignition phase, spherical organic particles were emitted similar to tar balls. During the flaming phase, small particles with chain like aggregates were formed. The particles consisted of single spherical particles, agglomerated particles in the form of chains or aggregates and organic particles with inclusions. The organic particles were found to consist mainly of C and O and trace amounts of Si, S, Mo, K and Al. The study suggested that these particles are found in the plumes of smoldering rather than flaming fires. Furthermore, these spherical organic particles were similar to tar balls and polymeric organic compounds that are emitted during biomass burning. During the char burning phase, non-carbonaceous material similar to ash is emitted as most of the volatile material has been released during the ignition and flaming phases. The non-carbonaceous particles were found to be larger in size than the particles emitted during the preceding phases and were irregular in shape.

The study further investigated ageing of particles emitted from a brazier (imbaua) by using two sampling points at 1 m and 5 m away from the brim of the brazier. When sampling close to the brim of the brazier during ignition and early pyrolysis, the filter used clogged up with a liquid, tarry substance. At 5 m from the imbaula rim, the particles had coalesced and cooled into distinct particles including large spherical organic particles (Makonese et al., 2019).

A study by Fletcher et al. (1997) conducted pyrolysis experiments and found that soot yield decrease slightly with increased temperatures and that the primary soot particles from coal combustion were in the 25 nm to 60 nm size range. Bulk sampling also indicated a large number of large soot particles in the size range 5 µm to 38 µm which are only formed when coal is combusted. Combustion of coal in an imbaula was also found to produce large carbonaceous soot particles with diameters of between 5 µm and 100 µm (Makonese et al., 2014). Using more efficient top down lighting methods was found to reduce both the particulate emissions as well as the diameter of the particulates formed.

Emissions from wood fired boilers were characterized by Torvela et al. (2014). Emissions were analysed under different combustion conditions, based on the concentration of CO

emissions. The study indicated that organic carbon and elemental carbon emissions significantly increased under intermediate (CO: 1–0 - 1000 mg/MJ) and smoldering conditions (CO: 10–0 - 5000 mg/MJ). Gaseous organic emissions were highest during the firing phase. The study found that emissions consisted mainly of fly ash, soot and particulate organic matter.

Studies have indicated that emissions from older wood stoves contain a significant portion of organic material and soot, while emissions from more modern stoves comprise mostly of inorganic alkali salts. In an older wood fired stove, the majority of emissions, up to 80%, were found to be organic carbon and elemental carbon (Nystrom, 2016).

Coal burning has been found to have a lower organic carbon/elemental carbon ratio than biomass burning. Adding coal to biomass increases the bed and flue gas temperatures as volatiles are released from coal at a slower rate. Coal also has a longer char burnout rate, which allows for higher temperatures to be reached. The combustion of coal along with biomass was found to reduce the concentrations of CO and organics including PACs and phenols, likely due to reduced breakthrough of pyrolysis products. However, overall emissions were higher with co-combustion with coal (Fitzpatrick, 2009).

In order to select an appropriate abatement technology, an understanding of the composition, size and morphology of the particulate matter emitted from wood and coal combustion is required. The particulate matter emissions are expected to have a narrow size distribution with more than 95% consisting of PM<sub>2.5</sub> particles and more than 80% <0.5 µm (Zhang et al., 2018). Previous studies have indicated that emissions from wood fired boilers consists mainly of fly ash, soot and particulate organic matter and it is expected that the PM<sub>2.5</sub> particles comprise mainly of organic aerosols (Torvela et al., 2014; Zhang et al., 2018). The abatement technology selected for this study should therefore be able to reduce primarily organic material comprised of particulate matter with a large portion of emissions below 0.5 µm.

#### **2.2.4. Atmospheric reactions and impacts of emissions**

Various studies have indicated that particulates and gasses emitted from combustion continue to react in the atmosphere. Once emitted, particles have been shown to transform into

clusters in the atmosphere that can reach sizes of over 100  $\mu\text{m}$ . Analysis of aerosol filter samples in Soweto, Gauteng Province, has shown the presence of large ( $>3 \mu\text{m}$ ) sized particles rather than the sub-micron aerosols that are generally expected (Wentzel et al., 1999). Particulates collected by the aerosol filters contained primarily carbonaceous agglomerates with diameters between 10 and 100  $\mu\text{m}$ . These agglomerates were spherical with internal structures that vary and included dendritic, sponge like as well as 'melted toffee' type internal structures. Mineral particles were found to be occasionally embedded or adhering to the carbonaceous particles. Due to the low bulk densities of the large particulates and their high surface to volume ratios, they stay airborne for longer than would typically be the case for particulates of that size. The results indicated that the conglomerates likely had a liquid coating, some of which was shed during impaction with the sampling filter (Wentzel et al., 1999).

A study on the optical characteristics of ground-based, light-absorbing aerosols in the Kwadela township in South Africa found that daily averaged light-absorbing aerosols contributed more to  $\text{PM}_{2.5}$  in winter as compared to summer (Xulu et al., 2020). Bimodal diurnal cycles, correlated with diurnal  $\text{PM}_{2.5}$  patterns, were seen in both summer and winter, and measurements in winter indicated the dominance of brown carbon (from biomass or biofuel burning or burning of low quality coal). At midday and at night in summer, measurements indicated more black carbon emissions, likely from sources such as diesel emissions (Xulu et al., 2020).

Pachauri et al. (2013) analysed individual aerosol particles collected during summer and winter in India. The study found a distinct seasonal variation in the amount of carbonaceous material present in the aerosols. Carbonaceous particles were found to be more abundant during winter months, which the authors attributed to increased combustion and stagnant meteorological conditions. A total of 3500 individual particles ranging between 2 and 70  $\mu\text{m}$  were analyzed using scanning electron microscopy with energy dispersive X-ray analysis (SEM/EDX). Carbonaceous particles made up approximately 25% of the total particles collected. The particles varied from soot chains to complex carbonaceous structures comprised of interconnected carbon spheres (Pachauri et al., 2013).

### 2.3. ADDRESSING DOMESTIC FUEL BURNING

The ultimate focus of interventions addressing domestic fuel use should be the reduction of emissions, which influences both indoor and ambient air quality (WHO, 2014). A South African study analyzing the economic impact of various air quality initiatives found that technology interventions in the domestic sector would be the most efficient way to reduce healthcare costs associated with urban air pollution (Leiman et al., 2007). The interventions analyzed included the method of starting a fire (top down ignition), improving household insulation, stove maintenance and electrification of households (Scorgie, 2012). The benefits associated with using a top down ignition methods were significant, with a high benefit to cost ratio. Housing insulation, as well as stove maintenance and replacement were also found to have positive benefit to cost ratios. However, the technologies looking at low smoke fuels in the domestic sector were not found to be economically feasible at their costs at the time of the study (Leiman et al., 2007).

In South-Eastern Europe, it was found that 30% of households were not adequately able to heat their homes at reasonable prices. To support these households, the EU launched the REACH project (Reduce Energy use and Change Habits) which reduced energy poverty through energy efficiency measures such as energy efficient lighting, insulation and behavioral changes to reduce energy costs (Amann 2018, 37). The study found that, despite only accounting for 2.6% of total energy use, domestic fuel burning contributed 46% of PM<sub>2.5</sub> primary emissions in the study area (EU-28), which is three times more than the contribution of vehicle emissions. The emissions in each member state were found to vary widely and depended on factors such as the prevalence of small combustion installations, fuel use and social and regulatory conditions.

The study further highlighted the need for an integrated approach in addressing such emissions and noted that improvements would need sustained intervention over several years. It was recommended that interventions to reduce domestic use of dirty fuels should be accompanied by measures to address fuel poverty. The study identified measures that were effective in reducing domestic fuel burning emissions including:

- administrative measures such as awareness raising, registration of sources and emission standards
- design provisions to improve solid fuel stoves and boilers and improved fuel standards



- financial incentives such as subsidies for the installation of fuel efficient technologies (as implemented in Austria)
- fuel substitution strategies and bans and restrictions on the use of solid fuel
- energy efficient building renovations and improved heat management
- strategies to address fuel poverty.

Solid fuel bans have been used in Europe to reduce emissions. In Poland the use of solid fuel was restricted in the city of Krakow from September 2019, where low stack emissions contributed 55% to PM<sub>10</sub>. Coal usage was replaced by expanding the city's gas distribution network, modernization the district heating system, and promotion of energy efficient buildings and the use of renewable energy. The intervention included subsidies to low income households (Amann, 2018).

The WHO recommended emission rate for household combustion of PM<sub>2.5</sub> is 0.23 mg/min for unvented sources and 0.80 mg/min for vented sources, and governments are encouraged to make use of interim measures to ultimately reach the guideline with priority given to measures that yield significant positive impacts. The phasing out of the use of unprocessed coal for household fuel use is recommended as evidence suggests that indoor emissions from coal burning are carcinogenic to humans (WHO, 2014).

In South Africa, the governmental strategy is cognizant of the importance of understanding the needs of households in developing interventions to ensure sustainability and developed a strategy to address air pollution in dense low-income settlements (DEA, 2019). Research has indicated that, in understanding domestic fuel burning and fuel usage, the functioning of the household and social dynamics must be understood (Friedl et al., 2008).

Interventions such as pollution limits or a phasing out strategy for solid fuels are not deemed suitable in the South African context, as it is mainly poor households that are affected by household emissions. The use of dirty fuels is typically driven by poverty, even though communities may recognize that emissions are detrimental to their health. The strategy highlighted funding concerns when interventions are rolled out on a large scale (DEA, 2019).

The strategy proposed that the following interventions be investigated as a minimum (DEA, 2019):

- solar technology
- clean stoves
- free basic electricity with efficient appliances
- subsidized liquefied petroleum gas (LPG)
- improving the energy efficiency of houses
- air quality issues should be considered in development planning initiatives
- the use of air quality offsets
- public awareness campaigns.

The interventions that have been investigated in South Africa include the electrification of households, the use of alternative fuels, improved household energy efficiency and encouraging the use of top down fire ignition methods, amongst others. A brief description of some of these interventions is given in the Sections 2.3.1 to 2.3.6.

### **2.3.1. Electrification of households**

The World Bank Group estimates that in 1990 an estimated 60% of South African households had access to electricity (World Bank, n.d.). The South African Government estimates put this figure at 36% at the end of 1993 (DME, 2001). To provide electricity services to unserved households, the National Electrification Programme (NEP) was launched. The target was to provide access to electricity to 66% by 2001. The National Electrification Programme was followed by the Integrated National Electrification Programme.

The NEP target was reached and South Africa has made significant progress in increasing the percentage of households with access to electricity, as shown in Figure 2.3. By 2021, 89.3% of South Africans had access to electricity, which is significantly greater than the average for Sub Saharan Africa (StatsSA 2022; World Bank, 2018).

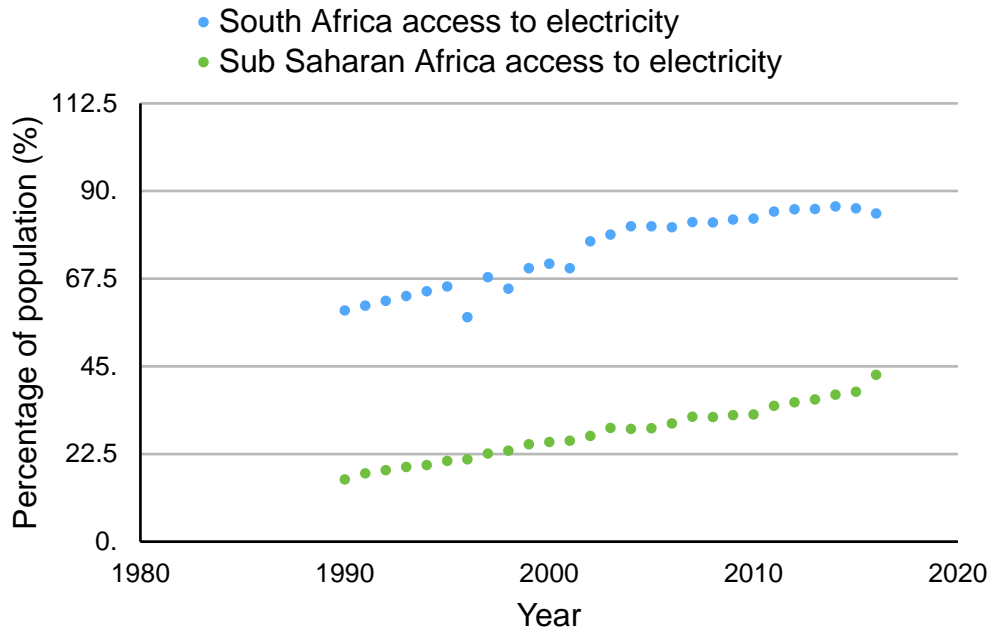


Figure 2.3. Comparing access to electricity between South Africa and Sub Saharan Africa (Source: World Bank Group)

To address the issue of the affordability of electricity, the Department of Minerals and Energy (DME) launched the Free Basic Electricity (FBE) programme in 2003, which provided for 50 MW of free basic electricity per low income household (Israel-Akinbo et al., 2018). An electricity tariff structure that increases price with increased usage could have the consequence of low income households limiting electricity usage by utilizing dirty fuels for space heating and cooking. During interruptions in electricity supply, households may also utilize dirty fuels as a backup (Friedl et al., 2008).

### 2.3.2. Top down fire making

The top down method of starting a fire produces less smoke as the combustion products travel through a hot zone, thereby encouraging more complete combustion (Wagner et al., 2005). In Europe, various awareness campaigns have been utilized to encourage top down emission techniques (Amann, 2018). In the South African context, it has been estimated that using a top down method of igniting fires could reduce PM emission by 50% and other pollutant emissions by 20% (Scorgie, 2012). A study by Makonese (2015) found that PM emissions from imbaulas could be reduced by an average of 80% when the top down method is

used and that, due to more complete combustion, a reduction in the formation of large carbonaceous agglomerates resulted.

A pilot study in eMbalenhle, Mpumalanga Province rolled out the top down method of fire making to reduce domestic emissions (Wagner et al., 2005). The project was started in 1998 and adopted a phased approach which included extensive community participation. In 2003, the project achieved its aim of reducing domestic fuel burning emissions by 50%.

### **2.3.3. Offsetting Projects**

Air quality offsets are a mechanism through which polluting industries invest in reducing emissions from another source in exchange for leniency from complying with their own emission limits (Langerman et al., 2018). A pilot offset study conducted by Eskom in Kwa-Zamokuhle, Mpumalanga Province showed that air quality in the area was poor and that ambient air quality limits for PM were exceeded on most winter days (Matimolane, 2017). The study found that for PM<sub>2.5</sub>, domestic fuel combustion was a significant source, with vehicles and secondary particulates accounting for 13 and 8% of PM<sub>2.5</sub> respectively. The air quality monitoring further indicated that emissions from domestic fuel burning were trapped under the inversion layer, particularly on low wind days.

The pilot study implemented various interventions proposed by an EScience and Nova Institute study (2013) to reduce domestic fuel burning including insulation of houses, the use of a Trombe wall (a wall designed to absorb energy from sunlight) to store energy and replacement of coal stoves with an LPG system. Matimolane (2017) investigated the success of the interventions after installation and found that the use of a Trombe wall was not deemed successful, as the installation was 'unsightly'. The pilot study further found that an electricity subsidy was not effective. Existing roof leaks had a negative impact on the ceiling installation, which were replaced by polyurethane foam with gypsum ceilings. The study highlighted the need for public participation and effective communication with households, as the implementation of interventions was done on a voluntary basis.

Offsetting projects are ongoing and include the provision of LPG to communities, as discussed in Section 2.3.4, and further investigation into the insulation of housing units.

#### **2.3.4. Fuel switching**

Domestic emissions can be reduced by encouraging households to replace coal and biomass burning with cleaner fuels such as low smoke fuels and LPG. For low smoke fuels to be a viable alternative, they need to be socially acceptable to households as well as cost effective and must conform to technical requirements such as heat produced, speed of cooking and ease of ignition (Scorgie et al., 2001). Households were generally not opposed to switching to low smoke fuels, provided that the low smoke fuel should have similar heating characteristics to coal, should have a similar cost to coal and must be suitable for use in existing appliances. The study concluded that the cost of low smoke fuels would have to be substantially reduced to be a viable alternative to coal and that none of the fuels included in the study had all the required characteristics to be a suitable substitute for coal.

In a survey conducted by Mdluli et al. (2010), 28% of respondents indicated that they would utilize low smoke fuel if it burned longer than coal, produced the same amount of heat and also emitted less smoke, but that they would only consider purchasing such a fuel if they had seen and tested it.

The offsetting study by Eskom investigated switching coal fired stoves in households with LPG gas and equipment (Matimolane 2017). The study found that households preferred the LPG systems to the use of coal stoves with 90% of participants opting to continue using LPG. On the use of LPG, it has been noted that this intervention can only be successfully implemented if an LPG distribution network is in place, which was not the case in the study area.

Biogas can be utilized as a source of energy by the anaerobic digestion of organic waste. In addition to the production of biogas, fertilizer is produced as a byproduct with provides additional benefits to the use of biogas. Smith et al. (2012) conducted a financial and economic cost benefit analysis on the use of biodigesters in rural communities and found that, while biodigesters were not a financially feasible investment for rural households, there were substantial economic benefits attached to the use of biodigesters from a broader social point of view. The study found that lives saved due to improved air quality was a substantial benefit representing 65.8% of the economic benefit.

A desktop study was conducted by Msibi and Kornelius (2017) to investigate the feasibility of biogas use in South African households. The study estimated the average energy needs of a household, calculated the biogas required to satisfy the household's energy needs and estimated the amount of waste required to generate the required biogas. The study concluded that biogas was a feasible alternative for households with access to cattle and pig waste. It was estimated that approximately 625 000 households could potentially benefit from the use of biogas, based on the availability of feedstock waste. Due to the low volumes generated per household, it was found not to be feasible to feed biodigesters solely with chicken, human and food waste.

The review of a pilot study conducted in the Eastern Cape Province indicated that approximately 65% of the installed biodigesters were not operational, mainly due to failures as a result of lack of operator skill or the failure of the digester biology (GIZ, 2016). In a biodigester, the pH, category of organic feed material, frequency of feeding and water availability determine the health of the microbes and therefore optimal functioning of the biodigester. There is therefore a need for training and support to biodigester beneficiaries to operate the biodigesters optimally and reduce failure rates. The study also found that biodigesters were not cost effective and that most biodigester installations in rural areas were donor funded (Semelane, 2018).

### **2.3.5. Provision of new stoves**

Emission reductions can be achieved by replacing old, damaged and inefficient stoves with modern stoves with improved designs. Studies have indicated that bottom lit down drafting (BLDD) devices can be manufactured quite easily and be customized to suit the intended use. It was found that such devices run much cleaner than traditionally used imbaulas and had reduced CO emissions. It is also expected that the PM emissions would be reduced, but the reduction was not quantified by the study (Pemberton-Pigott et al., 1999).

An investigation by EScience Associates and the Nova Institute (2013) noted that the use of coal and wood has been steadily declining and cautions that interventions such as new efficient stoves might slow down this declining trend, highlighting the need to evaluate potential unintended consequences of any intervention. The 1996 and 2011 census data indicated that the proportion of households making use of solid fuels was decreasing in South

Africa during this period, however there remains pockets of households that are still reliant on solid fuel (Pauw et al 2020).

### **2.3.6. Energy efficient housing**

The South African Government supplies approximately 100 000 subsidized houses per year (National Treasury, 2018). Ideally, houses should be built to be as energy efficient as possible to reduce the need for space heating. In line with this, the norms and standards that government provided housing must conform to were adjusted in 2014 to include improved energy efficient measures (DEA, 2019). However, houses built prior to the implementation of these norms and standards were not designed to be energy efficient, although they could be retrofitted with ceilings and ceiling insulation as well as improved insulation (Friedl et al., 2008).

Dense low-income communities, where residential air pollution is more pronounced, include households living in informal housing or houses that are poorly insulated, which leads to these communities requiring relatively more energy input to achieve thermal comfort than middle income households (DEA, 2019).

A survey by the Department of Energy assessed the thermal efficiency of housing by using dummy variables such as the presence of damp, damaged or broken windows and doors and leaky roofs, amongst others to assess the dwellings surveyed (DOE, 2012). Using this approach, the study found that 42% of houses were found to be thermally inefficient. Households that had a lower living standard or were non-electrified had the highest rate of thermal inefficiency, estimated to be above 85%. Households in urban informal areas were estimated to have thermally inefficient housing of 66%. Approximately a third of formal housing was found to be thermally inefficient, while 86% of informal housing was classified as thermally inefficient.

A study conducted in three settlements on the South African Highveld investigated the potential to use thermal insulation retrofits to improve indoor thermal conditions in the dwellings by measuring the daily mean indoor temperatures of dwellings with different levels of insulation (Matandirotya et al., 2019). The study found that the dwellings which were insulated

had higher daily mean indoor temperatures when compared to dwellings that were not adequately insulated and that thermal insulation of housing could be utilized to improve thermal comfort of households (Matandirotya et al., 2019).

### **2.3.7. Addressing domestic fuel burning**

The electrification of South African households has increased significantly, with nearly 90% of all households having access to electricity (StatsSA, 2022). Despite the rollout of electricity provision, many households still utilize solid fuels in line with an energy stacking model. The number of households that utilise solid fuel is also likely to be underestimated by the National Census and the General Household Survey in which households only report the main energy carrier used for each purpose (Pauw et al., 2022)).

Various interventions have been implemented in South Africa to address the emissions from domestic solid fuel burning including top-down fire making (Wagner et al., 2005), fuel switching (Scorgie et al., 2001; Mdluli et al., 2010; Matimolane, 2017) and energy efficient housing (Matandirotya et al., 2019; Matimolane, 2017). Some of these interventions were done as part of offsetting projects (Matimolane, 2017). While the overall number of households using solid fuel may have decreased, there remain pockets of households that are reliant on solid fuel (Pauw et al., 2022; StatsSA, 2022).

## **2.4. POTENTIAL FOR THE USE OF ABATEMENT TECHNOLOGY**

### **2.4.1. Background review**

Investigations and research into the reduction in emissions from household appliances appears to have been largely focused on improving combustion efficiency and little information seems to be available on secondary measures or end of pipe type measures to reduce emissions. The use of secondary measures to reduce emissions from small combustion sources in Europe was found to be limited due to the high cost and maintenance requirements of such installations which were limited to the use of electrostatic precipitators (ESPs) (Amann et al., 2018).



A patent of the United States of America details the invention of a polymer based filter to remove particulate matter from a gas stream. The polymer filter was made up of small diameter fibers that could be manufactured in a variety of ways (US Patent, 2004). While such polymer based filters would not be suitable for the temperatures encountered in the flues of domestic fuel burning devices, the principle of using a fibrous material could be applied to a more heat resistant material.

A review study by Lim et al. (2015) investigated the use of emission reduction technologies for small scale installations. The study evaluated several technologies that had been tested such as the use of additives, catalytic filters, electrostatic precipitators as well as technologies from the automotive industry. The study concluded that most technologies were still under development and had experienced challenges on implementation. The use of ESPs were found to be prohibitively expensive and had an added safety concern due to the high voltages employed.

Cheng et al. (2018) investigated the use of high gradient magnetic separation in capturing airborne particles. The study utilized a permanent magnet core to capture particulates, which was preferable to electromagnets as they require little to no external power. The study did not utilize a matrix within the collector to improve the gradient of the magnetic field. The study investigated the capture efficiency of  $\text{Fe}_3\text{O}_4$  particles and NaCl particles as a function of particle size. The study concluded that the use of a matrix such as a steel mesh is required to effectively capture particles smaller than 50  $\mu\text{m}$ .

Li et al. (2007) investigated the aggregation of fine ash particles from coal combustion to increase removal efficiency from traditional particulate matter separators. The study tested three samples from different regions in China in a uniform magnetic field. The fly ash particulates had a size range of 0.023 - 9.314  $\mu\text{m}$ . The removal efficiencies were lower than expected at 53%, 43% and 14% with increased removal efficiency with increased Fe concentrations.

Messerer et al. (2004) investigated the use of a miniature counterflow pipe bundle heat exchanger to remove soot particulates from diesel fuel emissions. The heat exchanger cools the flue gas, which causes the soot particles to migrate to the surface of the heat exchanger

as a result of thermophoresis and deposit on the surface of the tubes. Particle deposition efficiencies were found to be up to 45%.

In another study, Yamamoto et al. (2013) investigated the use of a heated carbon fiber filter to remove soot particles from diesel combustion. Without heating the filter, particles would accumulate on the filter, reducing the porosity significantly. By increasing the filter wall temperature using an electric heater, the study found that most of the particulates could be burned off, resulting in continuous filter regeneration. The study indicated that, while most of the particulates were burned off in the filter, new ultra-fine particles of less than 30 nm were formed.

Hukkanen et al. (2012) investigated the use of a catalytic combustor in reducing emissions from a wood fired boiler. The catalyst utilized consisted of three levels of metal wire mesh covered with a platinum and palladium catalyst. The catalyst layers were inserted into the stack. Due to the additional unburnt compounds that were oxidized by the catalyst, the O<sub>2</sub> content of the flue gas was decreased and the temperature increased. The catalyst was effective in removing CO from the flue gas with an overall reduction as high as 80% during the burn out phase. For the entire combustion cycle, reductions of 21% for CO, 14% for organic gaseous carbon and 30% of PM<sub>1</sub> was achieved. In this case, the flue gas temperatures were high enough to activate the catalyst, but the study notes that some residential heaters may not have sufficiently high flue gas temperatures to achieve this. The catalyst used was not dense and initially had a low pressure drop, but the pressure drop increased significantly if the catalyst became blocked. Catalysts can also become deactivated in the presence of compounds that become attached to its surface. The study notes that the catalyst used was inadequate as it required continuous surveillance, had to be cleaned regularly and cannot be used at low temperatures.

Ozil et al. (2009) investigated the use of two catalysts, a cordierite honeycomb monolith support and a metallic corrugated structure impregnated with an alumina washout. The study showed that the temperature of the flue gas of a wood fired boiler was too low during start up and shut down for the catalyst to be effective, which is also when the concentrations of CO and VOCs were highest. The study investigated the use of a heating system to improve the activity of the catalyst when fuel gas temperatures were below 300°C, which was

found to dramatically reduce the emissions of CO and VOCs, with CO reduction between 80 and 90%.

Paulsen et al. (2019) investigated the use of a chimneyless cookstove equipped with a potassium titanite catalyst on a cordierite monolith to reduce emissions from wood cooking. The stove achieved a particulate matter emission reduction of 36% compared to a stove with a blank monolith and a 26% reduction relative to a stove with no monolith. The addition of a blank monolith increased particulate matter and CO emissions compared to a stove without a monolith which was attributed to less airflow through the stove, leading to a change in the air-fuel ratio.

Although the technologies investigated for use on small scale domestic combustion units have shown that emission reduction is possible, all of the technologies had associated limitations making them unsuitable for wide scale implementation. There is therefore a need to explore further opportunities to investigate various cost effective options for emission reduction technologies that can be used on small scale domestic combustion units. The development of an effective abatement technology requires that it should be suitable for use under local conditions and that considerations such as cost, acceptability of use to the end user, locally available domestic fuel burning devices, and fuel used locally.

#### **2.4.2. Abatement methods**

Flue gas typically has a low particle loading and the particles are small in size (Xu, 2014). Perry et al. (1997) refers to particulates from combustion processes as 'fumes' and notes that these particulates have a diameter of less than 1  $\mu\text{m}$ . In the design of a separator, the most important size related particle property is the dynamic behavior of the particle. Particles larger than 100  $\mu\text{m}$  can be collected using gravitational methods or inertial methods. For particles below 100  $\mu\text{m}$ , the viscous regime dominates and the most useful size specification is the Stokes settling diameter. For particles smaller than 1  $\mu\text{m}$ , the Cunningham correction should be applied to the Stokes diameter.

In selecting the appropriate separator type, particle size plays an important role (Mueller, nd). The most challenging particle size to capture is the 0.1 to 2  $\mu\text{m}$  size range, as the forces for deposition by inertia are small. Particle flocculation occurs in this size range and particles may be discrete or loosely attached clusters. The degree of flocculation depends on the

concentration of the particulates in the gas stream, which influences the collection efficiency of the separator (Perry et al., 1997).

Particulates can be removed from the flue gas stream using non-catalytic methods such as filtering or scrubbing. The PM emissions can also be reduced by oxidizing the organic precursors of secondary particulate emissions using catalytic oxidation. The catalytic and non-catalytic methods available are set out in Sections 2.4.1.1 and 2.4.2.2.

#### 2.4.1.1. Non Catalytic Methods

The basic steps for the collection of particles in a separator are as follows:

1. Collection of the particulates
  - 1.1. application of a force that separates the particles from the gas stream
  - 1.2. sufficient retention time for the particles to move to the collection surface
2. Retention of the particles on the collection surface
3. Removal of particles from the deposition surface

The basic principles by which separators operate are gravitational deposition, flow line interception, inertial deposition, diffusional deposition and electrostatic deposition. Particle removal can also occur through scrubbing or filtration. Conditioning methods such as acoustic agglomeration can be utilized to improve the collection efficiency of separators.

Within a flue or separator, various forces are exerted on a particle in a gas stream. Gravitational forces act vertically downward on a particle. The viscous effect of the gas opposes the particle motion and exerts a drag force on the particle. A particle will experience centrifugal force due to angular motion which is perpendicular to the direction of the particle motion. Particles of less than 0.1  $\mu\text{m}$  experience Brownian movement due to the collisions between gas molecules and particles (Perry et al., 1997).

Physical forces such as the gravitational force, drag forces and inertial forces act on particles in separators and are dependent on the particle size, shape and velocity as well as the gas stream's density and viscosity. The ratio between the viscous and inertial forces acting on a particle is described by the Reynolds (Re) number. The Re number determines whether the

inertial or viscous regime is dominant and therefore whether laminar or turbulent motion results (Perry et al., 1997).

The flue gas consists of a heterogeneous mixture of gas and solids/liquids. Heterogeneous mixtures are separated by using mechanical-physical forces such as gravitational, centrifugal, mechanical or kinetic forces. The separation of gas and solid/liquid streams typically utilize the following technologies (Sorsamäki and Nappa, 2015):

- Gravity settlers
- Impingement separators
- Centrifugal (cyclones)
- Filters
- Wet scrubbers
- Electrostatic precipitators

Gravity settlers utilize the gravitational force exerted on a particle to remove solids from a gas stream. The separators are appropriate for low gas flow (Perry et al. 1997). Gravitation settling separators are generally only effective for particles larger than 42  $\mu\text{m}$ , as the settling velocity for smaller particles will necessitate the use of an excessively large separator (Perry et al., 1997).

Impingement separators provide surfaces that intercept a particle or fluid such as wire mesh separators. These separators typically have large voids and can be designed such that the gas has to change direction while moving through the voids. Particles are captured mainly through impingement. Impingement separators are mainly considered liquid separators as solids, viscous or sticky liquids plug the voids which decreases the efficiency of the separator (Mueller, nd).

Centrifugal separators such as cyclones are widely used to separate solids from gas streams. Particulates move towards the outer wall of the separator as a result of centrifugal acceleration (Perry et al., 1997). The minimum particle size that can be separated from a gas stream depends on the the number of turns the particle makes and the velocity of the gas (Mueller, nd). The collection efficiency for particles smaller than 5  $\mu\text{m}$  is low (Perry et al., 1997). Due to the small size of the particulates, centrifugal separation will not be suitable for this application.

Air filters utilise diffusion, impaction and interception to capture particles and can be classified as surface filters and depth filters. A variety of surface filter designs are utilized including mesh and perforated plate filters. Depth filters can be further classified into high or low solid filters (Xu, 2014). Conditioning may be required to separate particles smaller than 6  $\mu\text{m}$  and a commonly utilized method is coalescence which makes use of a fiber mat or surface on which agglomeration occurs until particles are large enough to shear off back into the gas stream. A fine fiber such as fiberglass can collect small aerosol particles which agglomerate until larger particles or droplets shear off and are then collected by a separator capable of removing larger, agglomerated particles (Mueller, nd). The pressure drop over the filter is an important consideration, as flue gasses must be able to vent to the atmosphere to avoid flue gas leaks into houses. Due to the presence of tar-like substances, filtration is unlikely to be sustainable due to the potential clogging of the filters.

Wet scrubbers utilise a liquid, normally water, to collect particulates. A wide variety of scrubber types have been developed such as condensation scrubbers, entrainment scrubbers, venturi separators, spray scrubbers and packed bed scrubbers (Perry et al., 1997). Wet scrubbing results in a contaminated water stream that must be disposed of, which is not ideal for household use.

Electrical precipitators (ESPs) apply an electrostatic field to charge and collect particles. Precipitators can be single stage where ionization and collection are combined or two stage where ionization is followed by particle collection. The field strength applied to the precipitator determines the behavior of the particulates. Particulates can be collected on parallel plates which produce a uniform field or concentric cylinders that produce a higher field closer to the cylinder (Perry et al., 1997). ESPs require electricity to operate, which adds a significant cost to households. Furthermore, electricity may not be available to operate the ESP in unelectrified households.

For the size range of the particulates in the flue gas, gravity settlers and centrifugal separators will not be suitable due to the low collection efficiencies. Electrostatic separators are theoretically capable of collecting the particulates but require the application of an electric field. The separator will therefore only be functional when electricity is supplied to the unit, which may not be available and adds an additional cost to the household. The utilization of

a scrubber requires the use of a scrubbing liquid which will require the management and disposal of a contaminated liquid effluent, which is thus not ideal for domestic applications.

#### 2.4.1.2. Catalytic Methods

Particulate matter emissions could be reduced by the oxidation of the organic particulate matter precursors such as VOCs and soot. The oxidation of VOCs has been extensively studied and the modeling of VOC catalytic combustion is complex due to the variability in experimental conditions, particularly in the case of mixtures (Spivey, 1987). The mechanism for catalytic oxidation depends on the type of catalyst used. Three models have been proposed for the catalytic oxidation of VOCs, namely the Langmuir-Hinshelwood (L-H), Eley-Rideal (E-R) and Mars-van Krevelen (MVK) models (He et al., 2019). In the L-H model, the reaction occurs between adsorbed oxygen and adsorbed VOC. The E-R model assumes that the reaction occurs between an adsorbed species and a gas phase species. According to the MVK model, the reaction occurs between the adsorbed VOCs and the oxygen in the catalyst. The metal oxide is reduced and immediately reoxidized by oxygen from the gas phase. The oxidation of VOCs over metal catalysts are generally described using the MVK model.

For a catalyst to be effective, fouling and catalyst poisoning must be considered. Carbonaceous deposits can form on the catalyst causing fouling (Li et al., 2009). Oxidation intermediates were found to be the most significant source of catalyst deactivation. The catalyst active sites can also be poisoned by chlorides, sulfites, bromides and nitrides. The suitability of a catalyst depends on the reversibility of the deactivation to allow for the reactivation of the catalyst (He et al., 2019). In general, the presence of water in emissions inhibits catalytic VOC oxidation, although a hydrophobic catalyst support can be utilized to minimize the interaction of water at the catalyst surface (He et al., 2019). The efficiency of the catalyst is dependent on the catalyst support properties such as specific surface area, pore structure and hydrophobicity.

In a review of the recent advances in the catalytic oxidation of VOCs since 1990, He et al. (2019) noted that, although the oxidation of VOCs has been extensively studied, very few studies were conducted under real world conditions. The study further noted that catalytic performance, reaction kinetics and the oxidation mechanism could be different in practical

applications. The behavior of VOC mixtures can be different from the behavior of single component systems as their relative reactivities and behavior are dependent on factors such as catalyst type, components present in the mixture and reactions conditions.

Volatile organic compounds can be oxidized using supported noble metal catalysts and metal oxide catalysts. The most commonly used noble metal catalysts are either Pt or Pd on an  $\text{Al}_2\text{O}_3$  or  $\text{SiO}_2$  support (Spivey, 1987). The carbon atom of CO adsorbs onto the Pt surface and Spivey (1987) postulated that a similar mechanism is involved for other VOCs. Noble metal catalysts generally are more active than metal oxide catalysts, but metal oxide catalysts are more resistant to certain catalyst poisons such as halogens, As and Pb. Importantly metal oxide catalysts have a lower cost and can be sufficiently reactive for some applications (Huang et al., 2015).

Metal oxide catalysts can be grouped according to their conductivity. N-type semi-conductors have an excess of electrons present in their lattice structure. CO oxidation occurs via lattice  $\text{O}^{2-}$  followed by oxide regeneration. P-type oxides are electron deficient in the lattice. Oxygen adsorption occurs readily on p-type metal oxides as electrons can be removed from cations to form reactive species such as  $\text{O}^\cdot$ . Oxidation occurs through adsorption of  $\text{O}_2$  which forms  $\text{O}^\cdot$  and then reacts with adsorbed CO. Adsorbed  $\text{O}_2$  species are more reactive than lattice oxide ions and therefore p-type catalysts are more active (Spivey, 1987). Insulators have relatively low conductivity and are generally not active catalysts.

Heterogeneous supported catalysts can be synthesized using a number of techniques. Coprecipitation involves mixing the salts of the active metal and the support to precipitate a combined metal-support precursor. Deposition precipitation occurs when a precursor solution undergoes a change in pH, temperature or evaporation and a precursor with low solubility forms that deposits on the support. The support functions as a nucleation site for the precursor. Impregnation and drying involves contacting a porous support with a solution containing the metal precursor. Water is commonly used as a solvent with inorganic salts and organic solvents are used with organometallic salts. In the case of wet impregnation, an excess amount of solution is used. Volume impregnation or dry impregnation utilizes just the amount of solvent to fit the pore volume of the support due to capillary pressure. With melt infiltration, the metal or metal precursor salt is physically mixed with the support and heated to above the melting temperature of the metal or metal salt (Munnik et al., 2015).



The most effective single metal catalysts have been found to be oxides of V, Cr, Mn, Fe, Co, Ni and Cu (Spivey, 1987). Cr based catalysts are highly active for VOC oxidation, but the Cr toxicity is problematic for catalyst disposal. Ce oxide catalysts have also shown to be highly active for VOC oxidation including chlorinated VOCs (Li et al., 2009). The high activity of Ce oxide catalysts has been attributed to its high oxygen storage capacity and ability to shuttle between  $\text{Ce}^{3+}$  and  $\text{Ce}^{4+}$  (He et al., 2019).

Mn catalysts have been extensively studied as they have high activity, durability and low toxicity. Mn oxides can occur in different crystal phases and can have various oxidation states. The ability to change oxidation states increases catalyst activity due to the increased oxygen mobility. Previous studies have indicated that the most reactive Mn oxide catalyst is  $\text{Mn}_3\text{O}_4$  followed by  $\text{Mn}_2\text{O}_3$  and  $\text{MnO}$ , which correlates with the oxygen mobility of the catalyst. Catalyst activity can be enhanced by the addition of K, Ca or Mg. The reactivity of Mn oxide is highly dependent on the morphology of the catalyst, with studies indicating that well defined morphological Mn oxide catalysts were suitable for VOC oxidation (Huang et al., 2015).

Gao et al. (2020) investigated the impact of the crystal structure of Mn oxide catalysts on the catalytic oxidation of soot. Different Mn precursors (sulfates, nitrates, acetates) were used to prepare the catalyst. Manganese catalysts were manufactured using colloidal solution combustion synthesis with calcination temperatures ranging from 550 to 950°C to obtain different crystalline structures and an amorphous phase. The study showed that the soot conversion curves with Mn oxide catalysts shifted to lower temperatures compared to non-catalysed reactions and that the amorphous Mn oxide catalyst was more active for soot oxidation which was ascribed to the low temperature reducibility of the catalyst, the abundance of  $\text{Mn}^{4+}$  ions and the increased surface oxygen availability. The soot conversion percentage was temperature dependent and increased at temperatures above 250°C. The soot particulates studied had a diameter of >25  $\mu\text{m}$  which exceeded the catalyst pore diameter, which can be addressed by creating mesopores or micropores. The Mn oxide catalysts were also effective in oxidizing NO with the maximum oxidation (over 50%) occurring at 350°C. Soot oxidation was further found to be enhanced when NO was present as was previously reported in literature.

Liu et al. (2017) used a Fe wire mesh to serve as a nucleation site for Mn-Fe bimetal oxides through growth on the Fe metal sites. Different morphologies were achieved by changing the Mn:Fe ratio. The catalysts were prepared using a water bath deposition method with urea and the precursors formed were calcined for four hours at 500°C. Ferric nitrate tetrahydrate was used as the source of Fe ions and manganese acetate tetrahydrate provided the Mn ions. The catalyst produced had good stability attributed to the good adhesion between the bimetal oxides and the wire mesh and was used in the selective catalytic reduction of NO to N<sub>2</sub>.

Augustin et al. (2015) utilised manganese acetate tetrahydrate and tetra ethylene glycol (TEG) in ethylene glycol (EG) to produce precursors that were calcined at different temperatures and under different atmospheres. Small particle sizes of less than 100 nm were reported and attributed to the use of tetra ethylene glycol and the relatively mild reaction conditions. The study found that the structure and morphology of the crystals produced depended on the calcination temperature as well as the Ar or O<sub>2</sub> atmosphere. The precursors were calcined under Ar flow for 2 hours at 350°C and 550°C to produce Mn<sub>3</sub>O<sub>4</sub> and α-Mn<sub>2</sub>O<sub>3</sub> respectively. To produce Mn<sub>5</sub>O<sub>8</sub> the precursor was calcined for five hours under O<sub>2</sub> flow. No further laboratory or field tests were conducted as part of the study.

Li et al. (2011) utilized polyethylene glycol (PEG) and KMnO<sub>4</sub> in distilled water to synthesize Mn<sub>3</sub>O<sub>4</sub> nanooctahedral shaped particles. The polyethylene glycol acted as the reducing agent as well as a “structure-directing” agent. The nanoparticles formed had an octahedral shape, a size of approximately 150 nm and a Mn/O ratio of 0.74. The PEG reduced the Mn<sup>7+</sup> to Mn<sup>4+</sup> or Mn<sup>3+</sup>. The PEG also reduced the random aggregation of nanoparticles and tailored the morphology of the nanoparticles. The concentration of the PEG as well as the reaction temperature was found to determine the role of the PEG in the reaction system. Lower PEG concentrations (less than 10%) resulted in fast aggregation of the nanoparticles. At 100°C the particles formed were nanorods and at a temperature of 180°C the nanoparticles transformed into a pseudo spherical shape. Samples were taken during the duration of the synthesis to determine the crystal growth evolution. The study found that the crystal growth followed a self-assembly mechanism followed by Ostwald ripening. The catalyst was tested for photodecomposition activity and it was found that the photocomposition activity of the Mn<sub>3</sub>O<sub>4</sub> nano-octahedra was superior to that of commercially available Mn<sub>3</sub>O<sub>4</sub> powders.

Liu et al. (2010) synthesized manganese oxide nanoplates with different shapes by using different organic additives in a polyol-based process. The nanoparticles were synthesized using manganese acetate and ethylene glycol with an organic additive. The precursors were calcined to produce  $Mn_2O_3$ . The reaction was performed at  $195^\circ C$  using 0.5 g of manganese acetate and 50 mL of ethylene glycol as well as an organic additive to control the shape of the particles formed. The suspension was heated for 30 min and a white precipitate formed after 10 min. The precipitate was rinsed with ethanol and calcined at  $500^\circ C$  for 2 hours. Nanoplates were formed when polyvinyl-pyrrolidone (0.4 g) was used and hexagonal nanoplates were formed when polyethylene glycol (5 mL) was added to the reaction. The study noted that the morphologies of the precursors were preserved when calcined and that the shape and size of the precursors did not change appreciably. The catalyst efficiency was not tested as part of the study.

A study by Sukhdev et al. (2020) also found that the morphology of the nanoparticles formed depended on the addition of a polymer such as polyethylene glycol, polyacrylamide, polyvinyl alcohol and so forth as reducing agents. The concentration of the polymer and the reaction temperature regulate the morphology of the nanoparticles formed.

Wojnarowicz et al. (2016) synthesized manganese doped ZnO nanoparticles using zinc acetate dihydrate and manganese acetate tetrahydrate using ethylene glycol as a solvent. Ethylene glycol was chosen as a solvent as it has weak reducing properties which prevents the precipitation of foreign phases caused by the change in the oxidation state of the  $Mn^{2+}$  ions. The particles formed had a spherical shape and the size of the particles decreased with increased dopant concentrations. The use of ethylene glycol therefore prevented a change in the oxidation state of the  $Mn^{2+}$ .

The polyol method is a well-known synthesis method involving dissolving a metal precursor in a poly alcohol such as a glycol solvent and heating the reaction solution to a refluxing temperature to produce metallic nanoparticles (Benseeba, 2013). The glycol functions as both the solvent for the precursor and the reducing agent during the synthesis. The glycols are further able to control particle growth by controlling nucleation, growth and agglomeration of the particles. The high boiling points of the glycols further allows higher synthesis temperatures required to form certain metal nanoparticles. Various polyalcohols are suitable

for polyol synthesis such as ethylene glycol, propylene glycol, tri ethylene glycol and tetra ethylene glycol, amongst others, and the selection of the appropriate reagent is dependent on the reaction temperature required and the reduction potential of the solvent (Rao et al., 2017).

Soot has complex physiochemical properties that depend on the fuel, combustion conditions and combustion device. Therefore, laboratory testwork typically uses model soot samples with uniform characteristics which differ from real world soot emissions, which have higher volatile, ash and moisture contents which can affect oxidation characteristics (Khaskheli et. al. 2022). Tests on gaseous pollutants such as CO typically investigate the oxidation of single component systems, however oxidation properties may differ in the case of a multi component system as will be the case in practical applications, where the flue gas is likely to contain a mixture of soot, and gaseous inorganic and organic pollutants. This was illustrated in a study conducted by Dos Santos et. al. (2014) which investigated the oxidation of a multicomponent system consisting of CO, hydrocarbons and soot using a Ce-Zr-Nd mixed oxide catalyst. The study showed that for the less active catalysts, there was a net increase in CO concentrations, as the catalyst was not active enough to oxidize the CO resulting from soot combustion. The multiple chemical components in the emissions may compete for active sites on the catalyst that can result in further inefficiency.

Volatile organic compounds can be oxidized using supported noble metal catalysts and metal oxide catalysts. Although noble metal catalysts are generally more active, metal catalysts are cheaper to manufacture and may still achieve an acceptable level of activity. The most effective single metal catalysts have been found to be oxides of V, Cr, Mn, Fe, Co, Ni and Cu. Of these, a Mn catalyst was selected for use in this study due to its low toxicity and low raw material cost. Mn particles can have different crystal structures and oxidation states, which have an impact on the catalytic activity towards oxidation of VOCs, which are precursors of organic particulate emissions. The polyol catalyst synthesis method described by Augustin et al. (2015) utilizes affordable reagents and mild reaction conditions to produce manganese oxide particles. The technique is also capable of producing Mn particles with varying structures and compositions and was therefore utilized in the synthesis of the catalyst in this study.

### 2.4.3. Abatement Design

Due to the expected size distribution of the emissions, non-catalytic methods are unlikely to achieve the design objectives as discussed in Section 2.4.2.1. The use of catalytic abatement technology is relatively understudied in South Africa, but has been investigated in other parts of the world (Paulsen et al., 2020). There is therefore a potential use for abatement technologies in the South African context to supplement the interventions already investigated and implemented.

Although catalytic methods have not been widely utilized in practical domestic applications, studies have shown effective soot reduction during laboratory testing (Gao, 2020). A base metal catalyst was used in this study due to the lower relative cost of required reagents compared to precious metal catalysts. Manganese was selected due to the results achieved with laboratory testing using soot Temperature Programmed Reduction (TPR) (Gao, 2020). Three catalyst preparation techniques were tested namely deposition precipitation, wet deposition and dry deposition, as further detailed in Chapter 3.

Data on the emission factors for various fuels from a range of studies reported in the literature was compared in Section 2.2.1. The results indicate that particulate loads of approximately 7.5 g/kg fuel can be expected for coal fired stoves and 2.75 g/kg for wood fired stoves. The loads provide an indication of the expected loading, but the loading will be dependent on the fuel type and stove type used. The emissions are expected to be dependent on combustion conditions and operator behavior and as such are expected to vary. Emissions are also expected to vary during the different stages of the combustion process. As the abatement will be in operation during the entire combustion cycle, it must accommodate the emissions from the combined combustion cycle.

The particulate matter emissions are expected to be comprised mainly of organic particles, soot and inorganic fly ash, which may react with each other and gaseous emissions in the combustion chamber and flue. The temperature of the flue gas, which is likely to depend on the positioning of the abatement device, will influence the catalyst efficiency as well as the aging of the particulates and their properties. Closer to the combustion chamber, sticky, tarry carbonaceous particles may form (Makonese et al., 2019). Various other chain like or cluster like particulates are also likely to be present (Forbes, 2012) as well as organic particles with

inorganic inclusions. A smaller fraction of inorganic fly ash emissions is expected, which may be larger in size than the organic particles (Zhang et al., 2018; Makonese et al., 2019).

The particulates are expected to be 95% PM<sub>2.5</sub> (Zhang et al., 2018; Fletcher et al., 1997), although larger carbonaceous soot particles can be expected from coal combustion with sizes varying between 5 µm and 100 µm (Fletcher et al. 1997; Makonese et al., 2014).

In order to be considered effective, the designed catalyst should conform to various safety and performance criteria. The catalyst must further be acceptable to the end user. It is expected that the requirements of an end of pipe technology for emission reduction from a domestic fuel burning device would preferably need to meet the following requirements and considerations:

- acceptable emission reduction
- acceptable to end users
- ease of installation
- safety (heat resistant, no release of fiber particles and use of non-toxic materials)
- installation possible on non-standard domestic combustion units
- cost effective
- light in weight
- low or no electricity requirements
- cleaning mechanism that is either automated/automatic or easy
- high air flow
- low pressure drop
- limited clogging or particle build up.

In order to utilise the catalyst in a domestic stove, the catalyst must be suspended on a catalyst support structure. The choice of the catalyst support structure considered the above requirements, particularly the requirements related to high air flow, low pressure drop, limited clogging and ease of installation and customisability.

## CHAPTER 3: EXPERIMENTAL METHODS

This chapter describes the approach that was followed to address the objectives of this research. The chapter sets out the catalyst synthesis methods utilized, followed by the methodology for investigating the catalyst structure, morphology and composition. The chapter further outlines catalyst field testing methodology and the flue gas particulate measurement methodology utilized to determine the efficacy of the catalyst.

### 3.1. PROTOTYPE ABATEMENT PRODUCTION

In order to be utilized in the cast iron stove, the manganese oxide catalyst was synthesized on a catalyst support base. A stainless steel mesh was used as catalyst support and the catalyst was prepared on the catalyst support using in-situ deposition, wet impregnation and dry impregnation. Once prepared, the catalyst was placed in the stove for field testwork. Further information on the catalyst synthesis is provided in Section 3.2.

The choice of the catalyst support was based on the risk of clogging, ease of installation, pressure drop, high air flow through the catalyst and cost amongst other parameters. A coarse 0.5 mm thick steel mesh was thus used as the catalyst support as shown in Figure 3.1.

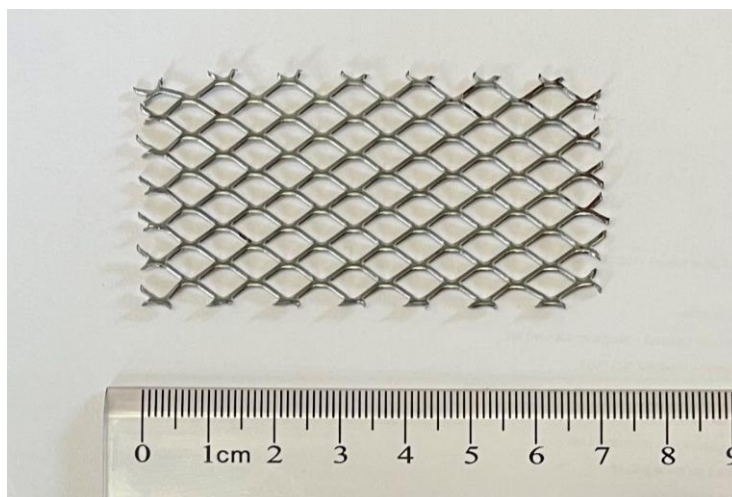


Figure 3.1. 0.5 mm thick steel mesh used as catalyst support

### 3.2. EXPERIMENTAL

Figure 3.2 provides an overview of the testwork conducted. Catalyst development testwork was done to determine the optimal method for the catalyst synthesis. Once the catalyst synthesis method was developed, the bulk catalysts were prepared and tested in a domestic stove. The detailed experimental plan is shown in Figure 3.3.

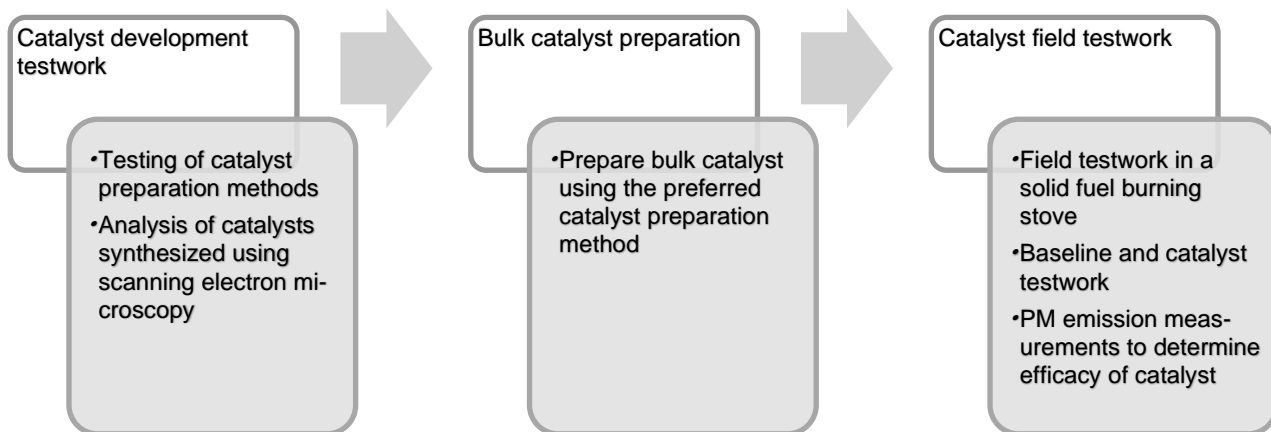


Figure 3.2. Experimental design



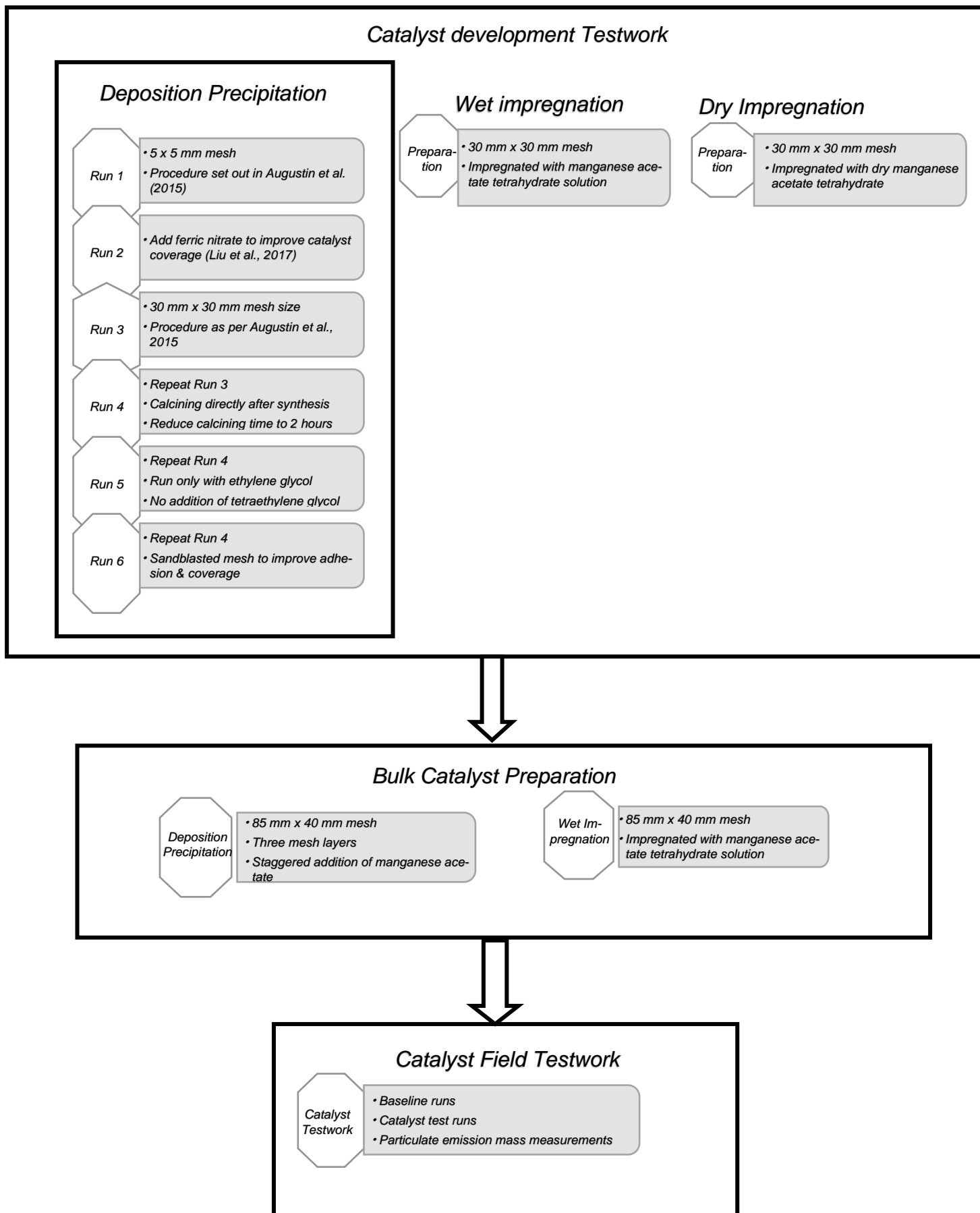


Figure 3.3. Overview of the experimental design

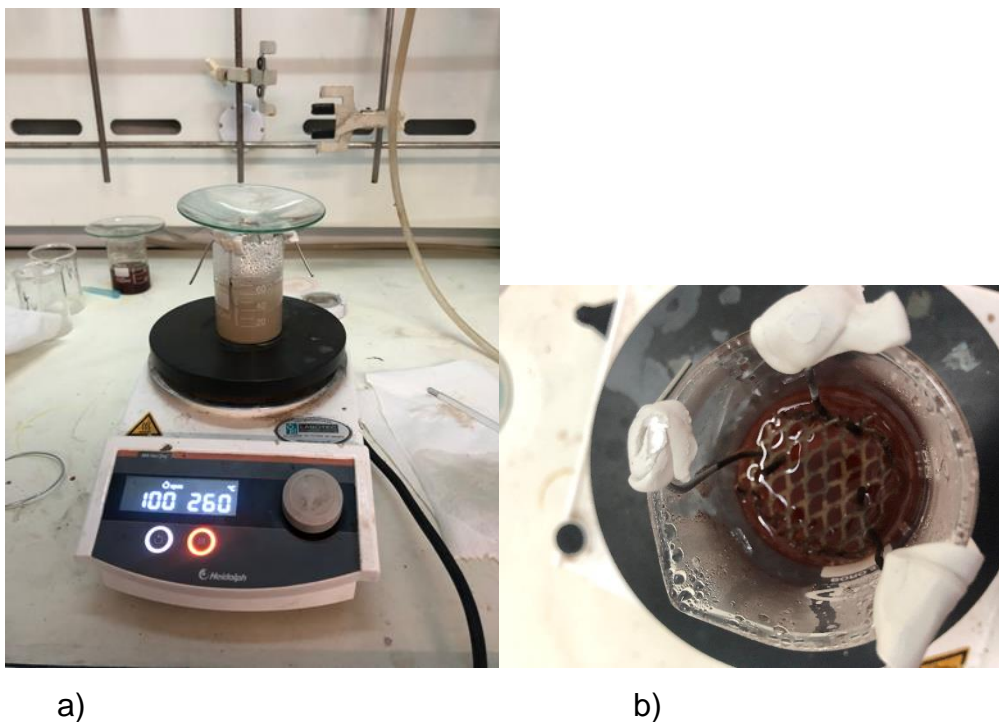
### 3.2.1. Catalyst development testwork

In order to determine the most suitable catalyst preparation method, catalysts were synthesized using precipitation, wet impregnation and dry impregnation techniques.

#### 3.2.1.1. Synthesis using Precipitation

A synthesis method based on that described in Augustin et al. (2015) was utilized to prepare the catalyst. This method was preferred due to the mild reaction conditions and the relatively low cost of the required reagents. Manganese (II) acetate tetrahydrate (>99%), tetraethylene glycol (99%), iron (III) nitrate nonahydrate (>98%) and ethylene glycol (>99%) were obtained from Sigma-Aldrich (South Africa). All reagents were used as received.

Typical test conditions were as follows: The reaction solution was prepared by dissolving manganese acetate tetrahydrate and tetraethylene glycol in ethylene glycol as detailed in each test run described below. The catalyst support mesh (commercially available 0.5 mm thick steel mesh obtained from Leroy Merlin Hardware Store) was rinsed using acetone prior to synthesis. The mesh was then suspended in the reaction solution using wire hooks secured to the beaker using rubber-based putty adhesive as shown in Figure 3.4. The mixture was then gradually heated on a magnetic stirrer hot plate (Heidolph, Germany) and stirred using a magnetic stirrer. The temperature of the reagent mixture was measured manually using a thermometer. The reagent solution was gradually heated to a temperature of 170°C to achieve the temperature required for the desired chemical reaction to occur. The catalyst which formed on the mesh substrate was removed from the reaction solution after precipitation occurred at 170°C and was rinsed with ethanol (>98%, Sigma-Aldrich). The samples were dried under argon (99.9%, Afrox) and were then transferred to a muffle furnace (Lenton, South Africa) at 550°C for five hours to calcine under stagnant air.



a)

b)

Figure 3.4. Catalyst preparation setup for precipitation tests a) side view and b) top view

In Test Run 1 a small piece of mesh (5 mm x 5 mm) was suspended in the reaction solution to determine whether the precipitate would form on the untreated mesh. 0.5 g of magnesium acetate was dissolved in 60 mL of ethylene glycol and 6 mL of tetraethylene glycol. The reaction solution was heated and stirred using a magnetic stirrer. At 120°C a brown precipitate formed which disappeared upon further heating. The mixture was heated for approximately 3.5 hours until a temperature of 170°C was reached and a light colored precipitate formed, likely manganese (II) oxide on account of the light pink colour. The reaction solution was left to cool and the precipitate was filtered using a Buchner funnel. The wire, mesh and precipitate were rinsed using ethanol and dried under argon gas. The precipitate, wire and mesh were calcined under stagnant air in a Lenton muffle furnace (Figure 3.5) at 550°C for five hours.



Figure 3.5. Samples were calcined in a Lenton muffle furnace

To increase coverage of the mesh, ferric nitrate (0.2 g) was added to the reaction solution in Test Run 2 and the same procedure was followed. The use of ferric nitrate was to provide Fe ions to produce a bimetal oxide with better adherence to the metal, similar to the study by Liu et al. (2017).

In Test Run 3, the procedure used for Test Run 1 was repeated using a larger piece of mesh (30 mm x 30 mm). To increase coverage, the surface of the mesh was roughened using sandpaper. The mesh was suspended in the reaction solution and secured using a putty like adhesive to minimise movement of the mesh. The reaction solution was heated and again turned brown at 120°C. The mixture was heated further and a light precipitate formed at 170°C after heating the reaction solution for 2 hours. The temperature was maintained at 170°C for a further two and a half hours. The reaction solution was left to cool and the precipitate was filtered. The mesh and precipitate were rinsed using ethanol and dried using argon gas. The light pink colored precipitate was left to dry overnight and turned dark brown in colour. Thereafter, the mesh was calcined at 550°C for two hours.

To determine whether morphological changes occur when the sample is exposed to air, Test Run 4 was conducted using the same procedure and mesh size as Test Run 3. After formation of the precipitate after 3 hours, the sample was removed from the reaction mixture, rinsed with ethanol and directly transferred to the furnace for calcining at 550°C for two hours. In order to improve catalyst adherence, the manganese acetate used was increased to 1 g.

To determine the impact of the tetra ethylene glycol (TEG) on the morphology and adherence of the catalyst to the mesh, Test Run 5 was conducted using the same procedure and mesh size as Test Run 4 without the addition of the TEG. The colour changes were similar to those observed during Test Run 1. The precipitate started forming once a temperature of 170°C was reached after two hours. The mesh was removed from the solution the next day, rinsed with ethanol, dried and calcined at 550°C for two hours.

In order to determine the impact of surface roughness on precipitate coverage, the mesh sample (30 mm x 30 mm) was sandblasted for Test Run 6 and the same procedure was followed as for Test Run 1. An overview of the experimental design is provided in Figure 3.3.

#### 3.2.1.2. Synthesis using wet and dry impregnation

Diefallah (1991) studied the kinetics of the thermal decomposition of manganese acetate tetrahydrate using isothermal and thermogravimetric techniques. The analysis indicated that the manganese acetate tetrahydrate loses water in two stages at temperatures slightly above room temperature to form an anhydrous salt. At a temperature of approximately 320°C the anhydrous salt decomposes to MnO with losses of CO<sub>2</sub> and acetone (Diefallah 1991, 2).

To produce the wet impregnation catalyst, a solution of 30 mL of deionized water (DI, 9.2 µS/cm<sup>3</sup> from a Milli-Q water purification system (Millipore, Bedford, MA, USA)) and 5 g of manganese acetate tetrahydrate was prepared and the sandblasted mesh dipped in the solution. The mesh was calcined directly for two hours at 400°C to form MnO (Diefallah 1991). The coating of the mesh was improved where the reaction solution pooled on the surface.

To produce the dry impregnation catalyst, the mesh was physically mixed with dry manganese acetate tetrahydrate and calcined at 550°C for two hours.

### **3.2.2. Bulk catalyst synthesis**

Two bulk catalysts were produced using deposition precipitation and wet impregnation. The deposition bulk catalyst was synthesized using 300 mL of ethylene glycol and 2.5 g of manganese acetate. Three 0.5 mm steel mesh sheets of a larger size that can be installed in the flue of the cast iron stove (85 mm x 40 mm) were suspended in the reagent mixture and the same procedure as Test Run 5 was followed without addition of TEG. When a temperature of 170°C was reached, a precipitate formed as shown in Figure 3.6. 2.4 g of additional manganese acetate was added the reaction solution in 0.8 g aliquots every 15 minutes. The precipitate which formed settled and did not remain in suspension. The mesh was removed from the reaction solution, rinsed with ethanol, dried under argon gas and calcined for two hours at 550°C.

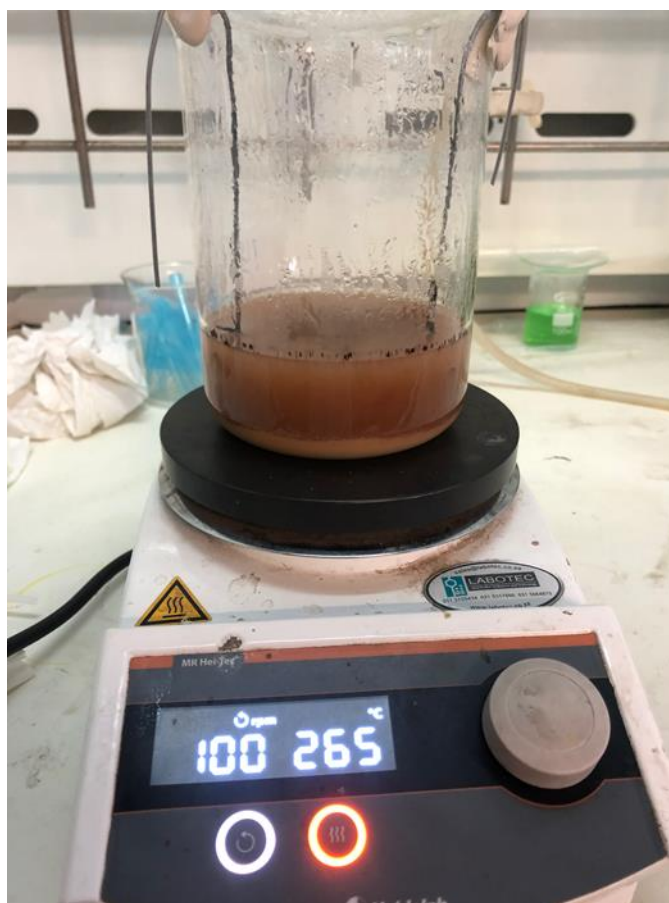


Figure 3.6. Reagent mixture at a measured temperature of 170°C. Precipitate can clearly be seen at the base of the beaker

The wet impregnation catalyst was synthesized using a concentrated solution of deionized water and manganese acetate tetrahydrate as described in Section 3.2.1.2.

### 3.3. Catalyst testwork

The experimental setup consisted of a one plate combustion device with a flue. The device used was a commercially available design with one cooking plate (Ndebele Appliances and Coal Stoves, Bronkhorstspuit, South Africa), which is representative of cooking stoves available in South Africa. The catalyst was positioned at the base of the flue where the highest flue temperatures were expected, as the catalyst efficiency is temperature dependent as discussed in Section 2.4.1.2. The experimental setup is shown in Figure 3.7. A flue or chimney was utilized to enhance the reproducibility of the sampling even though stoves without flues may also be in use in South Africa.

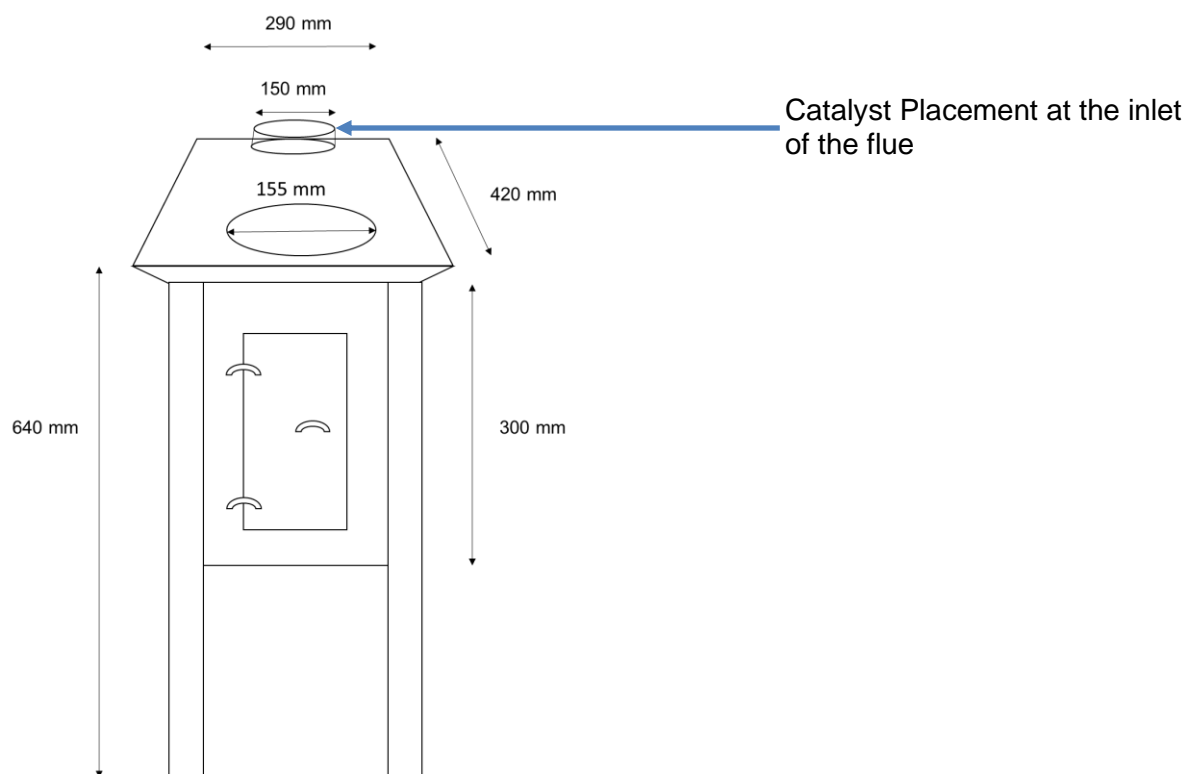


Figure 3.7. Experimental setup showing the stove and positioning of the catalyst

Baseline and catalytic test runs were conducted as shown in Table 3.1. Four baseline, three catalyst run repeats using the deposition catalyst, and one comparative catalyst test run using the wet deposition catalyst were conducted. A catalyst hot run (Filter #6) was conducted by sampling only during the flaming phase of the run to exclude the emissions resulting from ignition and flame out. Filter #2 was utilised as a field blank.



Table 3.1. Test Runs conducted

<b>Test Run</b>	<b>Type</b>	<b>Filter #</b>
Baseline 1	Baseline - Repeat 1	3
Baseline 2	Baseline - Repeat 2	4
Baseline 3	Baseline - Repeat 3	10
Baseline 4	Baseline - Repeat 4	1
Catalyst 1	Bulk Catalyst produced using deposition - Repeat 1	7
Catalyst 2	Bulk Catalyst produced using deposition - Repeat 2	8
Catalyst 3	Bulk Catalyst produced using deposition - Repeat 3	9
Catalyst Wet Impregnation	Bulk Catalyst produced using wet impregnation	5
Catalyst Hot Run	Bulk Catalyst produced using deposition - Sampling only during flaming phase of combustion	6

For each test run 100 g of soft wood sticks approximately 150 mm in length and 20 mm diameter were utilized and the combustion process was started using a single wax based firelighter ball. The wood was positioned in the same stacked manner for each run with the firelighter ball positioned in the middle. A single batch of wood purchased from a local hardware store was used to ensure consistency in composition. The soft wood was selected as fuel to improve the reproducibility of the test runs as the wood is more homogenous in size and composition when compared to hard wood or coal. The test runs were conducted under similar ambient conditions (ambient temperature, wind speed and precipitation) at the same time each day to improve reproducibility. The fuel used for the runs was sized, weighed and bagged and stored indoors to reduce fuel variability and to ensure consistent fuel moisture content. All the test runs were conducted over a two week period to ensure that tests were conducted within the same season and to limit any changes to the composition of the wood and firelighter balls. The runs were sampled over the entire combustion cycle from ignition

to extinction. For the Catalyst Runs, the catalyst was secured at the bottom of the flue as shown in Figure 3.8.



Figure 3.8. Catalyst secured at flue inlet to optimise the reaction temperature

### 3.4. Measurement methodology

Particulate concentrations were collected for gravimetric analysis using 37 mm styrene cassettes, as shown in Figure 3.9, with 37 mm polytetrafluoroethylene (PTFE) filters with a pore size of 2  $\mu\text{m}$  (Environmental Express, Charleston, South Carolina, USA). PTFE filters were selected as they are temperature resistant up to 260°C. A Gilian (GilAir Plus) personal sampling pump was used to collect particulates onto the filters at a sampling flow rate of 600  $\text{cm}^3/\text{min}$  for 10 min. A flow rate of 600  $\text{cm}^3/\text{min}$  was selected as it provided a stable flow rate with the filter in place. Ten cassettes were prepared using the method described in Appendix A. Sample filters were weighed using a Mettler Toledo microgram analytical balance in a temperature and humidity controlled environment as shown in Figure 3.10, using the procedure set out in Appendix B. Particulate matter was collected to provide a relative measure of the particulate matter emissions and was intended to provide an initial screening of the potential efficacy of the catalyst. Sampling was conducted over the entire burn sequence and commenced as soon as the firelighter was lit. It should be noted that the wood selected ignited within seconds of the firelighter being lit.



Figure 3.9. Three piece 37 mm styrene cassette



Figure 3.10. Measurement of PTFE filters using a Mettler Toledo microgram analytical balance

The flue gas flow rate was measured using a vane type Benetech GT8907 digital anemometer (Benetech, China). The flue external temperature was measured using an infrared thermometer (Shenzen FLUS Technology Company, China). The measurements were conducted at the base of the flue to ensure that the catalysts were exposed to similar temperatures across test runs. Particulate matter measurements were taken at 290 mm from the flue exit point to allow for the cooling of the flue gas to protect the equipment from damage. The measurement position is shown in Figure 3.11.

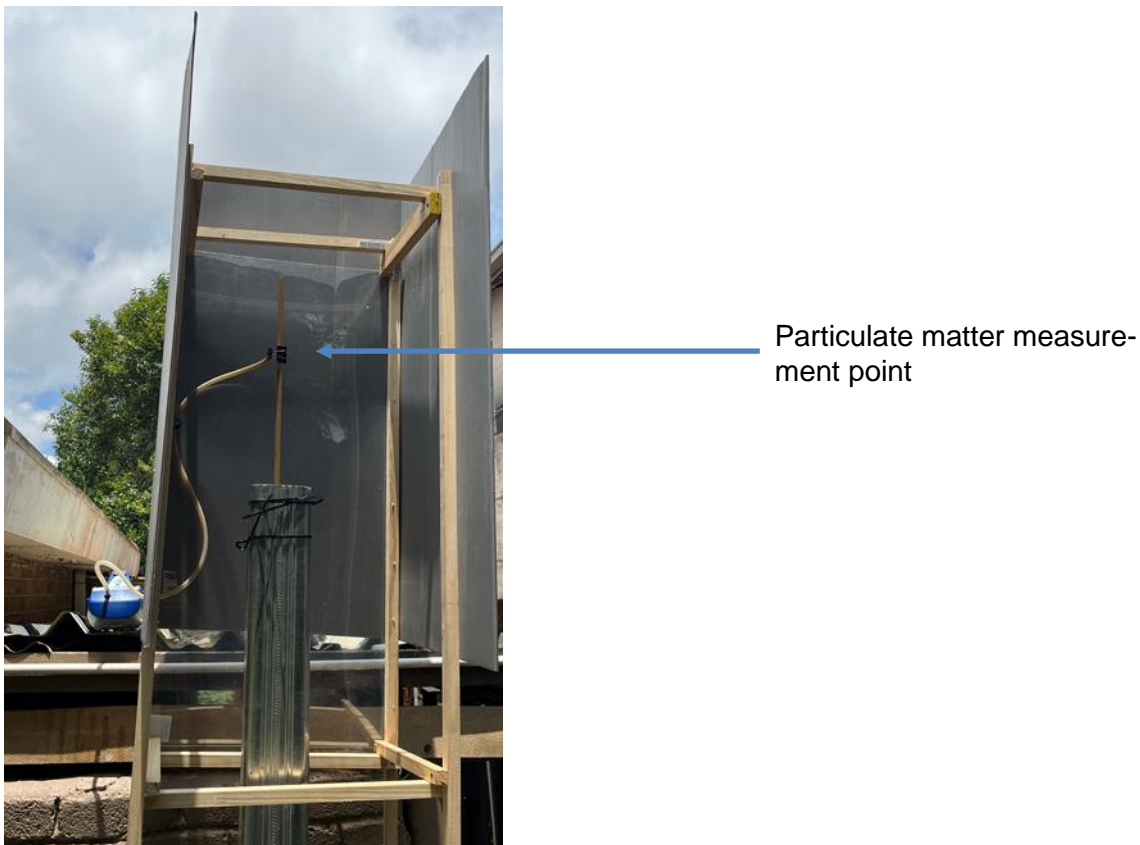


Figure 3.11. Flue gas measurement in the plume above the flue gas exit point

### 3.5. Characterization methodology

The catalyst samples produced were examined using Scanning Electron Microscopy (SEM) using a Zeiss Crossbeam 540 SEM at 20 kV to determine the morphology and particle size of the catalyst and to determine the catalyst coverage on the mesh substrate.

The filter samples were examined using the same instrument at 2 kV. A section of the center part of each filter was removed using a steel blade, mounted on an aluminum stub and sputter coated using Au to improve conductivity.

The catalyst samples were analysed using Energy Dispersive X-Ray (EDX) (OXFORD Link-ISIS-300 Zeiss, Germany) analysis to determine the semi-quantitative composition of the catalysts. The analysis was conducted on the entire mesh to investigate the catalyst coverage over the entire area of the mesh.

### 3.6. Quality Control and Assurance

A limited number of test runs were performed to serve as an initial screening to determine whether the catalyst was able to reduce particulate matter emissions, as set out in Section 3.3. In order to compare the baseline runs and catalyst runs, various quality control measures were taken to improve reproducibility of the tests. The tests were conducted under similar ambient conditions (ambient temperatures and wind speed) to ensure similar plume dispersion conditions. A single batch of wood fuel was used and the samples were weighed, bagged and stored indoors to maintain the wood moisture content. The wood sticks used were of similar shape and size and stacked in a consistent manner during testwork. The temperature at the base of the flue was measured to ensure that the catalyst was exposed to similar operating temperatures across the test runs. A wind box was utilized to minimize disturbance of the plume during sampling and particulate measurements were taken at a fixed sampling point as indicated in Figure 3.11.

A Gilian (GilAir Plus) personal sampling pump was used to collect particulates onto the filters and a flow rate of 600 cm<sup>3</sup>/min was selected as it provided a stable flow rate with the filter in place. The flow rate was checked using a bubble flow meter.

The procedure followed for the preparation of the cassettes is set out in Appendix A. Sample filters were weighed using a calibrated Mettler Toledo microgram analytical balance in a temperature and humidity controlled environment using the procedure set out in Appendix B.

## CHAPTER 4: RESULTS AND DISCUSSION

This chapter presents the results of the catalyst synthesis testwork and bulk catalyst preparation runs. The chapter further describes the results of the catalyst testwork in a household scale solid fuel stove.

### 4.1. CATALYST DEVELOPMENT TESTWORK

Samples of the catalyst were prepared as detailed in Sections 3.3.1 and 3.3.2. Catalyst preparation test runs were conducted to determine the appropriate procedure for the preparation of the bulk catalysts. Catalysts were prepared using precipitation, wet impregnation and dry impregnation.

#### 4.1.1. Synthesis using precipitation

The six catalyst synthesis runs using precipitation were conducted as described in Section 3.3.1.1. An example of the mesh samples before and after calcining are shown in Figure 4.1. The catalyst turned from a light pink colour to a black colour during calcination.

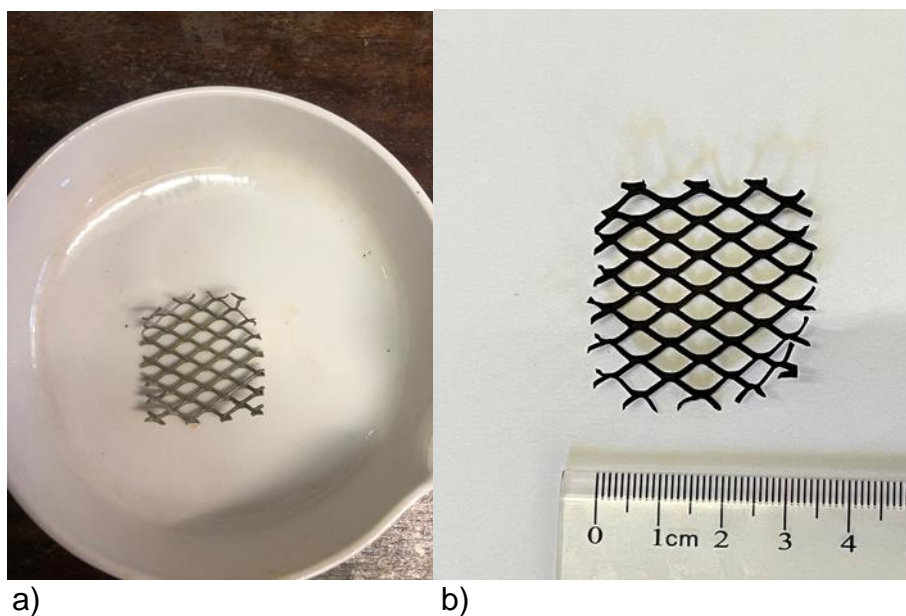
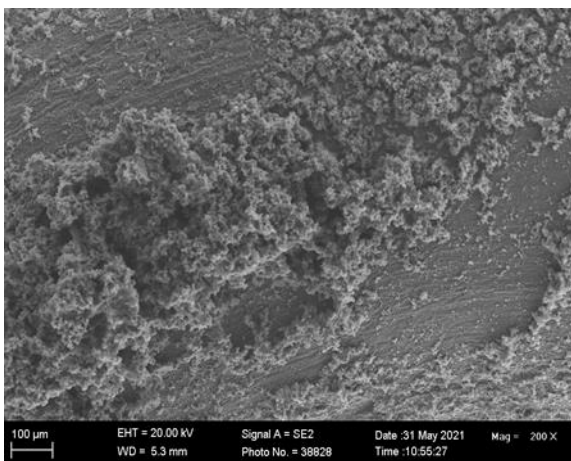


Figure 4.1. Mesh with precipitate before (a) and after (b) transfer to the muffle furnace

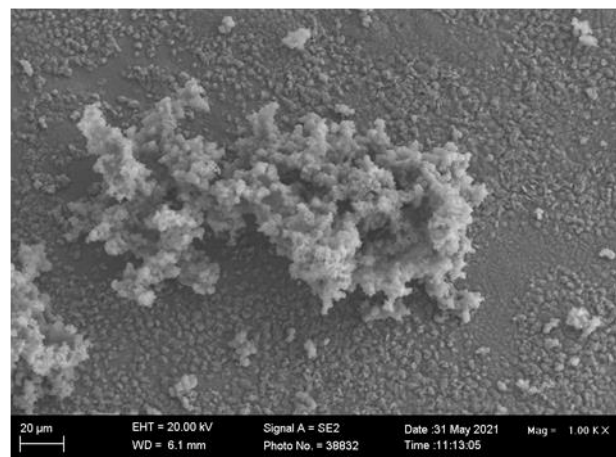


#### 4.1.1.1 Test Run 1

Test Run 1 utilised the synthesis methodology as set out in Augustin et al (2015) utilizing a 5 x 5 mm piece of mesh suspended in the reagent mixture. On parts of the mesh and wire, precipitate formed in clusters as evident from the SEM micrographs shown in Figure 4.2. At 10000 X magnification, clusters of spherical particles could be seen as shown in Figure 4.3. Although the precipitate formed on the wire mesh, the precipitate was patchy and did not cover a large percentage of the mesh surface.



a)



b)

Figure 4.2. SEM micrographs of the product of Test Run 1 utilising precipitation synthesis showing the precipitate formed on the wire mesh sample (200 X (a) and 1000 X (b) magnification)

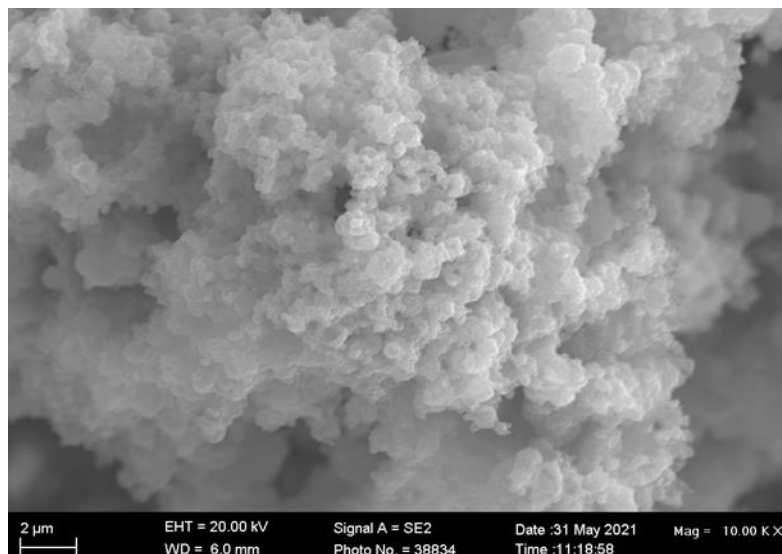


Figure 4.3. SEM micrograph showing spherical particle clusters at 10000 X magnification of the Test Run 1 sample prepared by precipitation synthesis

The samples were analysed using Energy Dispersive X-Ray (EDX) analysis to determine the semi-quantitative composition of the catalysts. The analysis confirmed that the precipitates formed during the precipitation runs as well as the wet impregnation runs are manganese oxides with carbon inclusions. Fe oxides were detected in the samples, likely from the mesh substrate. The EDX results are shown in Figures 4.4 and 4.5.

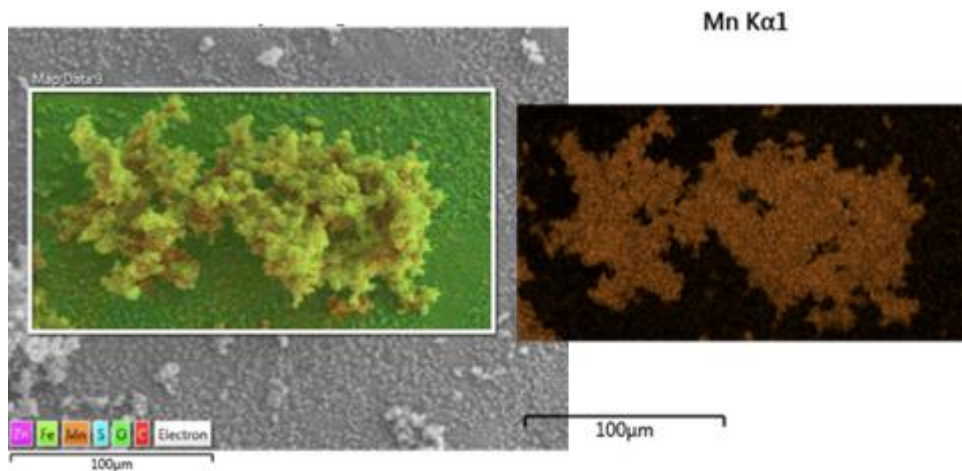


Figure 4.4. EDX results showing manganese oxide precipitate on the mesh (precipitation synthesis Test Run 1)

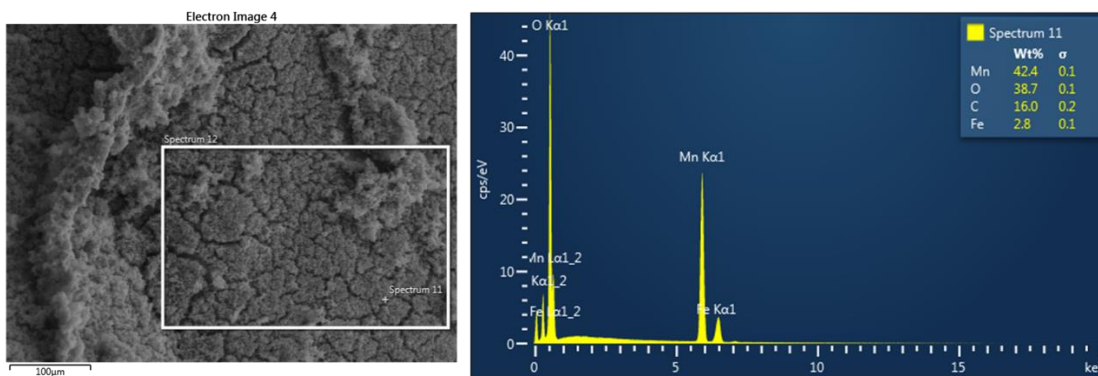


Figure 4.5. EDX results showing manganese oxide precipitate on the mesh (bulk synthesis preparation sample)

#### 4.1.1.2 Test Run 2

In Test Run 2, Test Run 1 was repeated with the addition of ferric nitrate. It was observed that the reaction solution turned dark brown and no visible precipitate formed. The reaction



conditions were not conducive to formation of the required product and ferric nitrate was thus not utilised in subsequent tests.

#### 4.1.1.3 Test Run 3

Test Run 3 utilised the same reaction conditions of Test Run 1 and the mesh was left to dry overnight prior to calcining. The catalyst synthesized from Test Run 3 formed clusters of precipitate on the mesh as shown in Figure 4.6. The coverage of the mesh was found to be visually similar to Test Run 1.

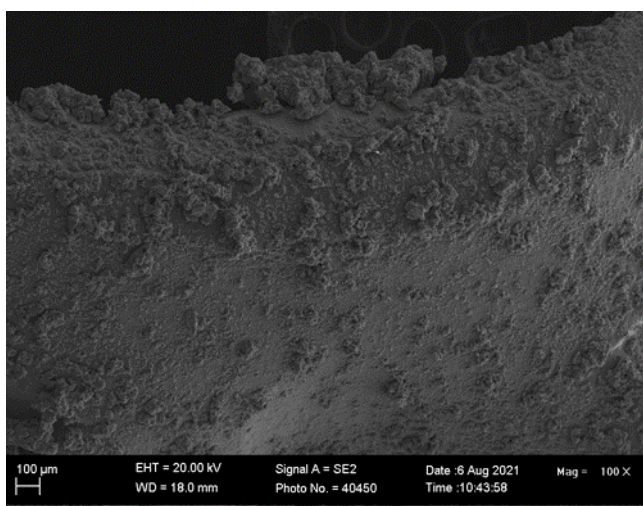
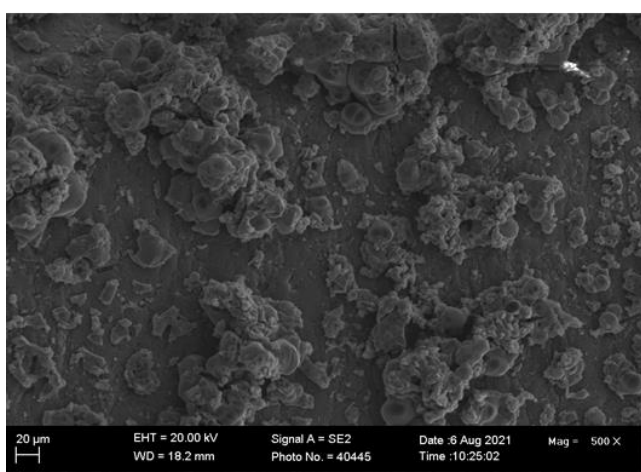
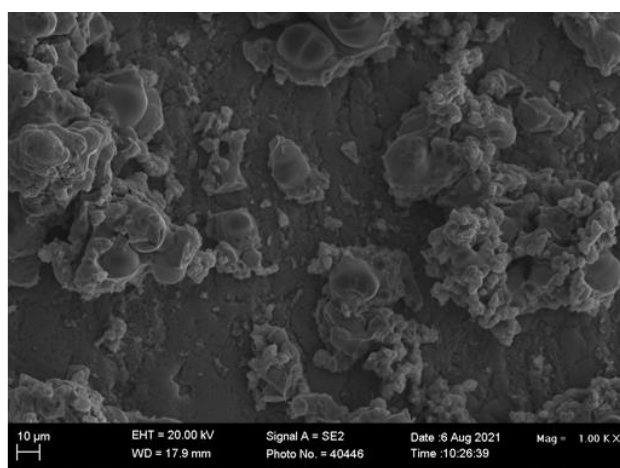


Figure 4.6. SEM micrograph showing clusters of precipitate at 100 X magnification formed from Test Run 3 of the precipitation synthesis

Under higher magnification the amorphous clusters can be distinguished, as shown in Figure 4.7.



a)



b)

Figure 4.7. SEM micrographs of the catalyst synthesized in Test Run 3 showing amorphous clusters of precipitate at 500 X (a) and 1000 X (b) magnification

When the rinsed and dried sample is exposed to air, the morphology of the sample changes significantly, as shown in Figure 4.8. The exposed sample does not have the spherical particle morphology and changes to an amorphous morphology. The morphology is expected to be spherical, as found in Augustin et al. (2015) and not amorphous.

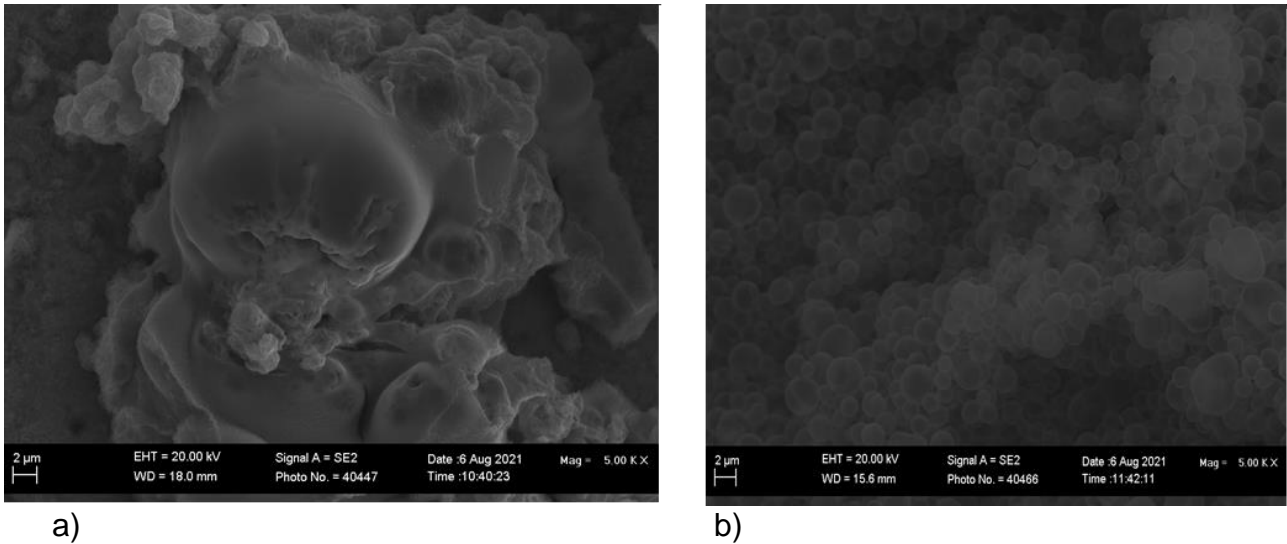


Figure 4.8. SEM micrographs at 5000 X magnification comparing the precipitate exposed to air prior to calcination (a) and sample transferred directly to the muffle furnace once rinsed and dried (b)

#### 4.1.1.4 Test Run 4

Test Run 4 utilised the same synthesis methodology as Test Run 1 with an increased manganese acetate tetrahydrate concentration to improve the catalyst coverage on the mesh. The mesh was calcined directly after synthesis and the calcining time reduced to 2 hours. For the catalyst synthesized from Test Run 4, the precipitate on the mesh could clearly be seen at 100 X magnification as shown in Figure 4.9.

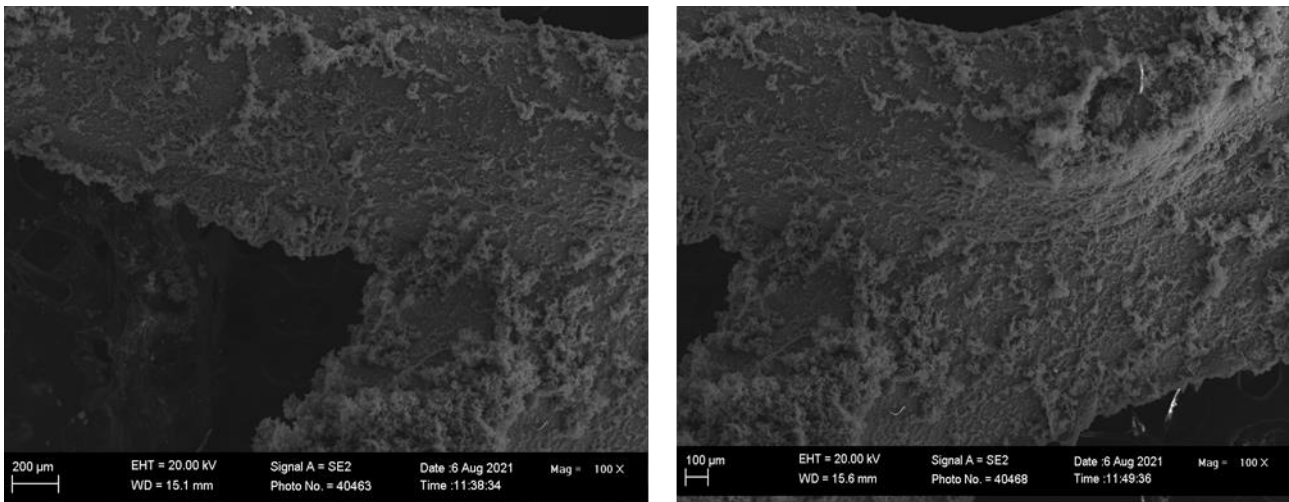


Figure 4.9. SEM micrographs of the catalyst synthesized from Test Run 4 showing precipitate on the mesh at 100 X magnification

The precipitate covered the mesh well and formed clusters of precipitate in places, as can be seen in Figure 4.10. The utilization of higher concentrations of manganese acetate tetrahydrate greatly improved the precipitate coverage on the mesh.

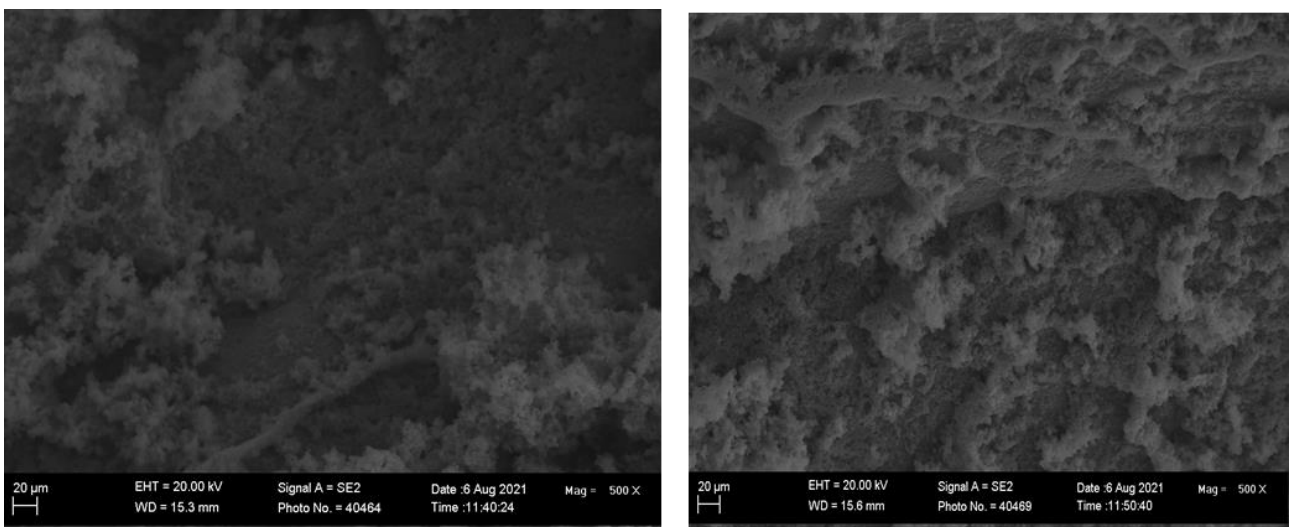
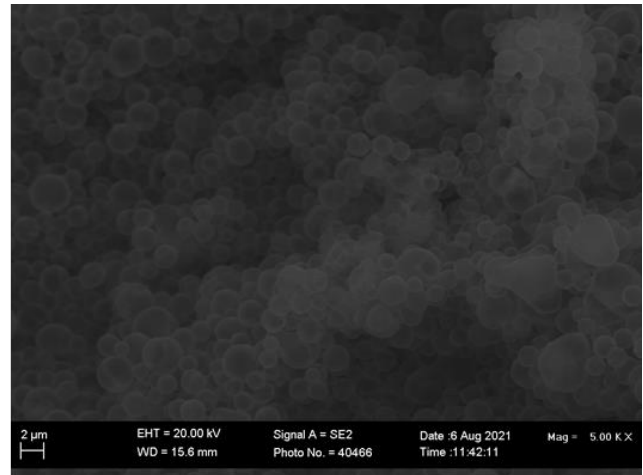


Figure 4.10. SEM micrographs of the catalyst synthesized from Test Run 4 showing precipitate coverage at 500 X magnification

The clusters were made up of spherical particles, as can be seen in Figure 4.11. The clusters have similar morphology to those observed for Test Run 1, indicating that oxidation prior to calcination impacts the morphology of the product significantly.



a)

b)

Figure 4.11. SEM micrographs showing clusters made up of spherical particles at 1000 X (a) and 5000 X (b) magnification produced from Test Run 4

At 10000 X magnification the individual spherical particles were evident, as shown in Figure 4.12.

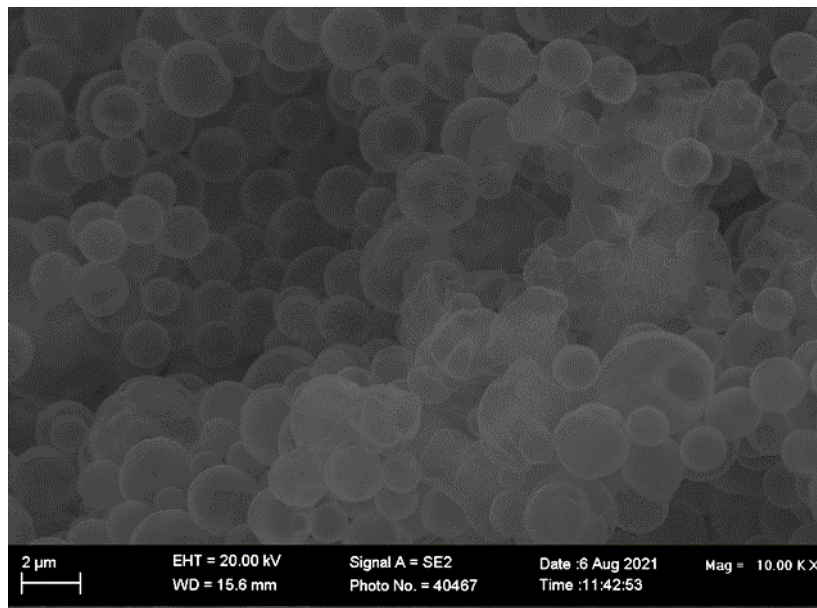


Figure 4.12. SEM micrograph showing the precipitate comprised of spherical particles shown at 10000 X magnification produced from Test Run 4

#### 4.1.1.5. Test Run 5

Test Run 5 utilised the same synthesis methodology as Test Run 4 without the addition of TEG. The catalyst synthesized from Test Run 5 showed full coverage on the mesh as shown in Figure 4.13.

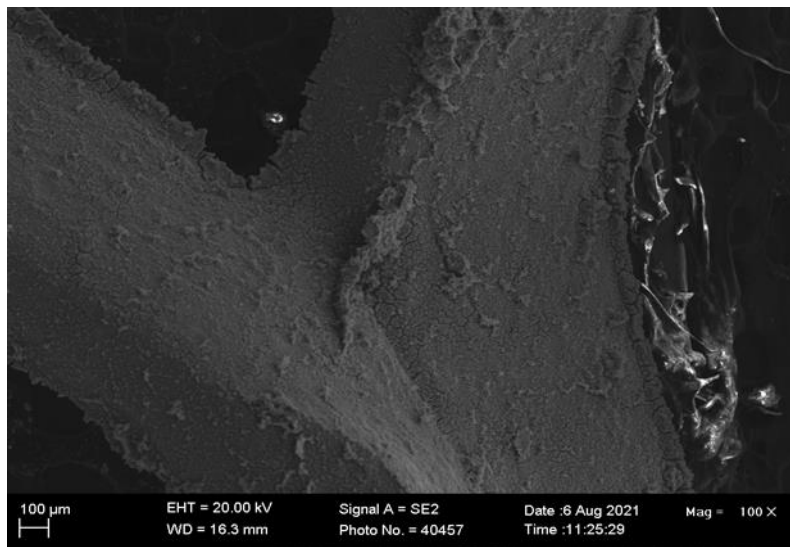


Figure 4.13. SEM micrograph showing the precipitate coverage at 100 X magnification for the catalyst produced from Test Run 5

At 500 X magnification it can be seen that the precipitate covered the mesh well as can be seen in Figure 4.14.

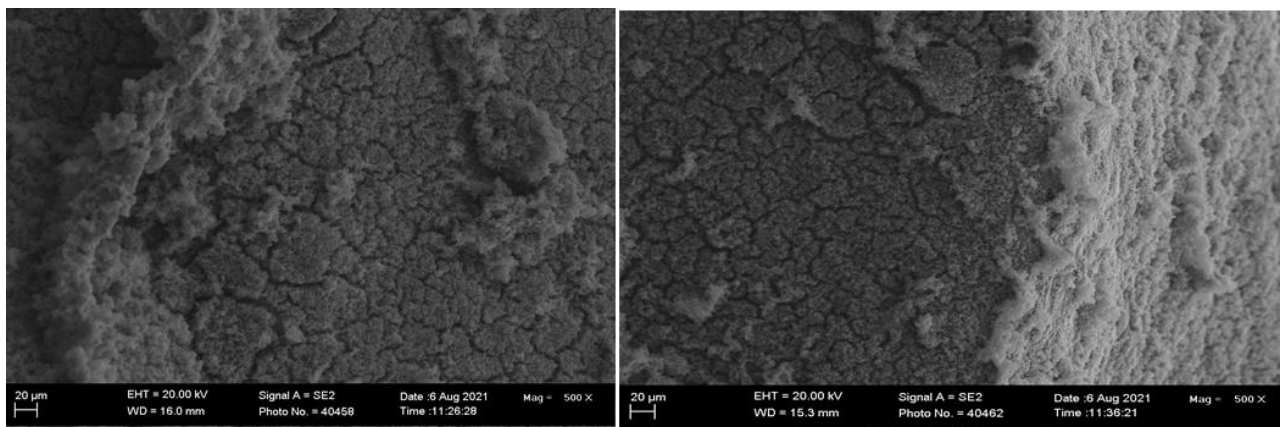
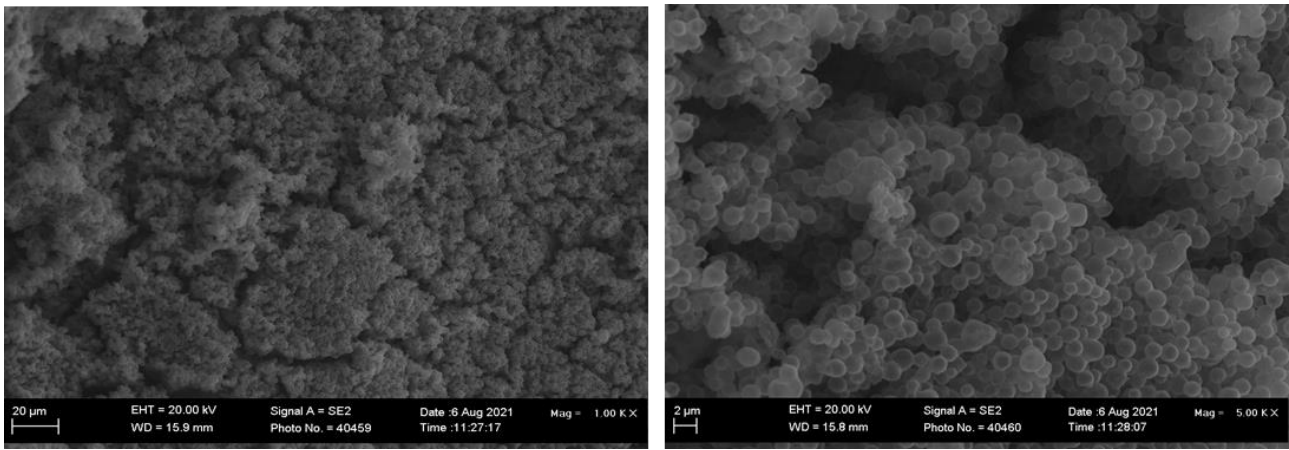


Figure 4.14. SEM micrographs showing the precipitate coverage at 500 X magnification for the catalyst produced from Test Run 5

The precipitate was comprised of spherical particles, as shown in Figure 4.15.





a)

b)

Figure 4.15. SEM micrographs showing the precipitate comprised of spherical particles at 1000 X (a) and 5000 X (b) magnification for the catalyst produced from Test Run 5

The spherical particles that make up the precipitate vary in size from 0.5 μm to 1.5 μm as shown in Figure 4.16. EDX analysis indicated that the spherical particles were manganese oxide particles.

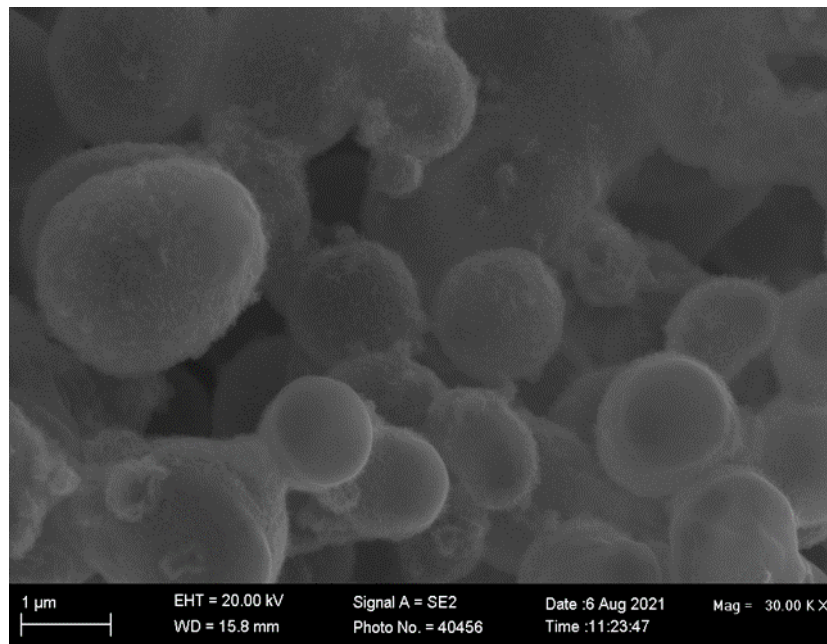
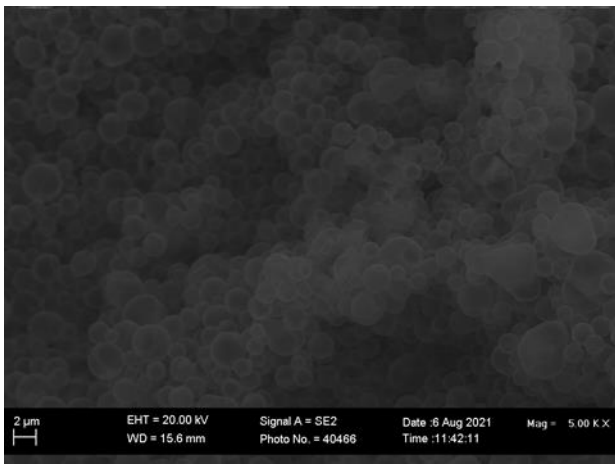
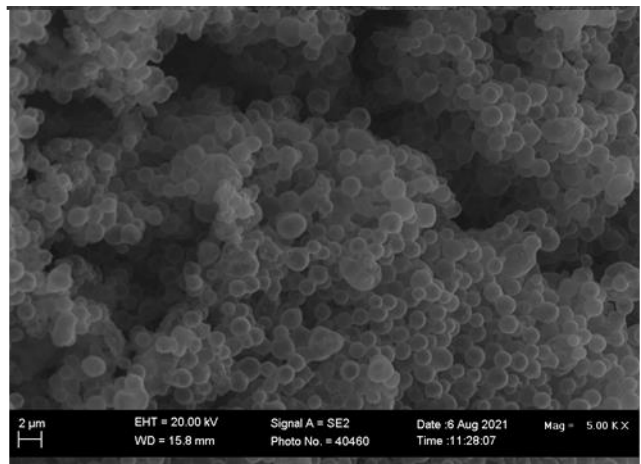


Figure 4.16. SEM micrographs showing spherical particles of various sizes at 30000 X magnification for the catalyst produced from Test Run 5

The addition of TEG does not appear to improve coverage of the mesh with catalyst particles and the precipitates appeared to have similar morphologies as shown in Figure 4.17.



a)

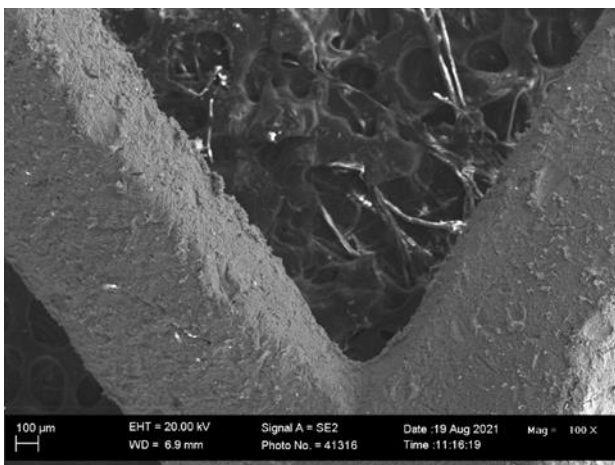


b)

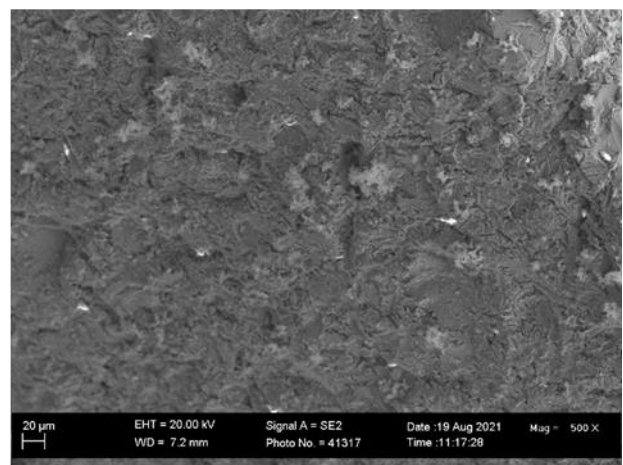
Figure 4.17. SEM micrographs at 5000 X magnification comparing the samples prepared with the addition of TEG (a) and samples prepared without TEG (b)

#### 4.1.1.6. Test Run 6

The results for Test Run 6 at magnifications of 100 X and 500 X are shown in Figure 4.18, in which the same synthesis conditions as for Test Run 1 were used except that here the wire mesh was sandblasted prior to synthesis. The roughened surface of the mesh can be seen with clusters of spherical particles. The catalyst adherence visually appears to be similar to Run 1, indicating that the increased manganese acetate concentrations used for Runs 4 and 5 greatly improves catalyst coverage and the sandblasting does not result in improved coverage.



a)



b)

Figure 4.18. SEM micrographs showing the catalyst prepared on a sandblasted mesh surface at 100 X (a) and 500 X (b) magnification produced from Test Run 6

The clusters of particles are shown in Figure 4.19 at 1000 X magnification. The clusters showed similar morphology to that of Run 1.

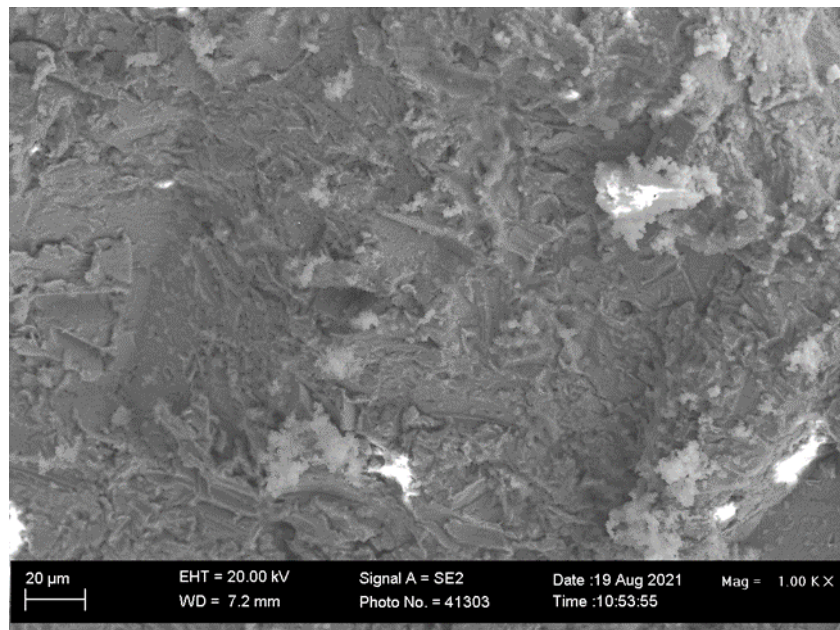


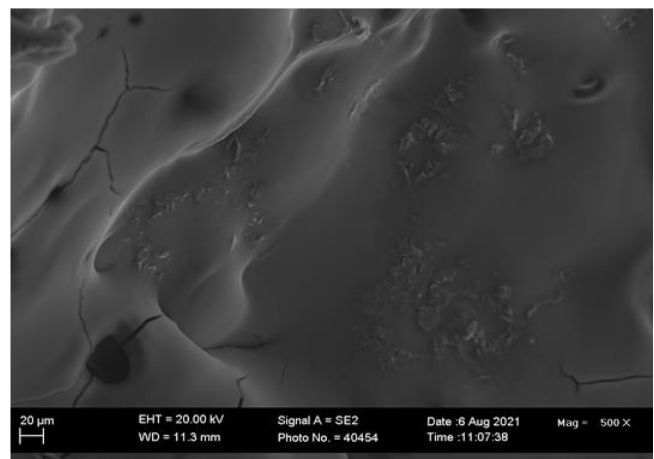
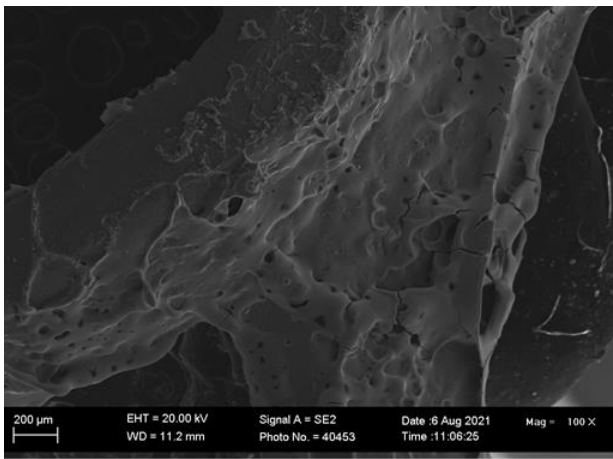
Figure 4.19. SEM micrograph showing the catalyst clusters at 1000 X magnification produced from Test Run 6

#### **4.1.2. Synthesis using wet and dry impregnation**

##### **4.1.2.1. Wet Impregnation Synthesis**

A mesh sample was prepared using 8 g of manganese acetate tetrahydrate in 30 mL of water. The sample was dipped in the solution, removed and calcined without drying at 550 °C for two hours. The catalyst sample was analysed using SEM and the results are shown in Figure 4.20.



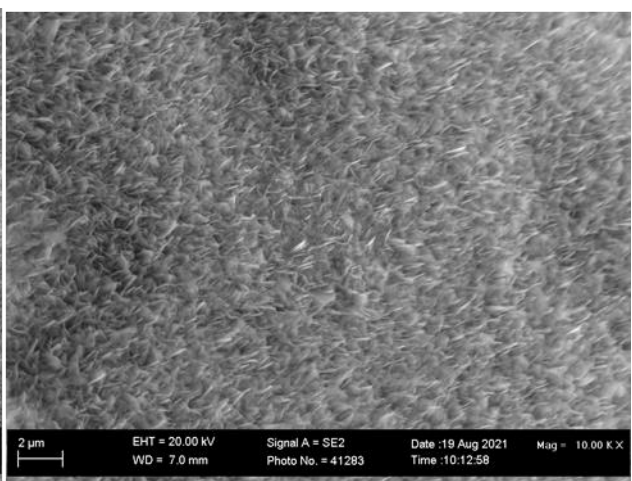
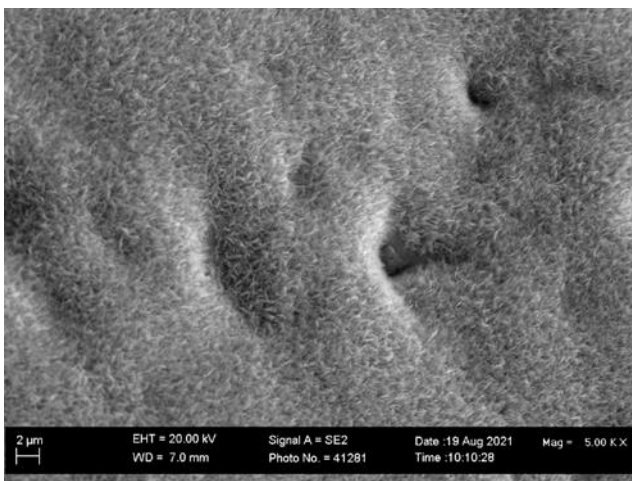


a)

b)

Figure 4.20. SEM micrographs showing the catalyst synthesized using wet impregnation at 100 X (a) and 500 X (b) magnification

At higher magnifications it can be seen that the mesh was covered in plate-like particles as shown in Figure 4.21. This indicates a different crystal structure to that obtained by the precipitation synthesis route.

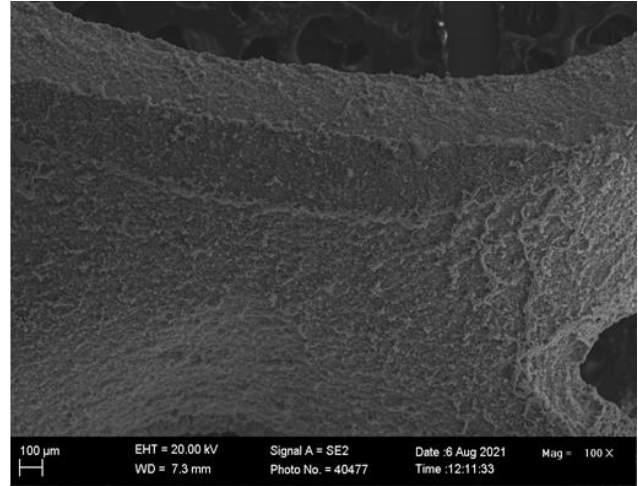
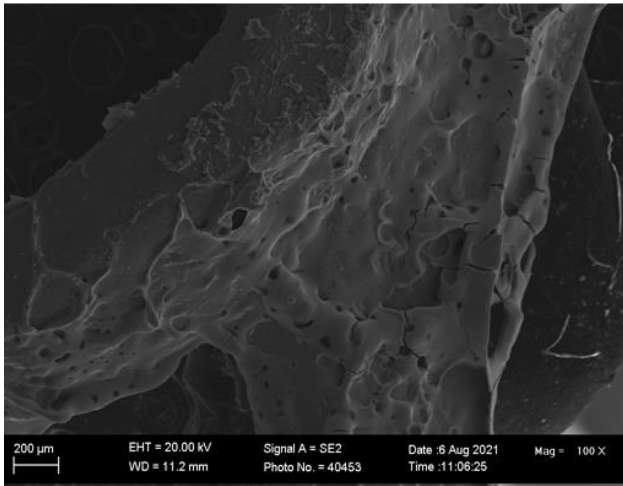


a)

b)

Figure 4.21. SEM micrographs showing the plate like coverage of the catalyst prepared using wet impregnation at 5000 X (a) and 10000 X (b) magnification

The morphology of the catalyst changed significantly depending on the synthesis method used. At magnifications of 100 X and 500 X the results indicated that spherical particles were formed when the synthesis was done using deposition precipitation and a relatively smooth manganese oxide deposit was formed using wet precipitation as shown in Figure 4.22. Good coverage of the catalyst on the mesh as achieved using both techniques.

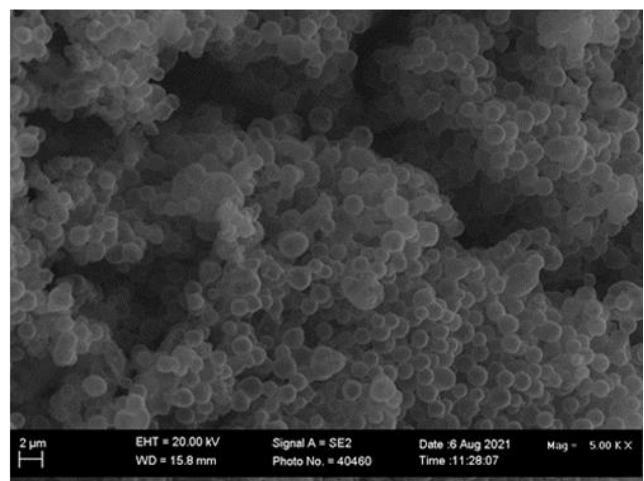
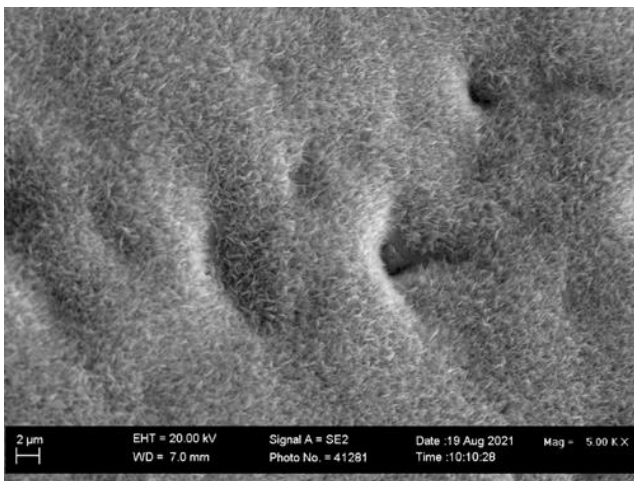


a)

b)

Figure 4.22. SEM micrographs comparing the catalysts synthesized using wet impregnation (left) and precipitation (right) techniques at 100 X magnification

At higher magnifications, the surface of the wet impregnation sample had a plate-like structure compared to the spherical structure of the sample prepared using precipitation as shown in Figure 4.23.



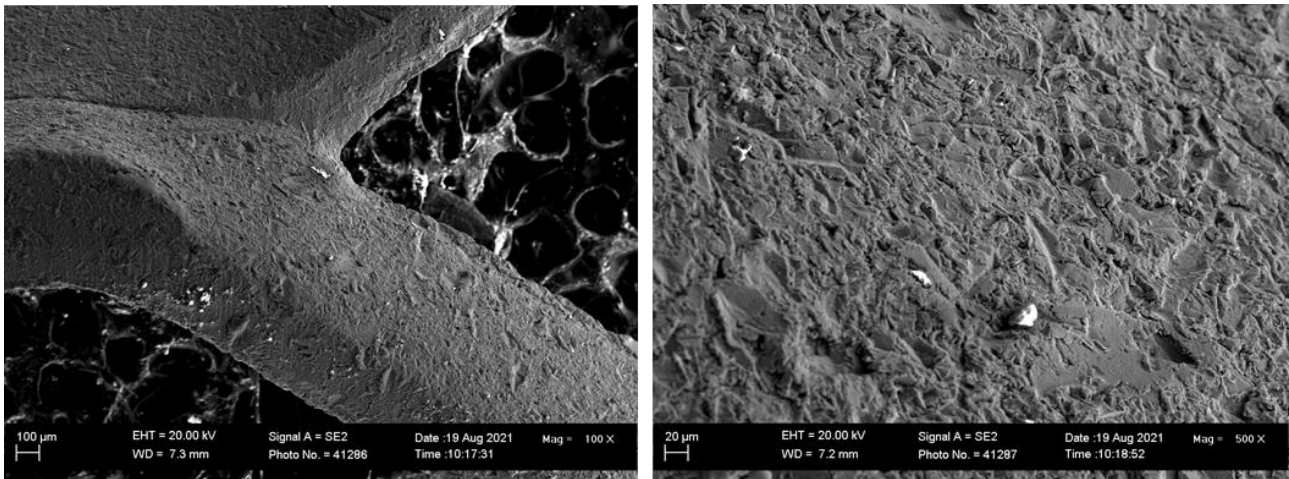
a)

b)

Figure 4.23. SEM micrographs comparing the surface of samples prepared using wet impregnation (a) and precipitation (b) at 5000 X magnification

#### 4.1.2.2. Dry Impregnation Synthesis

The catalyst was prepared using dry impregnation. As shown Figure 4.24, the coverage achieved was poor and the sandblasted mesh surface was still clearly visible.



a)

b)

Figure 4.24. SEM micrographs showing the catalyst prepared using dry impregnation on a sandblasted mesh at 100 X (a) and 500 X (b) magnification

## 4.2. BULK CATALYST PREPARATION

Both the optimized precipitation synthesis (Test Runs 4 and 5) and wet impregnation techniques achieved good coverage of the mesh substrate. The wet impregnation technique is a simpler process involving dipping the mesh into a concentrated solution of manganese acetate tetrahydrate prior to calcination, whereas the precipitation technique involves the gradual heating of the reagents to form a precipitate. The morphologies of the samples prepared were significantly different, as shown in Section 4.1.2.1. Bulk catalyst samples were prepared for testwork using both techniques. The sandblasting did not significantly improve coverage and the mesh used for the bulk synthesis was thus not sandblasted.

### 4.2.1. Bulk synthesis using precipitation

It was found that in order to achieve improved coverage, a higher concentration of manganese acetate tetrahydrate should be used than was used in the method described by Augustin et al. (2015). In the preparation of the bulk catalyst, the additional manganese acetate tetrahydrate was added incrementally as discussed in Section 3.3.2. The addition of tetraethyl glycol (Test Run 4) did not significantly change the coverage, morphology or particle size of the precipitate formed and was therefore not used in the synthesis of the bulk catalyst (as was done for Test Run 5). In order to preserve the morphology of the particles formed, the sample was transferred to the muffle furnace once rinsed. The prepared sample is shown in Figure 4.25.

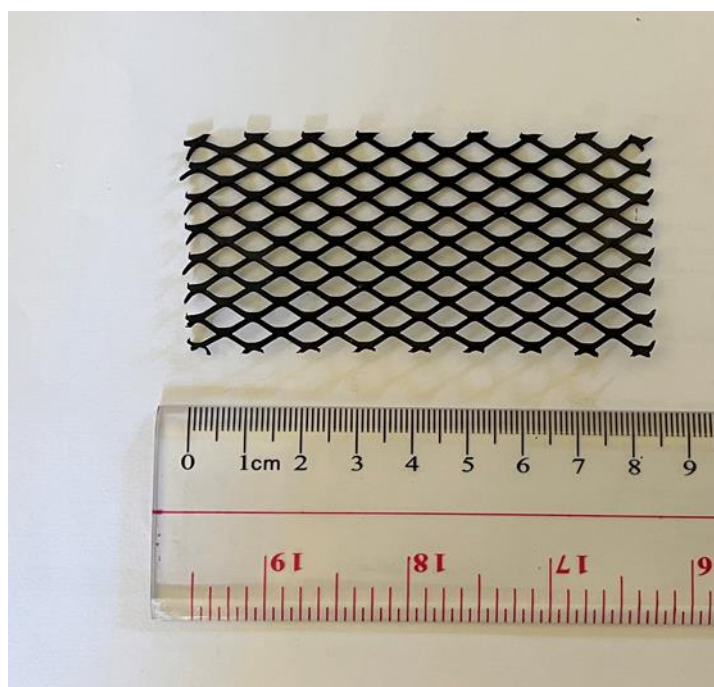


Figure 4.25. Mesh after synthesis and calcination from the bulk catalyst synthesis using precipitation

The sample was analysed using SEM. The results indicated that good coverage was achieved as shown in Figure 4.26.

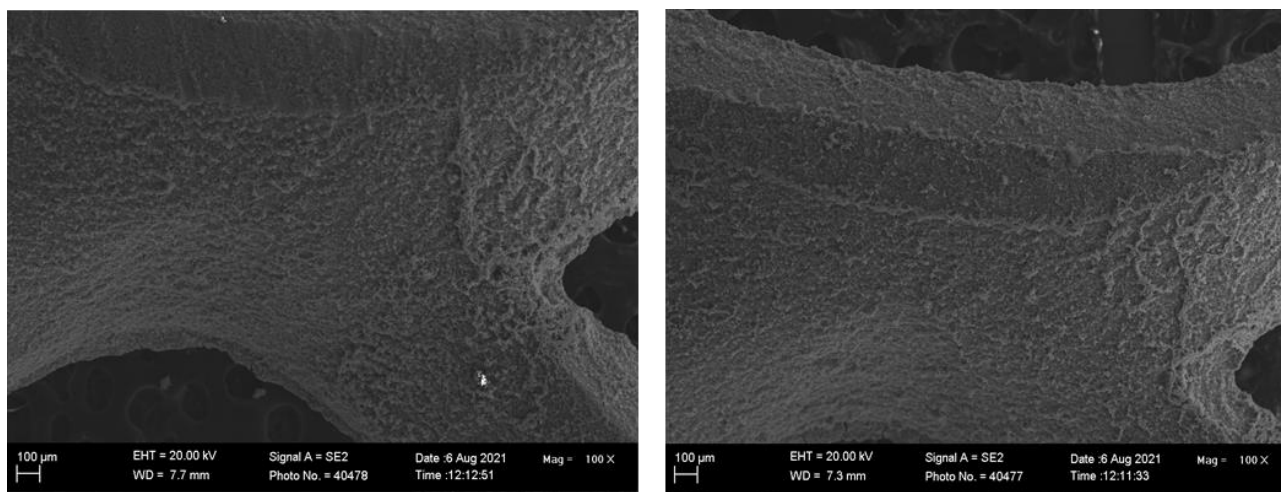
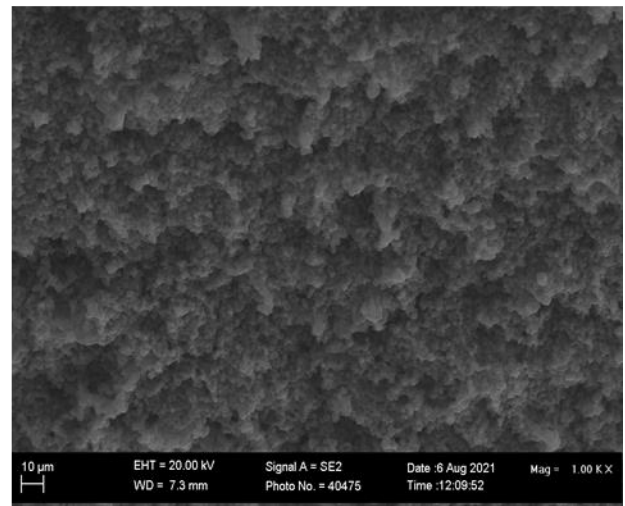
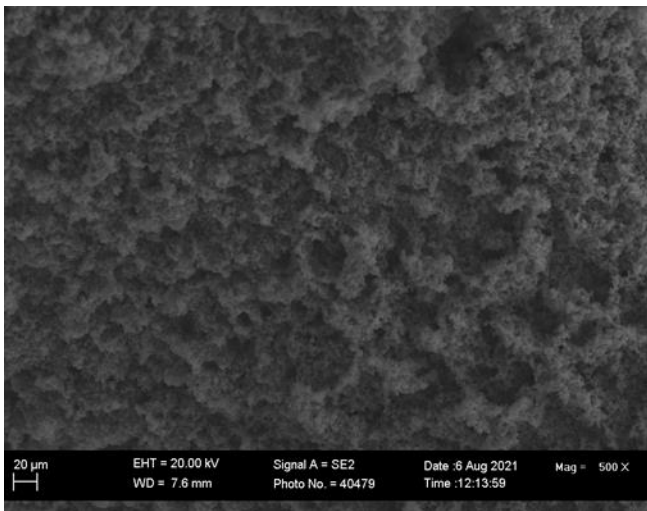


Figure 4.26. SEM micrographs showing the coverage of the precipitate on the mesh at 100 X magnification produced from the bulk catalyst synthesis using precipitation

The mesh was covered in precipitate several layers deep as can be seen in Figure 4.27.

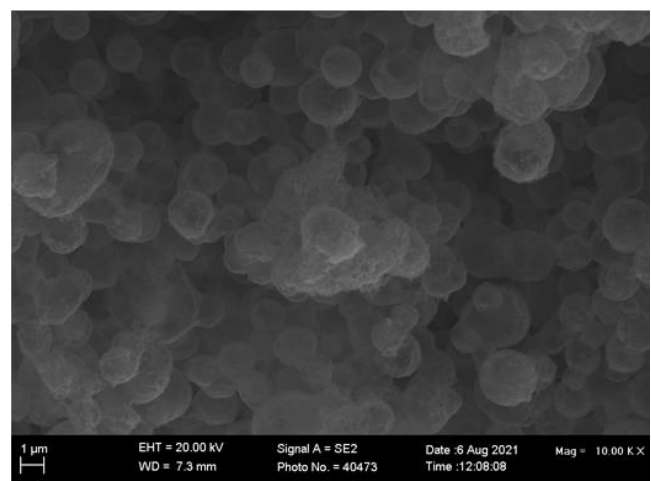
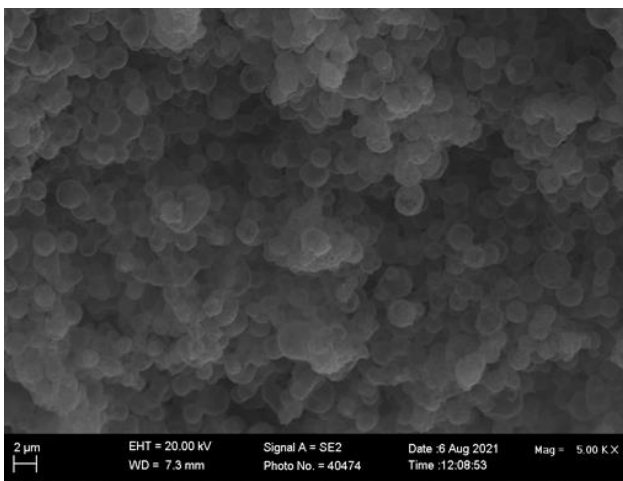


a)

b)

Figure 4.27. SEM micrographs showing the precipitate coverage at 500 X (a) and 1000 X (b) magnification produced from the bulk catalyst synthesis using precipitation

The precipitate was comprised of spherical particles with some agglomeration as shown in Figure 4.28.



a)

b)

Figure 4.28. SEM micrographs showing spherical particles with agglomeration at 5000 X (a) and 10000 X (b) magnification produced from the bulk catalyst synthesis using precipitation

Figure 4.29 indicates that the procedure can be successfully scaled up and that similar coverage and morphology was achieved to that obtained in the smaller test scale tests.



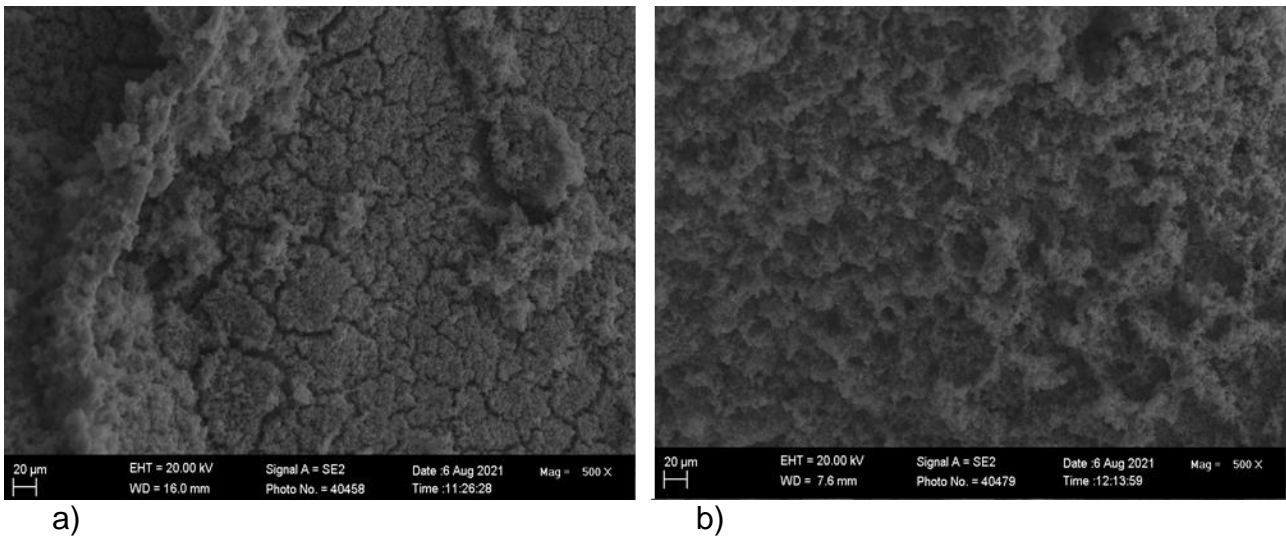


Figure 4.29. SEM micrographs at 500 X magnification comparing the catalyst synthesized from Test Run 5 (a) and synthesis of the bulk sample (b)

#### 4.2.2. Bulk synthesis using wet impregnation

A bulk catalyst was prepared using the same technique as set out in Section 4.1.2.1. The sample prepared using wet impregnation is shown in Figure 4.30. The catalyst covered the entire mesh, with similar morphology to that of the smaller test catalyst.

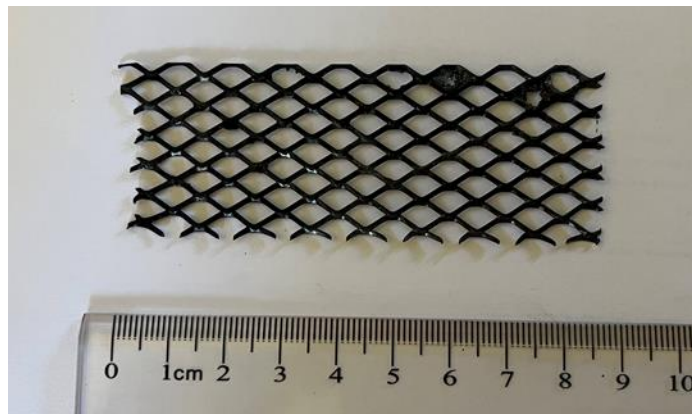


Figure 4.30. Substrate after wet impregnation and calcination

### 4.3. CATALYST TESTING

Test runs were conducted with and without the catalyst as set out in Section 3.3.3. The PTFE filters after sampling are shown in Figure 4.31. The filters were weighed using the procedure set out in Appendix B and the full gravimetric results are included in Appendix C. The masses obtained were divided by the total volume of flue gas sampled to account for

differences in sampling times and flow rates. The sample PM mass concentrations obtained are presented graphically in Figure 4.32.



Figure 4.31. PTFE filters with their numbered filter supports after the testwork sampling

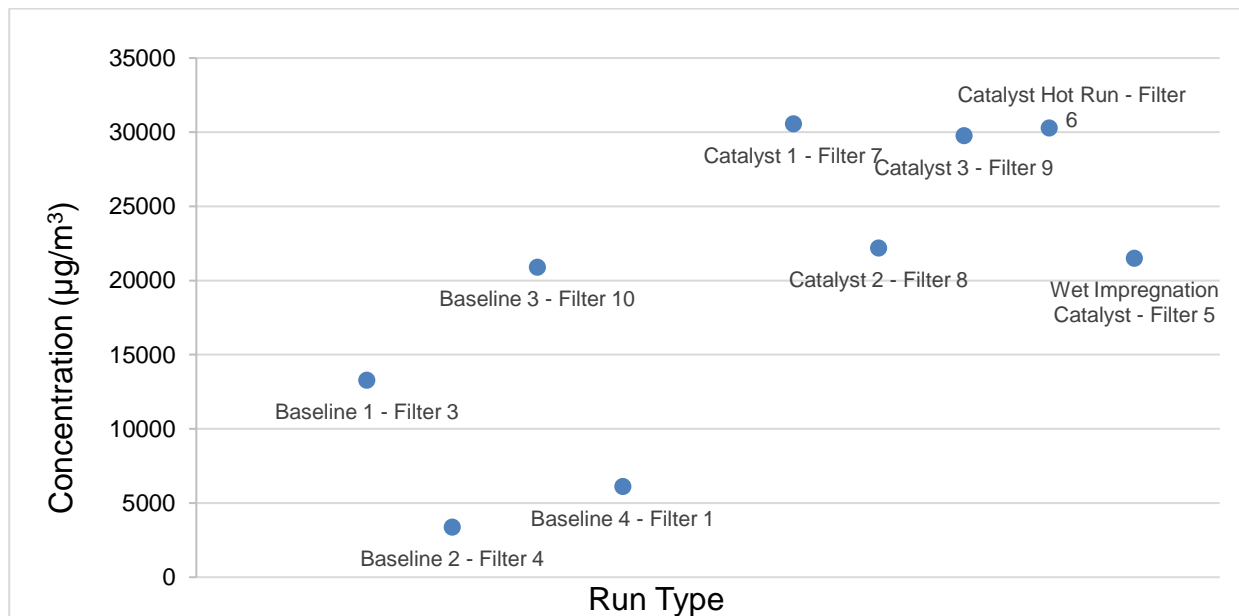


Figure 4.32. Measured total PM mass concentrations for the Baseline and Catalyst Runs

The results indicate, contrary to expectation, that higher concentrations of particulate matter were recorded for the Catalyst runs compared to the Baseline runs. Visual inspection of the

catalyst indicated that the emission were not due to the clogging of the catalyst. It was expected that due to the full oxidation of VOCs to CO<sub>2</sub> over the catalyst, secondary particulate matter would be reduced during the catalyst runs. To investigate the morphology of the particulate matter, Scanning Electron Microscopy (SEM) analysis was conducted on five of the samples. Two baseline samples (Filters 3 and 10), two catalyst samples (Filters 6 and 9) and the field blank sample (Filter 2) were selected for analysis.

The structure of the filter and the filter pores can be seen on the field blank sample (Filter 2) as shown in Figure 4.33.

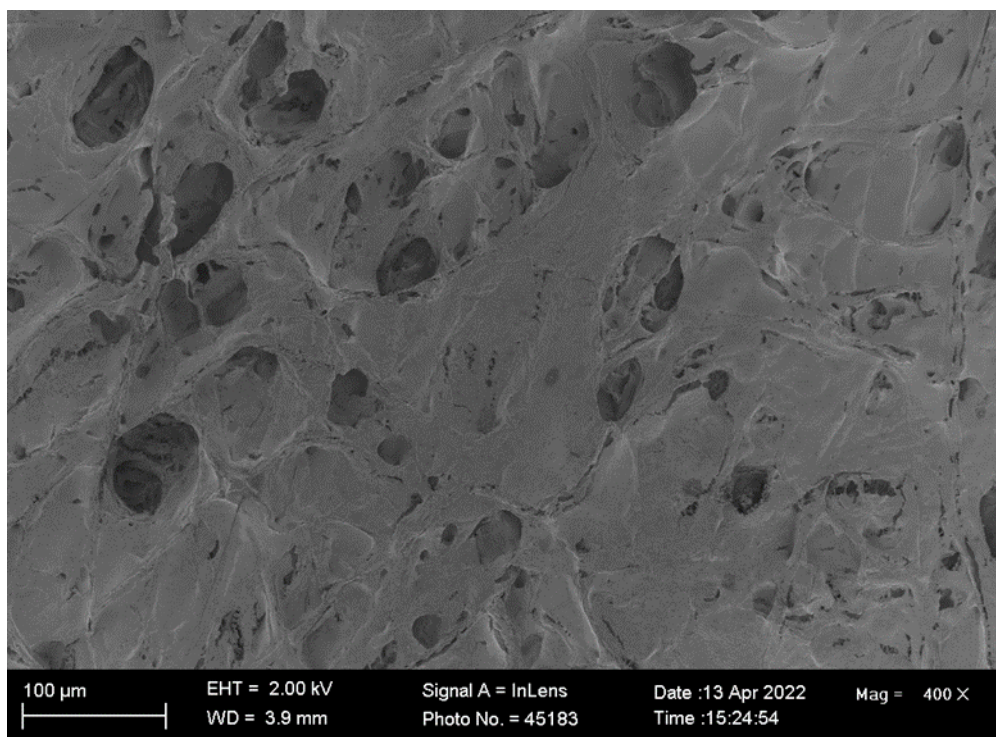


Figure 4.33. SEM micrograph of the field blank filter showing the structure of the filter and the pores (Filter 2) at 400 X magnification

At 400 X magnification, the Baseline Run samples appeared similar to the field blank sample as shown in Figures 4.34 and 4.35. At 5000 X magnification, chain-like structures could be seen within a few of the pores as shown in Figure 4.36.



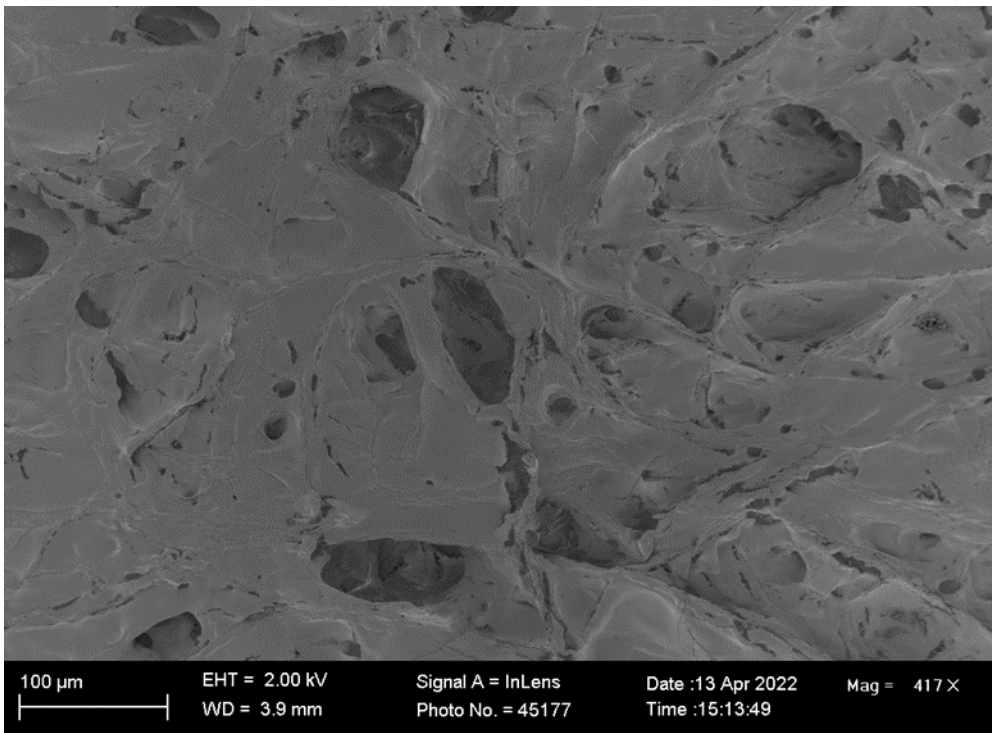


Figure 4.34. SEM micrograph of the Baseline Run 1 filter (Filter 3) at 417 X magnification

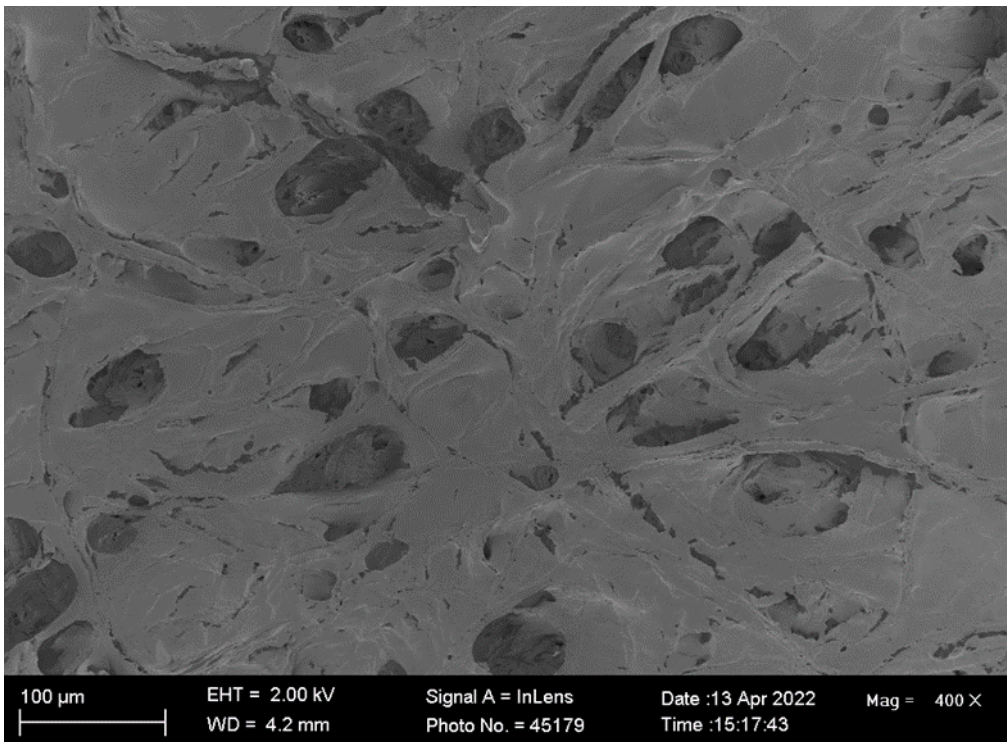


Figure 4.35. SEM micrograph of the Baseline Run 3 filter (Filter 10) at 400 X magnification

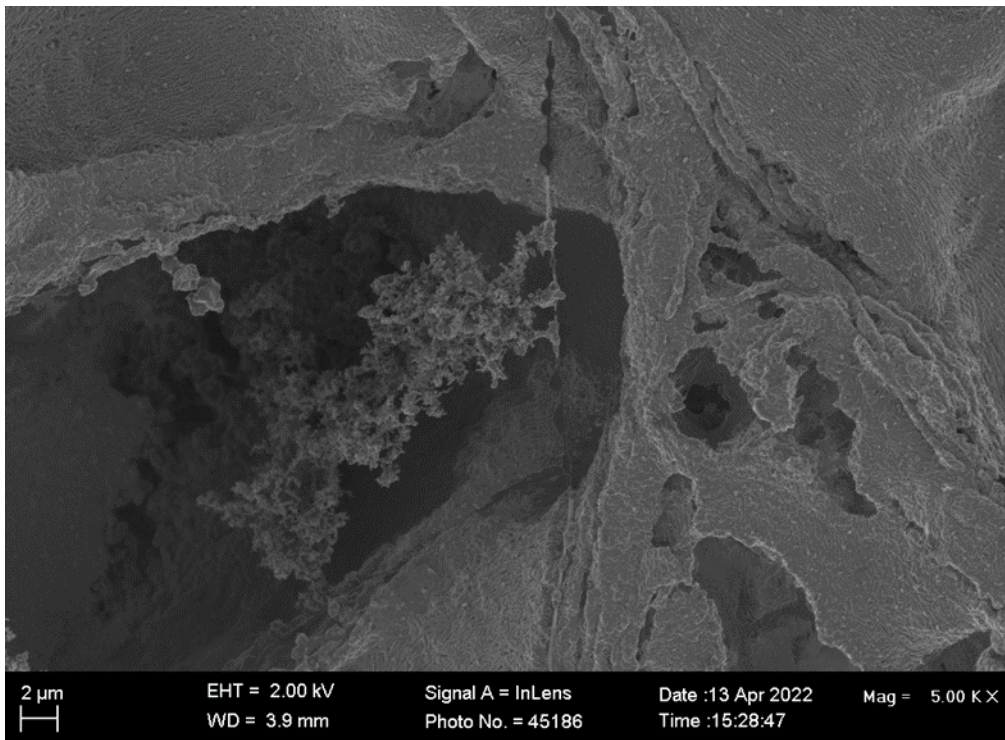


Figure 4.36. SEM micrograph of a chain-like structure, likely a soot aggregate, found in one of the pores for Baseline Run 3 (Filter 10)

For the catalyst runs, clusters of particles could be seen within the pores of the filters as shown in Figures 4.37 and 4.38. Both filters had particle clusters within the pores, but the Catalyst Hot Run which was sampled only during the flaming phase of the run (Filter 6) had fewer of these clusters likely due to the shorter sampling time of 5 min when compared to 10 min sampling time for the Catalyst Run (Filter 9).



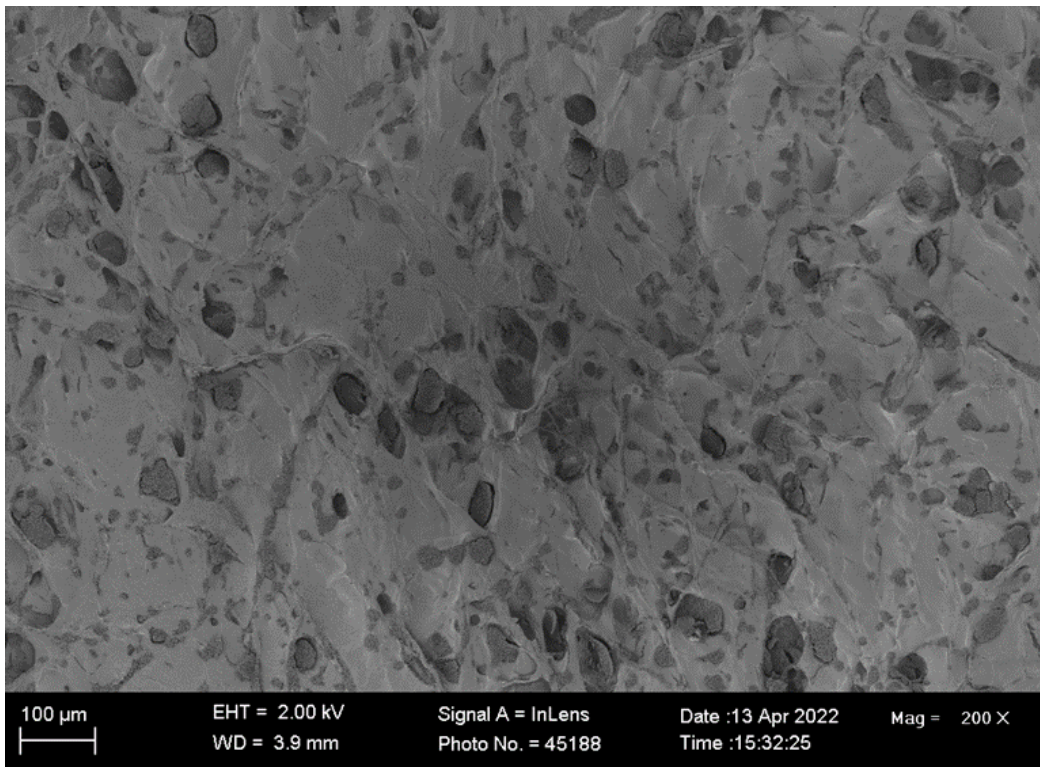


Figure 4.37. SEM micrograph showing particulate clusters in the pores of the filter from Catalyst Run 3 (Filter 9) at 200 X magnification

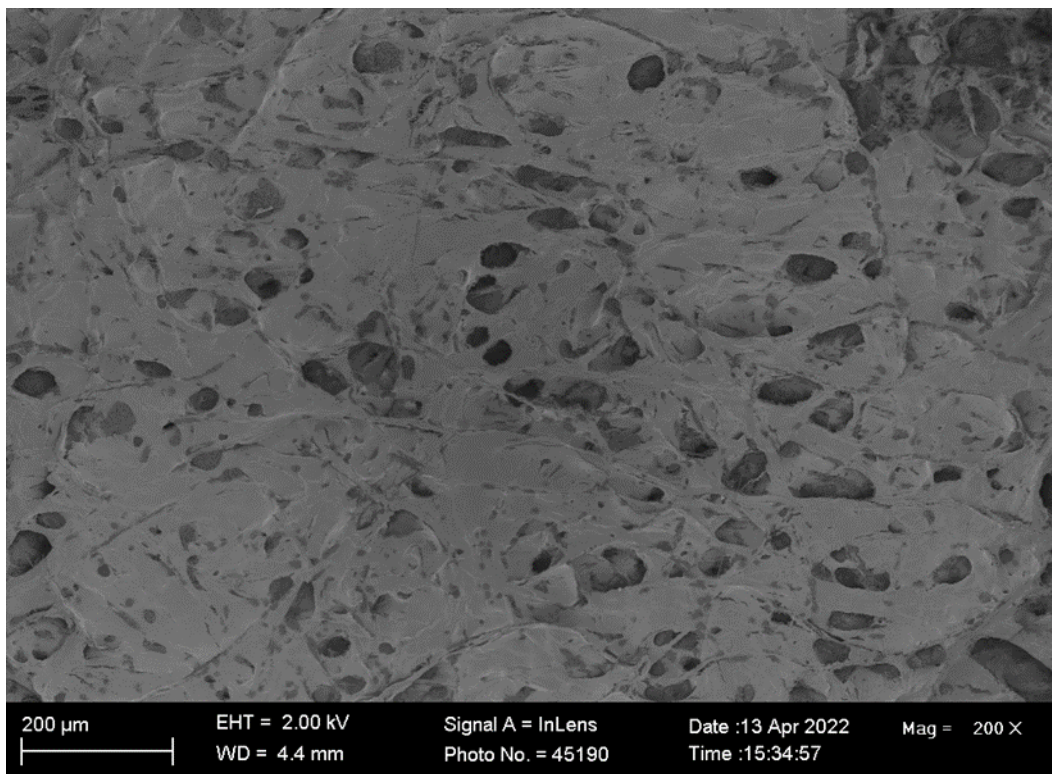


Figure 4.38. SEM micrograph (at 200 X magnification) of the Catalyst Hot Run Filter 6 showing fewer particulate clusters due to the shorter sampling time than the catalyst run

At higher magnification (1150 X), the clusters of particulates can be seen as shown in Figure 4.39.

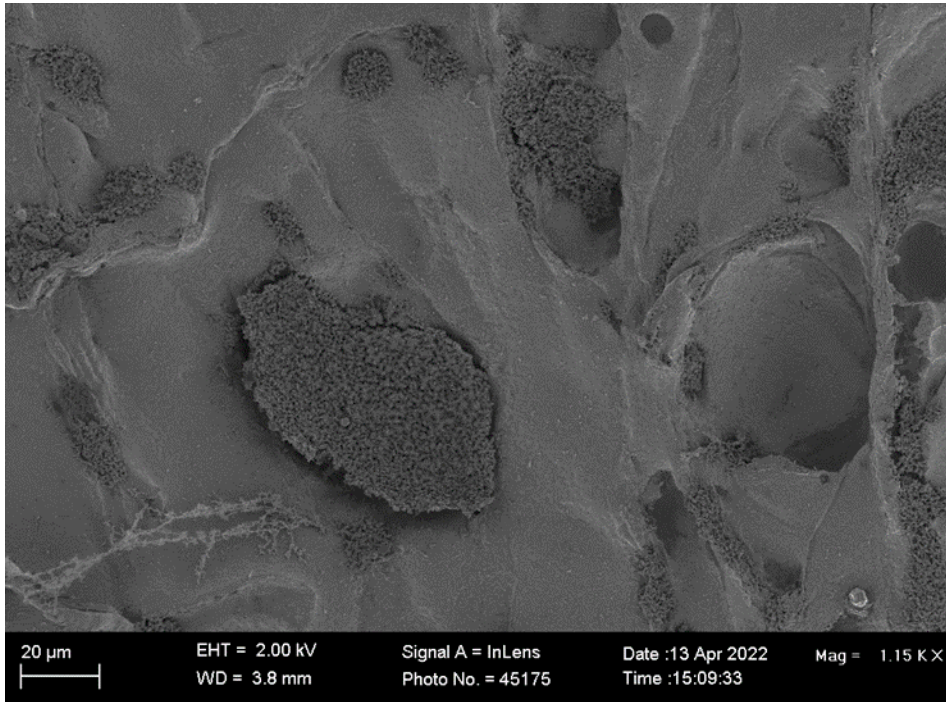


Figure 4.39. SEM micrograph (at 1150 X magnification) of Catalyst Run 3 (Filter 9) showing the particulate clusters

Figure 4.40 shows the clusters of particulates at 5000 X magnification along with a sharp edged particle, likely a fly ash particle.

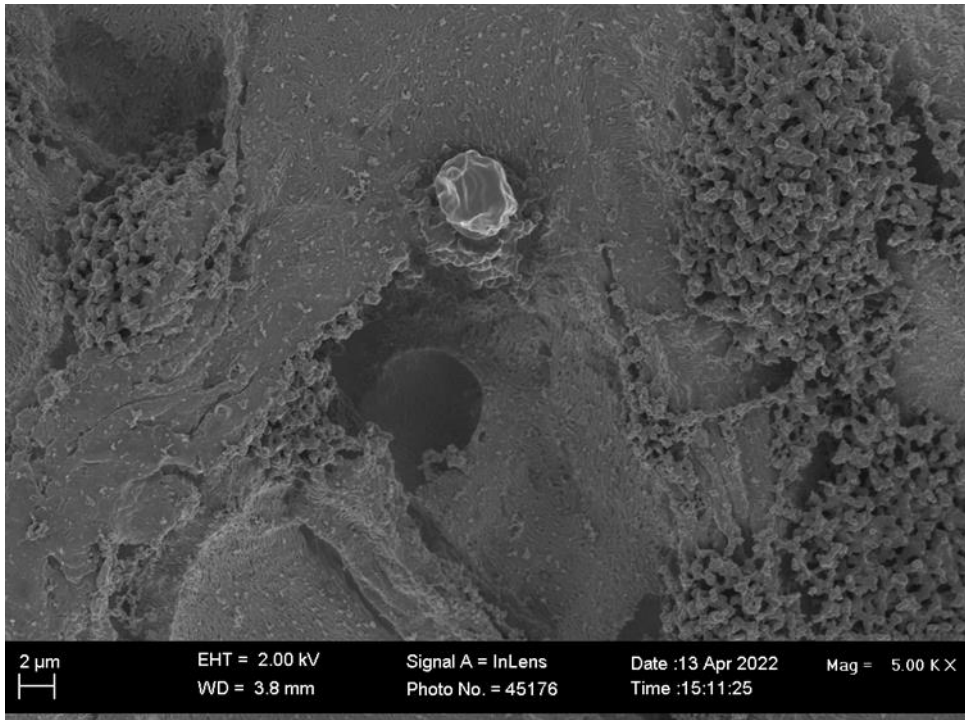
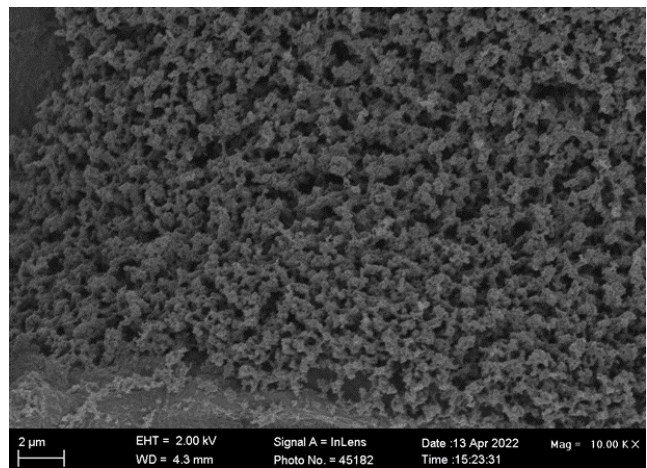
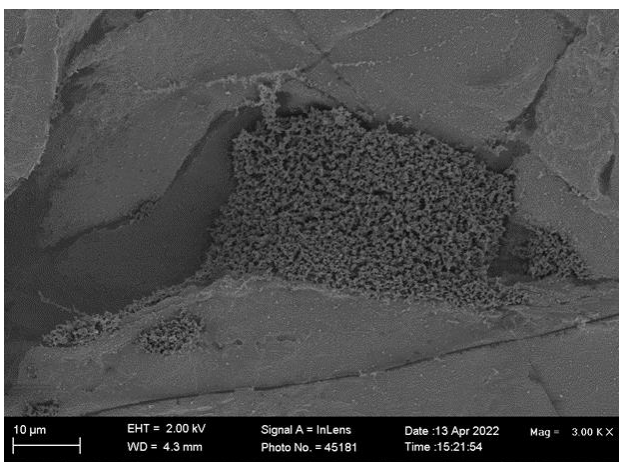


Figure 4.40. SEM micrograph (at 5000 X magnification) of Catalyst Run 3 (Filter 9) showing the spherical particulates and a sharp edged particle, likely fly ash particle

The clusters and chains can be seen at 3000 X and 10000 x magnification as shown in Figure 4.41.



a)

b)

Figure 4.41. SEM micrograph at 3000 X (a) and 10000 X (b) magnification showing spherical particles smaller than 1 μm in size for the Catalyst Hot Run (Filter 6)



Figure 4.42 shows the comparison between a catalyst run (a) and a baseline run (b) at 200 X magnification. Particulate clusters can clearly be seen in the pores of the filter for the catalyst run. Very few similar clusters could be seen on the baseline sample filter.

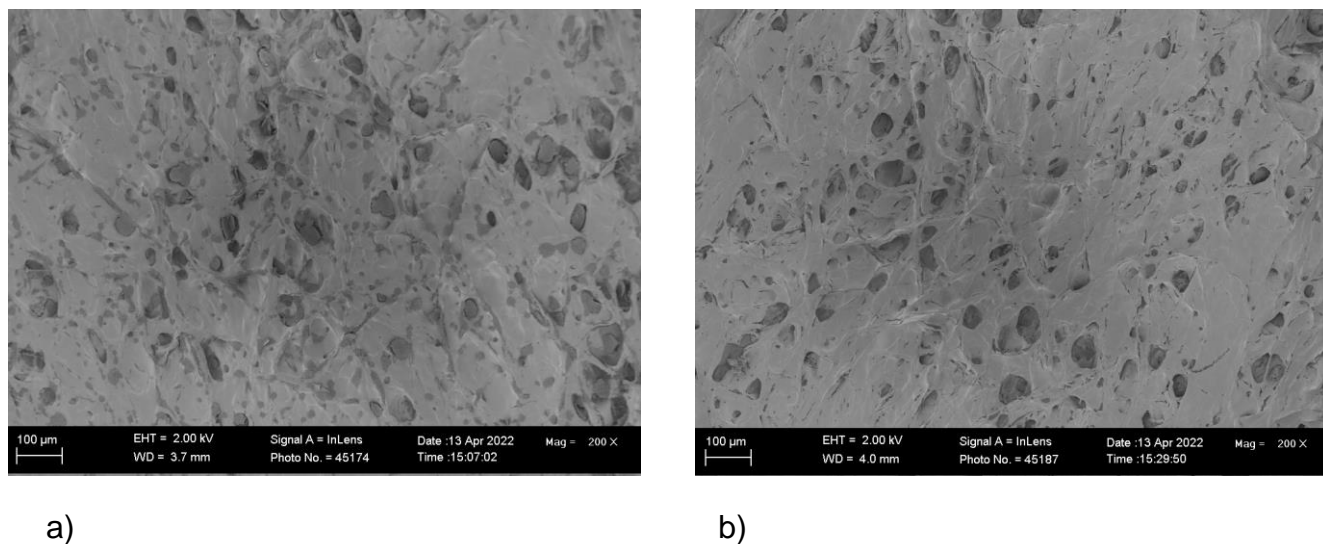


Figure 4.42. SEM micrographs comparing the filters from catalyst Run 3 (Filter 9) (a) to baseline Run 3 (Filter 10) (b) at 200 X magnification

Energy-dispersive X-ray spectroscopy (EDX) analysis was conducted at 15 kV on the samples to determine whether there was any detectable catalyst lost to the flue gas which would contribute to the PM load on the filters. Carbon and fluoride were detected by the EDX analysis due to the composition of the filter, although it was not possible to definitively determine whether the particulates formed were carbon-based due to the background carbon content of the filter.

The EDX analysis did not detect any manganese and the increased particulate mass on the filters used for the catalyst runs were therefore not as a result of macroscopic particles of the catalyst detaching from the support. Increased particulate matter could result from the dislodgement of very small metal particles from the catalyst which served as nucleation nodes for particle growth. The metallic nuclei would thus have a non-metal coating which may lead to non-detection by EDX.

The increase in particulate matter could also be caused by the impingement of particulate matter precursors on the catalyst. Particle growth occurs on the catalyst surface until the

particles formed are dislodged from the catalyst by the flue gas. If the catalyst does not oxidize the impinged pollutant efficiently, particle growth can occur with the increased residence time in the concentrated flue gas stream, resulting in chain like aggregates.

Various studies have shown that manganese oxide catalysts are able to oxidize CO, however previous studies investigating the use of manganese oxide catalysts for soot, CO and VOC reduction have mostly been conducted at laboratory scale and not under typical practical conditions. During laboratory testing, the soot or gas mixture has sufficient time to react and sufficient contact is achieved between the catalyst and the soot or gas (Khaskheli et. al. 2022). In a practical application, there will be much less contact time between the catalyst and the flue gas, which may impact on the efficiency of the catalyst.

## CHAPTER 5: CONCLUSIONS AND RECOMMENDATIONS

The catalyst was synthesized using three different synthesis methods and the synthesis using precipitation and wet deposition produced a manganese oxide catalyst with good coverage on the mesh support. The synthesis method used influenced the morphology of the catalyst. The catalyst synthesized using precipitation comprised of spherical particles and the wet deposition catalyst had a plate like structure. Both synthesis methods could be scaled up to produce bulk catalysts for field testwork. For future work, it is recommended that the mesh be weighed before and after synthesis to allow for quantification the mass of the catalyst deposited.

The catalyst testwork was conducted on the stove as-is (Baseline runs) and with the catalyst in place at the bottom of the flue (Catalyst runs). The testwork showed that an active catalyst can be synthesized in a facile and cost effective manner (as compared to precious metal catalysts) onto a mesh catalyst support which can be utilized in domestic fuel burning devices. The catalyst is easy to install and can be customised to fit non-standard domestic combustion units. The manganese based catalyst is heat resistant and does not release toxic materials. The catalyst is light in weight and requires no electricity to operate. During the limited test runs conducted, the catalyst did not clog, the airflow was not restricted and the stove vented as per the baseline runs. It is recommended that the catalyst be tested over a prolonged period to determine whether the catalyst regenerated due to the burn off of entrained particulate matter or whether it clogs over time. The number of consecutive cycles it can be used over should also be determined.

The total particulate concentrations were measured gravimetrically and the particle mass concentration of the catalyst runs were found to be higher than for the baseline runs. A limited number of test runs were performed as an initial screening and it is recommended that, should a suitable catalyst be synthesized, sufficient test runs be conducted to determine whether the difference between the catalyst and baseline runs is statistically significant. EDX analysis indicated that the increased particulate concentration on the catalyst runs was not likely to be as a result of macroscopic particles of the catalyst being dislodged from the support, as no manganese was detected. The catalyst therefore had good adherence to the catalyst support.



SEM analysis showed that the catalyst run filters had particulate clusters comprised of spherical particles in the pores of the filters. The baseline runs had very few, if any, of these particle clusters. The increased particulate matter could result from the dislodgement of very small metal particles from the catalyst which served as nucleation nodes for particle growth or could be caused by the impingement of particulate matter precursors on the catalyst followed by particle growth resulting in chain like aggregates. Measuring total particulate matter mass concentrations does not provide information on the morphology, surface chemistry, composition and size characterization of the particulates. It is recommended that more detailed analysis be conducted on the particulate matter to provide further insight into particulate formation.

Although the reaction mechanism of oxidation over a manganese oxide based catalyst is generally understood as being through the supply of oxygen from the crystal lattice, a detailed understanding of the elemental reactions are not well understood, particularly for multicomponent systems (Khaskheli et. al. 2022). An improved understanding of the reaction mechanism could lead to the optimisation of the catalyst activity.

The study measured particulate matter gravimetrically over the entire burn sequence. It is recommended that continuous particulate matter monitoring be conducted in future testwork to provide information on the performance of the catalyst during the different stages of combustion. It is further recommended that further testwork include the analysis of gaseous components such as CO, VOCs and CO<sub>2</sub> to determine the extent of oxidation of the particulate matter precursors.

It is recommended that a range of optimized, potentially active catalysts be tested to improve the oxidation of particulate matter precursors to CO<sub>2</sub>. Should a suitable catalyst be identified and synthesized, design optimization of the catalyst can be pursued which may include parameters such as the mesh configuration and type used as catalyst support and the number of catalyst layers used. It is recommended that an optimised catalyst be tested on a variety of fuels.

## REFERENCES

Albers PM, Wright CY, Voyi KVV and Mathee A (2015) 'Household fuel use and child respiratory ill health in two towns in Mpumalanga, South Africa', *South African Medical Journal*, vol. 105, no. 7, pp. 573 - 577.

Alemayehy YA, Asfaw SL and Terfie TA (2020) 'Exposure to urban particulate matter and its association with human health risks', *Environmental Science and Pollution Research International*, vol. 27, no. 22, pp. 27491-27506.

Amann M, Cofala J, Klimont Z, Nagl C, Schieder W (2018) *Measures to address air pollution from small combustion sources*, Report produced under Specific Agreement 11 under Framework Contract ENV.C.3/FRA/2013/00131 of DG - Environment of the European Commission.

Augustin M, Fenske D, Bardenhagen I, Westphal A, Knipper M, Plaggenborg T, Kolny-Olesiak J and Parisi J (2015) 'Manganese oxide phases and morphologies: A study on calcination temperature and atmospheric dependence', *Beilstein Journal of Nanotechnology*, vol. 6 pp. 47 - 59.

Benseeba F (2013) *Nanoparticle Technologies, From Lab to Market*, First Edition, Elsevier, ISBN: 9780080919270.

Chen SY, Song W, Lin HJ, Wang S, Biswas S, Mollahosseini M, Kuo CH, Gao PX and Suib SL (2016) 'Manganese Oxide Nano-Array Based Monolithic Catalysts: Tunable Morphology and High Efficiency for CO Oxidation', *ACS Applied Material Interfaces*, vol. 8, no. 12, pp. 7834–7842.

Cheng M.G, Murphy B, Moon J.W, Lutdka G.M and Cable-Dunlap P.R (2018) 'On the use of high-gradient magnetic force field in capturing airborne particles', *Journal of Aerosol Science*, vol. 120, pp. 22-31.

Cohen A.J, Brauer M, Burnett R, Ross Anderson H, Frostad J, Estep K, Balakrishnan K, Brunekreef B, Dandona L, Dandona R, Feigin V, Freedman G, Hubbell B, Jobling A, Kan H, Knibbs L, Liu Y, Martin R, Morawska L, Arden Pope III C, Shin H, Straif K, Shaddick G, Thomas M, Van Dingenen R, Van Donkelaar A, Vos T, Murray C.J.L, Forouzanfar M.H (2017) 'Estimates and 25-year trends of the global burden of disease attributable to ambient air pollution: an analysis of data from the Global Burden of Diseases Study 2015', *The Lancet*, vol. 389, pp. 1907–1918.

Damm O. and Triebel R (2008) *A synthesis report on biomass energy consumption and availability in South Africa*. A report prepared for ProBEC, GTZ, 2008.

Department of Energy (DOE 2012) *A survey of energy-related behaviour and perceptions in South Africa*, Human Sciences Research Council (HSRC)

Department of Environmental Affairs (2019) *National Environmental Management Air Quality Act 39 of 2004: Strategy to address air pollution in dense low-income settlements*, Government Notice GN666, 14 May 2019.

Department for International Development (2011). 'Potential of Small-Scale Biogas digesters in Sub-Saharan Africa'. *Interdisciplinary Expert Workshop*, 16-18 May 2011. Addis Ababa, Ethiopia. Available from: [http://r4d.dfid.gov.uk/PDF/Outputs/Energy/60820\\_workshop-Addis-Ababa-16-18May-2011.pdf](http://r4d.dfid.gov.uk/PDF/Outputs/Energy/60820_workshop-Addis-Ababa-16-18May-2011.pdf) (Accessed 18 June 2019).

Department of Mineral and Energy (2001) *National Electrification Programme (NEP) 1994 - 1999*, November 2001.

Diefallah EM (1992) 'Kinetic analysis of thermal decomposition reactions. Part VI. Thermal decomposition of manganese(II) acetate tetrahydrate', *Thermochimica Acta*, vol. 202 pp. 1-16.

EScience Associates (Pty) Ltd and the Nova Institute (2013) *Household emission offset pre-feasibility study for Eskom*, Presented to Eskom Holdings, Megawatt Park, Johannesburg, June 2013.

Fachinger F, Drewnic F, Giere R, Borrmann S (2017) 'How the user can influence particulate emissions from residential wood and pellet stoves: Emission factors for different fuels and burning conditions', *Atmospheric Environment*, vol. 158, pp. 216-226.

Fitzpatrick EM, Jones JM, Pourkashanian M, Ross AB, Williams A and Bartle KD (2008) 'Mechanistic Aspects of Soot Formation from the Combustion of Pine Wood', *Energy and Fuels*, vol. 22, no. 6, pp. 3771-3778.

Fitzpatrick EM, Bartle KD, Kubacki ML, Jones JM, Pourkashanian M, Ross AB, Williams A, Kubica K (2009) 'The mechanism of the formation of soot and other pollutants during the co-firing of coal and pine wood in a fixed bed combustor', *Fuel*, vol. 88, pp. 2409-2417.

Fletcher TH, Ma J, Rigby J, Bown AL and Webb BW (1997) 'Soot in coal combustion systems', *Progress in Energy Combustion Science*, vol. 23, pp. 283-301.

FRIDGE (2004) *Study to examine the potential socio-economic impact of measures to reduce air pollution from combustion*, Airshed Planning Professionals and Bentley West Management Consultants for Trade and Industry Chamber / Fund for Research into Industrial Development, Growth and Equity (FRIDGE), Johannesburg.

Friedl A., Holm D., John J, Kornelius G., Pauw C.J., Oosthuizen R. and van Niekerk A.S. (2008) *Air pollution in dense, low-income settlements in South Africa*, Prepared by The Nova Institute for the Department of Environmental Affairs and Tourism on behalf of Royal Danish Embassy.

Forbes PBC (2012) 'Particle emissions from household fires in South Africa', *WIT Transactions on Ecology and the Environment*, vol. 157, pp. 445-456.

Gao Y, Wang Y, Ciu C, Wang B, Liu W, Liu W and Wang L (2020) 'Amorphous manganese oxide as a highly active catalyst for soot oxidation', *Environmental Science and Pollution Research*, vol. 27, pp. 13448-13500.

GIZ (The Deutsche Gesellschaft für Internationale Zusammenarbeit GmbH) (2016). 'Analysis of the existing small-scale biogas projects in the Eastern Cape', South Africa.

He C, Cheng J, Zhang X, Douthwaite D, Pattison S and Hao Z (2019) 'Recent Advances in the Catalytic Oxidation of Volatile Organic Compounds: A Review Based on Pollutant Sorts and Sources', *Chemical Reviews*, vol. 119, pp. 4471-4568.

Hersey SP, Garland RM, Crosbie E, Shingler T, Sorooshian A, Piketh S and Burger R (2015) 'An overview of regional and local characteristics of aerosols in South Africa using satellite, ground and modeling data', *Atmospheric Chemistry and Physics*, vol. 15, pp. 4259-4278.

Huang H, Xu Y, Feng Q and Leung DY (2015) 'Low temperature catalytic oxidation of volatile organic compounds: a review', *Catalysis Science and Technology*, vol. 5, pp. 2649-2669.

Hukkanen A, Kaivosoja T, Sippula O, Jokiniemi J and Tissari J (2012) 'Reduction of gaseous and particulate emissions from small-scale wood combustion with a catalytic combustor', *Atmospheric Environment*, vol. 50, pp. 16 - 23.

Israel-Akinbo S, Snowball J and Fraser G (2018) 'The energy transition patterns of low-income households in South Africa: An evaluation of energy programme and policy', *Journal of Energy in Southern Africa*, vol. 29, no. 3, pp. 75 - 85.

Khaskheli AA, Xu L and Liu D (2022) 'Manganese oxide-based catalysts for soot oxidation: A review of recent advances and future directions', *Energy and Fuels*, vol. 36, pp. 7362-7381.

Kimemia DK, Annergarn HJ, Makonese T, Molapo V and Robinson J (2010) *Characterisation of domestic biomass combustion technologies used in Setswetla, Alexandra township, Gauteng, Proceedings of the Domestic Use of Energy (DUE) Conference, Cape Peninsula University of Technology, Cape Town, 29-31 March 2010.*

Langerman KE, Pauw CJ, Smith HJ, & Piketh SJ (2018) 'Moving households to cleaner energy through air quality offsets', *2018 International Conference on the Domestic Use of Energy (DUE)*, 2018 International Conference on the Domestic Use of Energy (DUE).

Leiman A, Standish B, Boting H, Van Zyl H (2007) 'Reducing the healthcare costs of urban air pollution: The South African experience', *Journal of Environmental Management*, vol. 84, pp. 27–37.

Li Y, Zhao C, Wu X, Lu D and Han S (2007) 'Aggregation experiments on fine fly ash particles in uniform magnetic field', *Powder Technology*, vol. 174, pp. 93-103.

Li WB, Wang JX and Gong H (2009) 'Catalytic combustion of VOCs on non-noble metal catalysts', *Catalysis Today*, vol. 148, pp. 81-87.

Li Y, Tan H, Yang XY, Goris B, Verbeeck J, Bals S, Colson P, Cloots R, Van Tendeloo G, and Su BL (2011) 'Well Shaped Mn<sub>3</sub>O<sub>4</sub> Nano-octahedra with Anomalous Magnetic Behavior and Enhanced Photodecomposition Properties', *Nano, Micro, Small*, vol. 7, no. 4, pp 475–483.

Lim MT, Phan A, Roddy D and Harvey A (2015) 'Technologies for measurement and mitigation of particulate emissions from domestic combustion of biomass: A review', *Renewable and Sustainable Energy Reviews*, no. 49, pp. 574-584.

Liu L, Yang Z, Liang H, Yang H, Yang Y (2010) 'Shape-controlled synthesis of manganese oxide nanoplates by a polyol-based precursor route', *Materials Letters*, vol. 64, pp. 891–893.

Liu J, Kang L, Li H, Maitarad P, Zhang J, Shi L and Zhang D (2017) 'Mn-Fe bi-metal oxides in situ created on metal wire mesh as monolith catalysts for selective catalytic reduction of NO with NH<sub>3</sub>', *Royal Society of Chemistry*, vol. 7, pp. 40444-40451.

Madubansi M and Shackleton CM (2006) 'Changing energy profiles on consumption patterns following electrification in five rural villages, South Africa', *Energy Policy*, vol. 34, no. 18, pp. 4081-4092.

Makonese T, Forbes P, Mudau L and Annergarn HJ (2014) 'Aerosol particle morphology of residential coal combustion smoke', *The Clean Air Journal*, vol. 24, no. 2, pp. 24 - 28.

Matandirotya NR, Cilliers DP, Burger RP, Language B, Pauw C and Piketh SJ (2019) 'The potential for domestic thermal insulation retrofits on the South African Highveld', *Clean Air Journal*, vol. 29, no. 1, pp. 21-28.

Matimolane M (2017) *Eskom air quality offset programme: Progress report March 2017*, Document number ENV17-R070.

Matsumoto T, Takanashi K, Kitigishi K, Shinoda K, Hieman JLC, Piquemal JY and Jeyadevan B (2015) 'Dissolution and reduction of cobalt ions in the polyol process using ethylene glycol: identification of the active species and its role', *New Journal of Chemistry*, vol. 37, pp. 5008 - 5018.

Messerer A, Niessner R and Pöschl U (2004) 'Miniature Pipe Bundle Heat Exchanger for Thermophoretic Deposition of Ultrafine Soot Aerosol Particles at High Flow Velocities', *Aerosol Science and Technology*, vol. 38, no.5, pp. 456-466.

Mdluli T and Vogel C (2010) 'Challenges to achieving a successful transition to a low carbon economy in South Africa: examples from poor urban communities', *Mitigation and Adaptation Strategies for Global Change, Springer*, vol. 15, no. 3, pp. 205-222.

Medical Research Council (MRC) (2008) *Risk factors South African Comparative Risk Assessment Summary Report*, Report by the Medical Research Counsel, Pretoria, South Africa, 1-19.

Msibi SS, Kornelius G (2017) 'Potential for domestic biogas as household energy supply in South Africa', *Journal of Energy in Southern Africa*, vol. 28, no. 2. pp. 1-13.

Mueller F (n.d.) *Fundamentals of gas solids/liquids separation*, Mueller Environmental Designs Inc, Houston, Texas.

Munnik P, De Jongh PE, and De Jong KP (2015) 'Recent Developments in the Synthesis of Supported Catalysts', *Chemical Reviews*, vol. 115, pp. 6687–6718.

Munyeza CF, Osano AM, Maghanga JK, Forbes PBC (2020) 'Polycyclic Aromatic Hydrocarbon Gaseous Emissions from Household Cooking Devices: A Kenyan Case Study', *Environmental Toxicology and Chemistry*, vol. 39, no. 3, pp. 538 - 547.

National Treasury (2018) *2018 Budget Estimates of National Expenditure: Vote 38 Human Settlements*, Report by National Treasury, South Africa.

Naidoo, S (2014) 'Quantification of emissions generated from domestic burning activities from townships in Johannesburg', *Clean Air Journal*, vol. 24, no. 1 , pp. 34-40.

Nkosi CN, Piketh SJ, Burger PR, Annergan HJ (2017) 'Variability of domestic burning habits in the South African Highveld: A case study in the KwaDela Township', *2017 International Conference on the Domestic Use of Energy, Cape Town*, 4-5 April 2017.

Nkosi NC, Piketh SJ and Burger R (2018) 'Fine PM emission factors from residential burning of solid fuels using traditional cast-iron stoves', *Clean Air Journal*, vol. 28, no. 1, pp. 35-41.

Norman R. and Cairncross E. and Witi R and Bradshaw D and the South African Comparative Risk Assessment Collaborating Group (2007) 'Estimating the burden of disease attributable to urban outdoor air pollution in South Africa in 2000', *South African Medical Journal*, vol. 97, no. 8, pp. 82–790.

Nystrom R (2016) 'Particle emissions from residential wood and biodiesel combustion', Doctoral Thesis, Umea University, Sweden.

Orasche J, Seidel T, Hartmann H, Schelle-Kreis J, Chow JC, Ruppert H and Zimmerman R (2012) 'Comparison of emissions from wood combustion. Part 1: Emission factors and characteristics from different small-scale residential heating appliances considering particulate matter and polycyclic aromatic (PAH)-related toxicological potential of particle-bound organic species', *Energy and Fuels*, vol, 26, pp. 6695-6704.

Ozil F, Tschamber V, Haas F and Trouve G (2009) 'Efficiency of catalytic processes for the reduction of CO and VOC emissions from wood combustion in domestic fireplaces', *Fuel Processing Technology*, vol. 90, pp. 1053-1061.



Paulsen AD, Kunsu TA, Carpenter AL, Amundsen TJ, Schwartz NR, Harrington J, Reed J, Alcorn B, Gattoni J and Yelvington PE (2019) 'Gaseous and particulate emissions from a chimneyless biomass cookstove equipped with a potassium catalyst', *Applied Energy*, vol. 235, pp. 369-378.

Pauw C, Fischer T, Weston M, Preston-Whyte F and Badenhorst. H (2006) *The elephant in the room: What do we know about urban wood use in South Africa?*

Pauw CJ, Murray HM and Howard MS (2022) 'The use of dirty fuels by low-income households on the South African Highveld', *Clean Air Journal*, vol. 32, no 1, pp. 1-17.

Pachauri T, Singla V, Satsangi A, Lakhani A, Maharaj Kumari K (2013) 'SEM-EDX Characterization of Individual Coarse Particles in Agra, India', *Aerosol and Air Quality Research*, vol. 13 pp. 523–536.

Pemberton-Pigott C, Annegarn H and Cook C (2009) 'Emission reductions from domestic coal burning: Practical application of combustion principles', *Proceedings of the Domestic Use of Energy (DUE) Conference, Cape Peninsula University of Technology, Cape Town, 14-16 April 2009*.

Perera IE and Litton CD (2015) 'Quantification of Optical and Physical Properties of Combustion-Generated Carbonaceous Aerosols (<PM<sub>2.5</sub>) Using Analytical and Microscopic Techniques', *Fire Technology*, vol. 51, no. 2, pp. 247-269.

Perry R and Green DW (1997) *Chemical Engineers Handbook*, 7th Edition, McGraw Hill Company Inc.

Rao B.G, Mukerjee D.M and reddy B.M (2017) *Nanostructures for Novel Therapy, Chapter 1: Novel approaches for preparation of nanoparticles*, Elsevier, pp 1-36.

Scorgie T (2012) 'Urban air quality management and planning in South Africa', PhD Thesis, University of the Witwatersrand, Johannesburg.

Seinfeld JH and Pandis SN (2016) *Atmospheric Chemistry and Physics: From Air Pollution to Climate Change*, Third Edition, Wiley and Sons Inc, New Jersey.

Semelane MS and Tazvinga H (2018) 'A sustainable method for micro scale biodigesters in South Africa'.

Shen G, Xue M, Chen Y, Yang C, Li W, Shen H, Huang Y, Zhang Y, Chen H, Zhu Y, Wu H, Ding A and Tao S (2014) 'Comparison of carbonaceous particulate matter emission factors among different solid fuels burned in residential stoves', *Atmospheric Environment*, vol. 89, pp. 337-345.

Shezi B and Wright CY (2018) 'Household air pollution exposure and respiratory health outcomes: a narrative review update of the South African epidemiological evidence', *Clean Air Journal*, vol. 28, no. 1, pp. 43-56.

Smith MT, Schroenn Goebel J and Blignaut JN (2012) 'The financial and economic feasibility of rural household biodigesters for poor communities in South Africa', Master of Commerce Thesis, University of KwaZulu Natal, Durban.

Smith KR, Bruce N, Balakrishnan K, Adair-Rohani H, Balmes J, Chafe Z, Dherani M, Hosgood HD, Mehta S, Pope D, Rehfuess E, and others in the HAP CRA Risk Expert Group (2014) 'Millions dead: How do we know and what does it mean? Methods used in the comparative risk assessment of household air pollution', *Annual Review of Public Health*, vol. 35, pp. 185-106.

Sorsamäki L and Nappa M (2015) *Design and selection of separation processes, research Report* (VTT-R-06143-15) prepared for VTT Technical Research Centre of Finland Ltd.

South African-German Energy Programme (SAGEN) 2016. 'Biogas industry in South Africa, An assessment of the skills need and estimation of the job potential', May 2016.

Spivey JJ (1987) 'Complete Catalytic Oxidation of Volatile Organics', *Industrial Engineering Chemical Research*, vol. 26, pp. 2165-2180.

Department of Statistics (StatsSA 2022) *General Household Survey 2021*, Department of Statistics, South Africa, Pretoria.

Sukhdev A, Challa M, Narayani L, Manjunatha AS, Deepthi PR, Angadi JV, Kumar PM Pasha M (2020) 'Synthesis, phase transformation, and morphology of hausmannite Mn<sub>3</sub>O<sub>4</sub> nanoparticles: photocatalytic and antibacterial investigations', *Heliyon*, vol. 6.

Torvela T, Tissari J, Sippula O, Kaivosoja T, Leskinen J, Viren A, Lahde A and Jokiniemi J (2014) 'Effect of wood combustion conditions on the morphology of freshly emitted fine particles', *Atmospheric Environment*, vol. 89, pp. 65-76.

Wagner NJ, Schoonraad P, Swanepoel P, van Niekerk A, Scholtz C, Kornelius G, Julies A, Pretorius O, Wasserman J and Muller A (2005) 'Results of domestic smoke reduction programmes at eMbalenhle (Mpumalanga) and Zamdela (Free State)', *NACA Conference*, September 2005.

Wentzel M, Annergarn HJ, Helas G, Weinbruch S, Balogh AG and Stiele JS (1999) 'Giant dendritic carbonaceous particles in Soweto aerosols', *South African Journal of Science*, vol. 95, pp. 141-145.

Wright CY, Garland RM, Thambiran T, Forbes PBC, Diab R and Oosthuizen MA (2017) Air quality and human health impacts in South Africa,

Wojnarowicz J, Mukhovskiy R, Pietrzykowska E, Kusnieruk S, Mizeracki J and Lojkowski W (2016) 'Microwave solvothermal synthesis and characterization of manganese-doped ZnO nanoparticles', *Beilstein Journal of Nanotechnology*, vol 7, pp 721–732.

World Bank Group Database (n.d.), Accessed 26 May 2018, < <https://data.worldbank.org/indicator/eq.elc.accs.zs>>

World Health Organization (2014) *WHO guidelines for indoor air quality: household fuel combustion*, WHO Press, World Health Organization, Geneva, Switzerland.

Xu Z (2014) *Fundamentals of Air Cleaning Technology and Its Application in Cleanrooms*, Springer, Berlin, Heidelberg.

Xulu NA, Piketh SJ, Feig GT, Lack DA and Garland RM (2020) 'Characterising light-absorbing aerosols in a low-income settlement in South Africa', *Aerosol and Air Quality Research*, vol. 20, pp. 1812-1832.

Yamamoto K, Fujikake F and Matsui K (2013) 'Non-catalytic after-treatment for diesel particulates using carbon-fiber filter and experimental validation', *Proceedings of the Combustion Institute*, no. 34, pp. 2865 - 2875.

Zhang J, Smith KR, Ma Y, Ye S, Jiang F, Qi W, Liu P, Khalil MAK, Rasmussen RA and Thorneloe SA (2000) 'Greenhouse gasses and other airborne pollutants from household stoves in China: a database for emission factors', *Atmospheric Environment*, vol. 34, pp. 4537-4549.

Zhang R, Liu C, Zhou G, Sun J, Liu N, Hsu PC, Wang H, Qiu Y, Zhao J, Wu T, Zhao W and Cui Y (2018) 'Morphology and property investigation of primary particulate matter particles from different sources', *Nano Research*, vol. 11, no. 6, pp. 3182-3192.

## Appendix A: Method for preparing cassettes

### PARTICULATES NOT OTHERWISE REGULATED, TOTAL 0500

DEFINITION: total aerosol mass CAS: NONE RTECS: NONE

METHOD: 0500, Issue 2

EVALUATION: FULL

Issue 1: 15 February 1984

Issue 2: 15 August 1994

OSHA : 15 mg/m<sup>3</sup>

NIOSH: no REL

ACGIH: 10 mg/m<sup>3</sup>, total dust less than  
1% quartz

PROPERTIES: contains no asbestos and quartz  
less than 1%

SYNONYMS: nuisance dusts; particulates not otherwise classified

SAMPLING		MEASUREMENT	
<b>SAMPLER:</b>	FILTER (tared 37-mm, 5- $\mu$ m PVC filter)	<b>TECHNIQUE:</b>	GRAVIMETRIC (FILTER WEIGHT)
<b>FLOW RATE:</b>	1 to 2 L/min	<b>ANALYTE:</b>	airborne particulate material
<b>VOL-MIN:</b>	7 L @ 15 mg/m <sup>3</sup>	<b>BALANCE:</b>	0.001 mg sensitivity; use same balance before and after sample collection
<b>-MAX:</b>	133 L @ 15 mg/m <sup>3</sup>	<b>CALIBRATION:</b>	National Institute of Standards and Technology Class S-1.1 weights or ASTM Class 1 weights
<b>SHIPMENT:</b>	routine	<b>RANGE:</b>	0.1 to 2 mg per sample
<b>SAMPLE STABILITY:</b>	indefinitely	<b>ESTIMATED LOD:</b>	0.03 mg per sample
<b>BLANKS:</b>	2 to 10 field blanks per set	<b>PRECISION (<math>\bar{s}_j</math>):</b>	0.026 [2]
<b>BULK SAMPLE:</b>	none required		
ACCURACY			
<b>RANGE STUDIED:</b>	8 to 28 mg/m <sup>3</sup>		
<b>BIAS:</b>	0.01%		
<b>OVERALL PRECISION (<math>\bar{s}_{rt}</math>):</b>	0.056 [1]		
<b>ACCURACY:</b>	$\pm 11.04\%$		

**APPLICABILITY:** The working range is 1 to 20 mg/m<sup>3</sup> for a 100-L air sample. This method is nonspecific and determines the total dust concentration to which a worker is exposed. It may be applied, e.g., to gravimetric determination of fibrous glass [3] in addition to the other ACGIH particulates not otherwise regulated [4].

**INTERFERENCES:** Organic and volatile particulate matter may be removed by dry ashing [3].

**OTHER METHODS:** This method is similar to the criteria document method for fibrous glass [3] and Method 5000 for carbon black. This method replaces Method S349 [5]. Impingers and direct-reading instruments may be used to collect total dust samples, but these have limitations for personal sampling.

**EQUIPMENT:**

1. Sampler: 37-mm PVC, 2- to 5- $\mu$ m pore size membrane or equivalent hydrophobic filter and supporting pad in 37-mm cassette filter holder.
  2. Personal sampling pump, 1 to 2 L/min, with flexible connecting tubing.
  3. Microbalance, capable of weighing to 0.001 mg.
  4. Static neutralizer: e.g., Po-210; replace nine months after the production date.
  5. Forceps (preferably nylon).
  6. Environmental chamber or room for balance (e.g., 20 °C  $\pm$  1 °C and 50%  $\pm$  5% RH).
- 

**SPECIAL PRECAUTIONS:** None.

---

**PREPARATION OF FILTERS BEFORE SAMPLING:**

1. Equilibrate the filters in an environmentally controlled weighing area or chamber for at least 2 h.  
NOTE: An environmentally controlled chamber is desirable, but not required.
2. Number the backup pads with a ballpoint pen and place them, numbered side down, in filter cassette bottom sections.
3. Weigh the filters in an environmentally controlled area or chamber. Record the filter tare weight,  $W_1$  (mg).
  - a. Zero the balance before each weighing.
  - b. Handle the filter with forceps. Pass the filter over an antistatic radiation source. Repeat this step if filter does not release easily from the forceps or if filter attracts balance pan. Static electricity can cause erroneous weight readings.
4. Assemble the filter in the filter cassettes and close firmly so that leakage around the filter will not occur. Place a plug in each opening of the filter cassette. Place a cellulose shrink band around the filter cassette, allow to dry and mark with the same number as the backup pad.

**SAMPLING:**

5. Calibrate each personal sampling pump with a representative sampler in line.
6. Sample at 1 to 2 L/min for a total sample volume of 7 to 133 L. Do not exceed a total filter loading of approximately 2 mg total dust. Take two to four replicate samples for each batch of field samples for quality assurance on the sampling procedure.

**SAMPLE PREPARATION:**

7. Wipe dust from the external surface of the filter cassette with a moist paper towel to minimize contamination. Discard the paper towel.
8. Remove the top and bottom plugs from the filter cassette. Equilibrate for at least 2 h in the balance room.
9. Remove the cassette band, pry open the cassette, and remove the filter gently to avoid loss of dust.  
NOTE: If the filter adheres to the underside of the cassette top, very gently lift away by using the dull side of a scalpel blade. This must be done carefully or the filter will tear.

**CALIBRATION AND QUALITY CONTROL:**

10. Zero the microbalance before all weighings. Use the same microbalance for weighing filters before and after sample collection. Maintain and calibrate the balance with National Institute of Standards and Technology Class S-1.1 or ASTM Class 1 weights.

11. The set of replicate samples should be exposed to the same dust environment, either in a laboratory dust chamber [7] or in the field [8]. The quality control samples must be taken with the same equipment, procedures and personnel used in the routine field samples. The relative standard deviation calculated from these replicates should be recorded on control charts and action taken when the precision is out of control [7].

**MEASUREMENT:**

12. Weigh each filter, including field blanks. Record the post-sampling weight,  $W_2$  (mg). Record anything remarkable about a filter (e.g., overload, leakage, wet, torn, etc.)

**CALCULATIONS:**

13. Calculate the concentration of total particulate,  $C$  ( $\text{mg}/\text{m}^3$ ), in the air volume sampled,  $V$  (L):

$$C = \frac{(W_2 - W_1) - (B_2 - B_1) \cdot 10^3}{V}, \text{ mg}/\text{m}^3.$$

where:  $W_1$  = tare weight of filter before sampling (mg)  
 $W_2$  = post-sampling weight of sample-containing filter (mg)  
 $B_1$  = mean tare weight of blank filters (mg)  
 $B_2$  = mean post-sampling weight of blank filters (mg)

**EVALUATION OF METHOD:**

Lab testing with blank filters and generated atmospheres of carbon black was done at 8 to 28  $\text{mg}/\text{m}^3$  [2,6]. Precision and accuracy data are given on page 0500-1.

**REFERENCES:**

- [1] NIOSH Manual of Analytical Methods, 3rd ed., NMAM 5000, DHHS (NIOSH) Publication No. 84-100 (1984).
- [2] Unpublished data from Non-textile Cotton Study, NIOSH/DRDS/EIB.
- [3] NIOSH Criteria for a Recommended Standard ... Occupational Exposure to Fibrous Glass, U.S. Department of Health, Education, and Welfare, Publ. (NIOSH) 77-152, 119-142 (1977).
- [4] 1993-1994 Threshold Limit Values and Biological Exposure Indices, Appendix D, ACGIH, Cincinnati, OH (1993).
- [5] NIOSH Manual of Analytical Methods, 2nd ed., V. 3, S349, U.S. Department of Health, Education, and Welfare, Publ. (NIOSH) 77-157-C (1977).
- [6] Documentation of the NIOSH Validation Tests, S262 and S349, U.S. Department of Health, Education, and Welfare, Publ. (NIOSH) 77-185 (1977).
- [7] Bowman, J.D., D.L. Bartley, G.M. Breuer, L.J. Doemeny, and D.J. Murdock. Accuracy Criteria Recommended for the Certification of Gravimetric Coal Mine Dust Personal Samplers. NTIS Pub. No. PB 85-222446 (1984).
- [8] Breslin, J.A., S.J. Page, and R.A. Jankowski. Precision of Personal Sampling of Respirable Dust in Coal Mines, U.S. Bureau of Mines Report of Investigations #8740 (1983).

**METHOD REVISED BY:**

Jerry Clere and Frank Hearl, P.E., NIOSH/DRDS.

## Appendix B: Method for weighing sample filters

### Mettler Microgram balance

#### Weighing procedure: Reference and sample filters

1. Download logged data from data-logging environmental monitor
2. Check if environmental conditions in the laboratory was maintained for the previous 24 hours within the prescribed limits
  - Dry air temperature =  $21 \pm 1.0^{\circ}\text{C}$
  - Relative humidity =  $50 \pm 5\%$
3. Record environmental conditions immediately prior to weighing reference filters
4. Ensure balance is level
5. Weigh a mass of 2 grams repeatedly until repeatability is reached. Repeatability = min and max of three (3) consecutive weights does not differ with more than one (1) percent from the average
6. Close balance and tare the balance
7. Open balance and place three (3) reference (control) filters on the weighing grid.  
Note: Use Three (3) reference (control) filters for each 10 sample filters
8. Close balance and start count down timer
9. Allow 30 seconds for balance to stabilise
10. Note reading on the balance immediately when settling time has expired
11. Remove reference (control) filters from the weighing chamber and hold it next to the weighing chamber. Take care not to breath over the filters
12. Close the balance door and wait for the balance to return to zero
13. If balance does not return to zero:
  - Discard all weighing results
  - Inspect the balance pan for dust or any other obstacle
  - Tare the balance
  - REWEIGH filters
  - Balance should not otherwise be tarred between weighing filters
14. Follow Steps 7 – 13 to obtain 3 consecutive weights for the three (3) reference (control) filters
15. Proceed to weigh 10 individual sample filters by following Steps 7 – 13
16. After weighing the ten (10) sample filters, weigh the three (3) reference filters again using Steps 7 - 13
17. Record environmental conditions immediately after weighing reference filters
18. If the maximum and minimum weight of reference (control) filters differ more than one (1) percent from the average, discard results and re-weigh
19. Place weighed filters with a clearly marked support pad in a clean filter cassette holder.

**Note: Weigh sampling filters in the shortest possible time period.**



## Appendix C: Filter masses (raw data)

	Date	Mass 1	Mass 2	Mass 3	Date	Mass 1	Mass 2	Mass 3
		µg	µg	µg		µg	µg	µg
Pre	18/02/2021	298397	298394	298389	25/03/2022	298397	298396	298396
	Temp: 21.1°C	RH:52			Temp: 20.5°C	RH: 50		
Post		298395	298393	298394		298395	298392	298393
	Filter #	Date	Filter Mass (µg)			Pump #	Flow Rate Setting (cm <sup>3</sup> /min)	Sampling Time (min)
Pre	1	18/02/2022	101055	101054	101053	2	600	9
Post		25/02/2022	101109	101108	101110			
Pre	2	18/02/2022	100003	100001	99998	2	600	10
Post		25/02/2022	100011	100010	100010			
Pre	3	18/02/2022	102938	102935	102935	2	600	10
Post		25/02/2022	103067	103069	103070			
Pre	4	18/02/2022	104327	104323	104325	2	600	10
Post		25/02/2022	104359	104358	104359			
Pre	5	18/02/2022	104488	104487	104484	2	600	10
Post		25/02/2022	104702	104701	104701			
Pre	6	18/02/2022	102276	102273	102273	2	600	5
Post		25/02/2022	102427	102425	102424			
Pre	7	18/02/2022	101227	101225	101225	2	600	10
Post		25/02/2022	101531	101532	101531			
Pre	8	18/02/2022	103949	103949	103950	2	600	9
Post		25/02/2022	104150	104149	104148			
Pre	9	18/02/2022	98122	98121	98120	2	600	10
Post		25/02/2022	98418	98419	98419			
Pre	10	18/02/2022	101844	101842	101843	2	600	9
Post		25/02/2022	102033	102030	102030			

## **Appendix D: Journal Article**

This article was accepted for publication by the Clean Air Journal in February 2023.

# Studies into the reduction of domestic fuel burning emissions by means of facile catalytic abatement technology

Marilize Steyn\*<sup>1</sup>, Nicolaas Claassen<sup>2</sup> and Patricia B.C. Forbes<sup>3\*</sup>

<sup>1</sup> Department of Geography, Geoinformatics and Meteorology, University of Pretoria, Pretoria 0028, South Africa, [marilizeg@gmail.com](mailto:marilizeg@gmail.com)

<sup>2</sup> Faculty of Health Sciences, Division of Environmental and Occupational Health, University of Pretoria, Pretoria 0028, South Africa, [nico.claassen@up.ac.za](mailto:nico.claassen@up.ac.za)

<sup>3</sup> Department of Chemistry, University of Pretoria, Pretoria 0028, South Africa, [patricia.forbes@up.ac.za](mailto:patricia.forbes@up.ac.za) <https://orcid.org/0000-0003-3453-9162>

\*Corresponding author

The negative health and socio-economic impacts of emissions associated with domestic fuel burning are widely recognized. Although there has been much progress in the provision of electricity to households in South Africa, many still rely on solid fuel sources such as wood and coal. While various investigations have been done on reducing household emissions by reducing the use of polluting fuels and improvements in combustion efficiency, comparatively fewer studies have been conducted on the reduction of emissions through emission reduction using abatement technology. Catalytic oxidation could be utilized to oxidize particulate matter precursors such as volatile organic compounds and soot particles to reduce secondary particulate formation. Although catalytic methods have not been effectively utilized in practical domestic applications, studies have shown effective soot reduction during laboratory testing. This study investigated the synthesis and use of a manganese oxide based catalyst to reduce particulate matter from domestic fuel burning stoves. The catalyst was synthesized onto a mesh substrate and inserted into the flue of the stove. During field testing, the presence of the catalyst increased the mass of particulate matter collected onto PTFE filters used for gravimetric analysis, with Scanning Electron Microscopy (SEM) analysis showing spherical particles in the pores of the filters used during the catalytic runs. The baseline runs had very few of these particle clusters. Energy Dispersive X-Ray (EDX) analysis of the catalyst run filters did not detect manganese, revealing that increased particulate concentrations were not as a result of macroscopic particles of the catalyst being dislodged from the support. Dislodgement of very small metal particles from the catalyst could, however serve as nucleation nodes for particle growth which would have a non-metal coating leading to the non-detection of manganese. The increase in particulate matter could also be caused by the impingement of particulate matter precursors on the catalyst followed by particle growth and dislodgement into the flue gas. The testwork showed that an active catalyst can be synthesized onto a mesh catalyst support in a relatively simple and cost-effective manner, which can be utilized in domestic fuel burning devices. It is recommended that a range of optimized, potentially active catalysts be tested to improve the oxidation of particulate matter precursors to carbon dioxide.

Keywords: household air pollution; particulate matter; domestic fuel burning; catalytic reduction.

## 1. Introduction

### 1.1 Domestic fuel burning

The negative health and socio-economic impacts of emissions associated with domestic fuel burning are widely recognized. The Global Burden of Diseases Study estimated that household air pollution was responsible for 2.8

million deaths and 85.6 million disability adjusted life years (DALYs) globally in 2015 (Cohen et al 2017). The study concluded that household fuel burning contributed significantly to mortality in low- and middle-income countries. The 1996 and 2011 census data indicates that the proportion of households making use of solid fuels decreased in South Africa during this

period, however there remain pockets of households that are still reliant on solid fuel (Pauw et al 2020). Areas that experience the highest impact of domestic fuel burning would be densely populated with a high density of emission sources. The negative impacts of household emissions are exacerbated by the fact that they are released in the breathing zone of individuals (DEA 2019). Globally, the greatest negative health impact of domestic energy use is from incomplete combustion of fuels in low efficiency stoves and lighting devices (WHO 2014).

Although there has been much progress in the provision of electricity to households in South Africa, many still rely on solid fuel sources such as wood and coal (Israel-Akinbo et al 2018). A study by Israel-Akinbo et al. (2018) examined how poor households transition from traditional energy carriers such as wood to modern energy carriers such as electricity, biofuels and liquefied petroleum gas. In the case of energy usage for heating purposes, households would not necessarily switch to modern fuels as income rises, in line with the energy stacking model, where households use a combination of energy carriers on the upper and lower stages of the energy ladder depending on their needs. An earlier study conducted by the then Department of Energy (presently the Department of Minerals and Energy) came to a similar conclusion as their results indicated that poorer households relied on multiple sources of energy regardless of electrification status, which further points to an energy stacking model rather than the energy ladder theory (DOE 2012).

A South African study analyzing the economic impact of various air quality initiatives found that technology interventions in the domestic sector would be the most efficient way to reduce healthcare costs associated with urban air pollution (Leiman et al 2007). The interventions that have been investigated in South Africa include the electrification of households, the use of alternative fuels, improved household energy efficiency and encouraging the use of top down fire ignition methods, amongst others (Matimolane 2017, Msibi and Kornelius 2017, Mdluli et al 2010, Wagner et al 2005, Scorgie 2012, Makonese 2015).

While various investigations have been done on reducing household emissions by reducing the use of polluting fuels and improvements in

combustion efficiency, comparatively fewer studies have been conducted on the reduction of emissions using abatement technology.

The aim of this study was to investigate the potential of particulate matter emission reduction in the domestic sector using an appropriate abatement technology. The study thus investigated the emissions that are likely to arise from domestic fuel burning and the available catalytic and non-catalytic abatement technologies for the reduction of the particulate emissions reported in the literature. The study sought to identify, synthesise and test a suitable abatement technique to decrease particulate matter emissions from domestic fuel burning devices.

## **1.2 Implementation of abatement technologies**

### *1.2.1 Previous studies*

Investigations and research into the reduction in emissions from household appliances appears to have been largely focused on improving combustion efficiency and little information seems to be available on secondary or end of pipe type measures to reduce emissions. The use of secondary measures to reduce emissions from small combustion sources in Europe was found to be limited due to the high cost and maintenance requirements of such installations which were limited to the use of electrostatic precipitators (ESPs) (Amann et al 2018).

A review by Lim et al (2015) investigated the use of emission reduction technologies for small scale installations. The study evaluated several technologies that had been tested such as the use of additives, catalytic filters, electrostatic precipitators as well as technologies from the automotive industry. It was concluded that most technologies were still under development and had experienced challenges on implementation.

Cheng et al (2018) investigated the use of high gradient magnetic separation in capturing airborne particles but it achieved low capture efficiency for particles smaller than 50  $\mu\text{m}$ .

In another study, Yamamoto et al (2013) investigated the use of a heated carbon fiber filter to remove soot particles from diesel combustion. Without heating the filter, particles would accumulate on the filter, reducing the porosity significantly. By increasing the filter wall temperature using an electric heater, the study found that most of the particulates could be burned off,

resulting in continuous filter regeneration. The study indicated that, while most of the particulates were burned off in the filter, new ultra-fine particles of less than 30 nm were formed, which may have an impact on human health.

Hukkanen et al (2012) investigated the use of a catalytic combustor in reducing emissions from a wood fired boiler. The catalyst utilized consisted of metal wire mesh covered with a platinum and palladium catalyst. For the entire combustion cycle, reductions of 21% for CO, 14% for organic gaseous carbon and 30% of PM<sub>1</sub> was achieved. In this case, the flue gas temperatures were high enough to activate the catalyst, but the study notes that some residential heaters may not have sufficiently high flue gas temperatures to achieve this. A major disadvantage of this technology is the high cost of the precious metals used as catalysts.

Ozil et al (2009) investigated the use of two catalysts, a cordierite honeycomb monolith support and a metallic corrugated structure impregnated with an alumina washout. The study showed that the temperature of the flue gas of a wood fired boiler was too low during start up and shut down for the catalyst to be effective and the use of a heating system was found to dramatically reduce the emissions of CO and VOCs, with a CO reduction of between 80 and 90% being achieved.

### 1.2.2 Emissions from domestic fuel burning

Flue gas from domestic solid fuel combustion typically has a low particle loading and the particles are small in size (Xu 2014); specifically the particulates are expected to be 95% PM<sub>2.5</sub> (Zhang et al 2018).

Previous studies have indicated that the particulate matter emissions from solid fuel burning comprised mainly of organic particles, soot and inorganic fly ash (Zhang et al 2018, Torvela et al 2014, Nystrom 2016, Makonese et al 2019). These particulates are also expected to react with each other and with gaseous emissions in the combustion chamber and flue. The temperature of the flue gas, which is likely to depend on the positioning of the abatement device, will influence the catalyst efficiency as well as both the aging of the particulates and their properties. Closer to the combustion chamber, sticky, tarry carbonaceous particles may form (Makonese et al 2019). Various other chain-like or cluster-like particulates are also likely to be pre-

sent (Forbes 2012). In addition, organic particles with inorganic inclusions may form. A smaller fraction of inorganic fly ash emissions is expected, which may be larger in size than the organic particles (Zhang et al 2018, Makonese et al 2019).

### 1.2.3 Catalytic abatement

The collection efficiency for particles smaller than 5 µm, as is expected in flue gas streams, is low and non-catalytic methods are unlikely to achieve a meaningful reduction in particulate matter concentration (Perry et al 1997). Catalytic oxidation could be utilized to oxidize particulate matter precursors such as volatile organic compounds and soot particles to reduce secondary particulate formation. Catalytic abatement allows users to utilise the available fuel, with reduced negative health outcomes. Although catalytic methods have not been effectively utilized in practical domestic applications, studies have shown effective soot reduction during laboratory testing (Gao et al 2020).

Volatile organic matter and soot can be oxidized using supported noble metal catalysts and metal oxide catalysts. Noble metal catalysts generally are more active than metal oxide catalysts, but metal oxide catalysts are more resistant to certain catalyst poisons such as halogens, As and Pb. Metal oxide catalysts importantly have a substantially lower cost and can be sufficiently reactive for some applications (Huang et al 2015) and were therefore selected for this study. The most effective single metal catalysts have been found to be oxides of V, Cr, Mn, Fe, Co, Ni and Cu (Spivey 1987). Manganese was selected for this study due to the promising results achieved with laboratory testing (Gao et al 2020). The results indicated that the soot conversion percentage was temperature dependent and increased at temperatures above 250°C. Furthermore, manganese oxide catalysts have low toxicity, low raw material cost and a diversity of crystalline structures which determine the catalytic activity (Huang et al 2015). In this study, a manganese oxide based catalyst was prepared and characterized. It was then tested for potential local application, utilizing a commercial domestic stove.

## 2. Methods

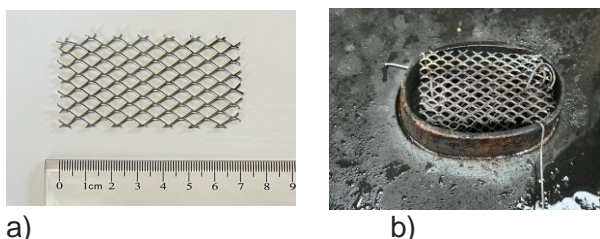
### 2.1 Catalyst Requirements

In order to be considered effective, the designed catalyst should conform to various safety and performance criteria such as acceptable emission reduction, limited clogging, ease of installation, heat resistance, cost effectiveness and the catalyst should be non-toxic. Installation should be possible on non-standardised units, should be self-cleaning or easy to clean with little or no electricity required for operation. The catalyst must further be acceptable to the end user.

Emissions are also expected to vary during the different stages of the combustion process. As the abatement will be in operation during the entire combustion cycle, it should accommodate the emissions from the combined combustion cycle.

### 2.2 Catalyst Synthesis

Three catalyst preparation techniques were tested namely precipitation, wet deposition and dry deposition. The choice of the catalyst support was based on the risk of clogging, ease of installation, minimizing pressure drop, high air flow through the catalyst, and cost, amongst other parameters. A coarse 0.5 mm thick steel mesh was thus used as the catalyst support for direct use in domestic flues as shown in Figure 1.



a) i. Figure 1. 0.5 mm thick steel mesh used as catalyst support (a) for installation at the base of the flue (b)

The synthesis utilizing precipitation was based on the polyol method, which is well-known for producing metallic nanoparticles (Augustin et al 2015, Li et al 2011, Liu et al 2010, Sukhdev et al 2020). A glycol solvent such as ethylene glycol functions as a solvent for the metal precursors as well as functioning as the reducing agent (Benseeba 2013, Rao et al

2017). The glycol further controls particle formation by controlling nucleation, growth and agglomeration of the particles. The method described by Augustin et al (2015) utilizes mild reaction conditions to produce manganese oxide particles with varying structures and compositions and was therefore used as a basis for the synthesis of the manganese oxide catalyst in this project.

Manganese (II) acetate tetrahydrate (>99%), tetraethylene glycol (99%), iron (III) nitrate nonahydrate (>98%) and ethylene glycol (>99%) were obtained from Sigma-Aldrich (South Africa). All reagents were used as received.

Typical test conditions were as follows: The reaction solution was prepared using 0.5 g of magnesium acetate dissolved in 60 mL of ethylene glycol and 6 mL of tetraethylene glycol (TEG). The catalyst support mesh (commercially available 0.5 mm thick steel mesh obtained from Leroy Merlin Hardware Store) was washed using acetone prior to synthesis. The mesh was then suspended in the reaction mixture using wire hooks secured to the beaker using rubber-based putty adhesive. The mixture was then gradually heated on a magnetic stirrer hot plate (Heidolph, Germany) and stirred using a magnetic stirrer. The temperature of the reagent mixture was measured manually using a thermometer. The reagent mixture was gradually heated to a temperature of 170°C. Samples were removed from the reaction mixture after precipitation occurred at 170°C and were washed using ethanol (>98%, Sigma-Aldrich). The samples were dried under argon (99.9%, Afrox) and were then transferred to a muffle furnace (Lenton, South Africa) at 550°C for five hours to calcine under stagnant air.

The wet deposition catalyst was synthesized by dipping the catalyst support into a concentrated manganese acetate tetrahydrate solution prior to calcining. A mesh sample was prepared using 8 g of manganese acetate tetrahydrate in 30 mL of water. The sample was dipped in the solution, removed and calcined without drying at 550°C for two hours.

The dry deposition catalyst was covered in dry manganese acetate tetrahydrate powder prior to calcining at 550°C for two hours.

### 2.3 Catalyst Testing Methodology

The experimental setup consisted of a commercial one plate combustion device with a flue as shown in Figure 2 (Ndebele Appliances and

Coal Stoves, Bronkhorstspuit, South Africa), which is representative of cooking stoves available in South Africa.

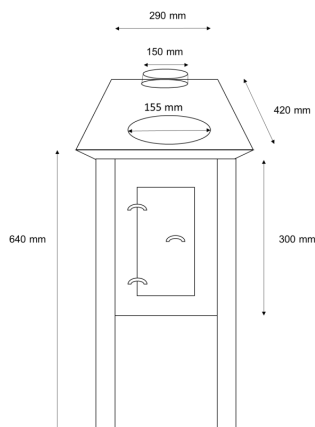


Figure 2. Diagram of the one-plate stove employed in testing of the catalyst

Bulk catalysts were produced using precipitation and wet impregnation. The catalyst was positioned at the base of the flue where the highest flue temperatures were expected, as laboratory testing had indicated that the catalyst was only effective temperatures above 250°C (Gao et al, 2020).

For each test run, 100 g of soft wood sticks approximately 150 mm in length and 20 x 20 mm diameter were utilized and the combustion process was started using a single wax based firelighter ball. The soft wood was selected as fuel to improve the reproducibility of the test runs as the wood is more homogenous in size and composition when compared to hard wood or coal. The test runs were conducted under similar ambient conditions at the same time each day to improve reproducibility. The fuel used for the runs was sized, weighed and bagged to reduce fuel variability and to ensure consistent fuel moisture content.

## 2.4 Measurement Methodology

The flue gas flow rate was measured using a vane type digital anemometer (Benetech, China). The flue temperature was measured using an infrared thermometer (Shenzen FLUS Technology Company, China). Measurements were taken at 290 mm from the flue exit point to allow for the cooling of the flue gas.

Particulate concentrations were collected for gravimetric analysis using 37 mm polystyrene cassettes, with 37 mm polytetrafluoroethylene

(PTFE) filters with a pore size of 2  $\mu\text{m}$  (Environmental Express, South Carolina, USA). PTFE filters were selected as they are temperature resistant up to 260°C. A Gilian (GilAir Plus) personal sampling pump was used to collect particulates onto the filters at a sampling flow rate of 600 mL/min for 10 min. The positioning of the sampling probe could potentially influence the size distribution of the particulate matter sampled, favouring the capture of finer particles. For this study non-isokinetic sampling was considered adequate as the study was interested in whether the catalyst affected the particulate matter formation in a relative manner, and not to quantify the emissions or derive emission factors. Sample filters were weighed using a Mettler Toledo microgram analytical balance in a temperature (221 $\pm$ 1°C) and humidity (50 $\pm$ 5%) controlled environment.

## 2.5 Catalyst and PTFE Filter Analysis

The catalyst samples produced were examined using Scanning Electron Microscopy (SEM) using a Zeiss Crossbeam 540 SEM at 20 kV to determine the morphology and particle size of the catalyst and to determine the catalyst coverage on the mesh substrate.

The catalyst samples were analysed using Energy Dispersive X-Ray (EDX) (OXFORD Link-ISIS-300 Zeiss, Germany) analysis to determine the semi-quantitative composition of the catalysts.

The PTFE filter samples were examined using the same SEM instrument at 2 kV. A section of the center part of each filter was removed using a steel blade, mounted on an aluminum stub and sputter coated with Au to improve conductivity.

## 3. Results and Discussion

### 3.1 Catalyst Synthesis

#### 3.1.1 Synthesis using precipitation

A test sample was prepared using the procedure described in Section 2.2. The synthesis was optimized by changing the initial concentrations of manganese acetate tetrahydrate and TEG used to prepare the reaction mixture. The test sample was produced utilizing a 5 x 5 mm piece of mesh suspended in the reagent mixture. Although the precipitate formed on the wire mesh, the precipitate was patchy and did not



cover a large percentage of the mesh surface. The Energy Dispersive X-Ray (EDX) analysis confirmed that the precipitates formed during the precipitation runs were manganese oxides with carbon inclusions.

The test run was repeated with an increased manganese acetate tetrahydrate mass of 1 g to improve the catalyst coverage on the mesh. The mesh was calcined directly after synthesis and the calcining time was reduced to 2 hours to ensure that the catalyst was calcined directly after synthesis. The precipitate on the mesh could clearly be seen at 100 X magnification as shown in Figure 3. The precipitate covered the mesh well and formed clusters of precipitate in places. The utilization of higher concentrations of manganese acetate tetrahydrate greatly improved the precipitate coverage on the mesh.

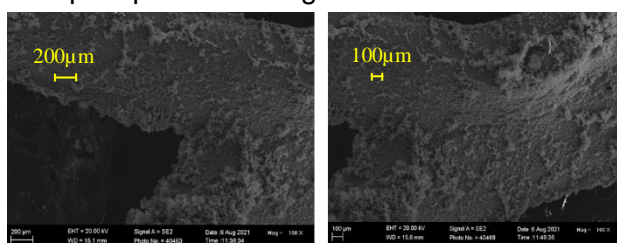


Figure 3. SEM micrographs of the catalyst synthesized using increased manganese acetate tetrahydrate concentrations showing precipitate on the mesh at 100 X magnification

To investigate the impact of the addition of TEG on the coverage and morphology of the catalyst, the previous test was repeated without the addition of TEG. The precipitate formed had good coverage, as shown in Figure 4.

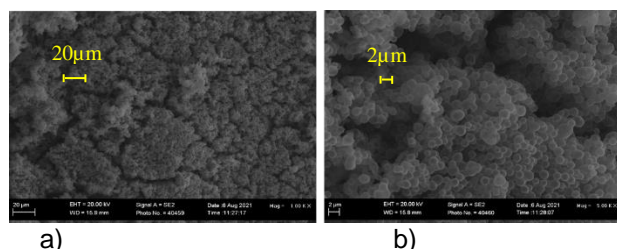


Figure 4. SEM micrographs showing the precipitate comprised of spherical particles at 1000 X (a) and 5000 X (b) magnification for the catalyst produced without the addition of TEG

The addition of TEG did not appear to improve coverage of the mesh with catalyst particles and the precipitates appeared to have similar morphologies as shown in Figure 5.

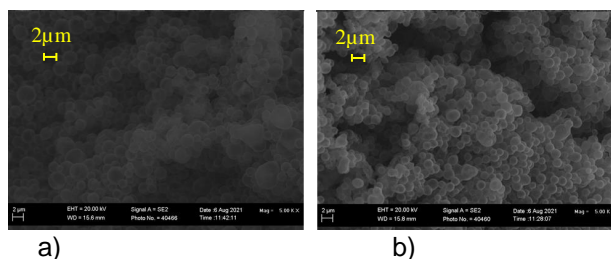


Figure 5. SEM micrographs at 5000 X magnification comparing the samples prepared with the addition of TEG (a) and samples prepared without TEG (b)

### 3.1.2 Synthesis using wet and dry deposition

A relatively smooth manganese oxide deposit was formed using wet precipitation and good coverage of the catalyst on the mesh was achieved as shown in Figure 6.

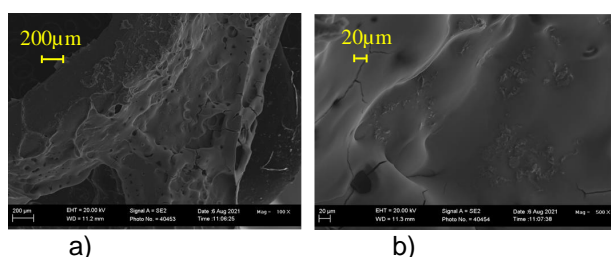


Figure 6. SEM micrographs showing the catalyst synthesized using wet impregnation at 100 X (a) and 500 X (b) magnification

The morphology of the catalyst changed significantly depending on the synthesis method used. At higher magnifications, the surface of the wet impregnation sample had a plate-like structure compared to the spherical, agglomerated particle type structure of the sample prepared using precipitation as shown in Figure 7.

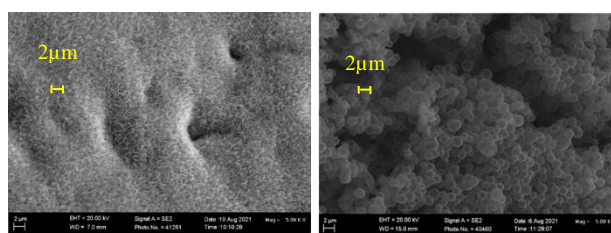


Figure 7. SEM micrographs comparing the surface of samples prepared using wet impregnation (a) and precipitation (b) at 5000 X magnification

The catalyst prepared using dry impregnation did not achieve good coverage and the mesh substrate was still clearly visible.



### 3.1.3 Bulk catalyst preparation

Both the optimized precipitation synthesis and wet impregnation techniques achieved good coverage of the mesh substrate. The wet impregnation technique is a simpler process involving dipping the mesh into a concentrated solution of manganese acetate tetrahydrate prior to calcination, whereas the precipitation technique involves the gradual heating of the reagents to form a precipitate. The morphologies of the samples prepared were significantly different, as shown in paragraph 3.1.2.

The sample was analysed using SEM. The results indicated that that the procedure can be successfully scaled up and that similar coverage and morphology was achieved to that obtained in the smaller test scale tests as shown in Figure 8.

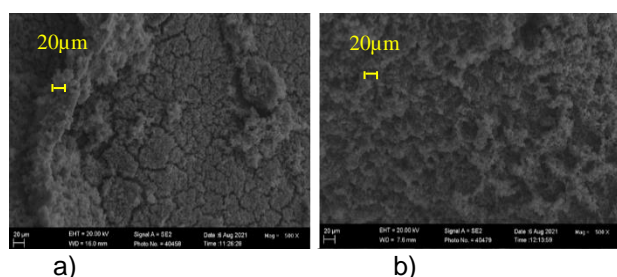
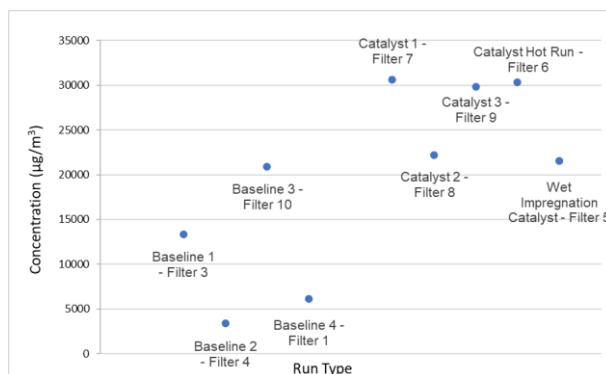


Figure 8. SEM micrographs at 500 X magnification comparing the catalyst synthesized from the optimized test run (a) and synthesis of the bulk sample (b)

### 3.2 Catalyst testing

Bulk catalyst samples were prepared for testwork using both techniques and were then field tested.

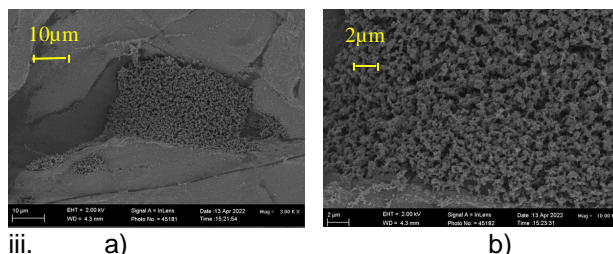
The gravimetric analysis results indicated that relatively higher mass concentrations of particulate matter were recorded for the catalyst runs compared to the baseline runs as shown in Figure 9. It was expected that due to the oxidation of VOCs over the catalyst, secondary particulate matter would be reduced during the catalyst runs.



ii. Figure 9. Comparison of the gravimetric results for the catalyst and baseline runs

To investigate the cause of the increased particulate matter, Scanning Electron Microscopy (SEM) analysis was conducted on five of the samples. Two baseline samples (Filters 3 and 10), two catalyst samples (Filters 6 and 9) and the field blank sample (Filter 2) were selected for analysis.

For the catalyst runs, clusters of particles could be seen within the pores of the filters, as shown in Figure 10. Both filters had particle clusters within the pores, but the Catalyst Hot Run which was sampled only during the flaming phase of the run and therefore for a shorter period (Filter 6) had fewer of these clusters.



iii. a) and b) Figure 10. SEM micrograph at 3000 X (a) and 10000 X (b) magnification showing spherical particles smaller than 1 µm in size for the Catalyst Hot Run (Filter 6)

Particulate clusters can clearly be seen in the pores of the filter for the catalyst run. Very few similar clusters could be seen on the baseline sample filter as shown in Figure 11.

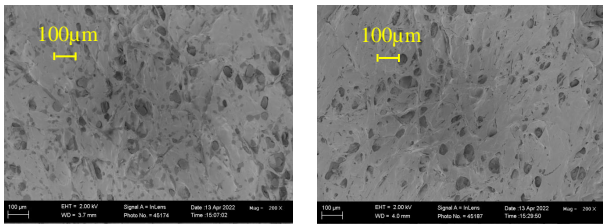


Figure 11. SEM micrographs comparing the filters from catalyst Run 3 (Filter 9) (a) to baseline Run 3 (Filter 10) (b) at 200 X magnification

Energy-dispersive X-ray spectroscopy (EDX) analysis was conducted at 15 kV on the samples to determine whether there was any detectable catalyst lost to the flue gas which would contribute to the PM load on the filters. Carbon and fluoride were detected by the EDX analysis due to the composition of the filter, therefore it was not possible to definitively determine whether the particulates formed were carbon-based due to the background carbon content of the filter. The EDX analysis did not detect any manganese and the increased particulate mass on the filters used for the catalyst runs were therefore not as a result of macroscopic particles of the catalyst detaching from the support.

#### 4. Conclusions and Recommendations

The testwork showed that an active catalyst can be synthesized in a facile and cost effective manner onto a mesh catalyst support which can be utilized in domestic fuel burning devices. The catalyst is easy to install and can be customised to fit non-standard domestic combustion units. The manganese based catalyst is heat resistant and does not release toxic materials. The catalyst is light in weight and requires no electricity to operate. During the limited test runs conducted, the catalyst did not clog, the airflow was not restricted and the stove vented as per the baseline runs. It is recommended that the catalyst be tested over a prolonged period to determine whether the catalyst remains self-cleaning or whether it clogs over time. The number of consecutive cycles it can be used over should also be determined (in this study four cycles were successfully tested in this regard).

The total particulate concentrations were measured gravimetrically and the particle mass concentration of the catalyst runs were found to be higher than for the baseline runs. EDX analysis indicated that the increased particulate concentration on the catalyst runs was not likely

to be as a result of macroscopic particles of the catalyst being dislodged from the support, as no manganese was detected. The catalyst therefore had good adherence to the catalyst support.

SEM analysis showed that the catalyst run filters had particulate clusters comprised of spherical particles in the pores of the filters. The baseline runs had very few, if any, of these particle clusters. The increased particulate matter could result from the dislodgement of very small metal particles from the catalyst which served as nucleation nodes for particle growth. The metallic nuclei may have had a non-metal coating which may lead to non-detection by EDX. The increase in particulate matter could also be caused by the impingement of particulate matter precursors on the catalyst. Particle growth occurs on the catalyst surface. If the catalyst does not oxidize the impinged pollutant efficiently, particle growth can occur until the particles formed are dislodged from the catalyst by the flue gas, resulting in chain like aggregates. Measuring total particulate matter mass concentrations does not provide information on the morphology, surface chemistry, composition and size characterization of the particulates. It is thus recommended that more detailed analysis be conducted on the particulate matter to provide further insight into secondary particulate formation.

Although the reaction mechanism of oxidation over a manganese oxide based catalyst is generally understood as being through the supply of oxygen from the crystal lattice, a detailed understanding of the elemental reactions are not well understood, particularly for multicomponent systems (Khaskheli et. al. 2022). An improved understanding of the reaction mechanism could lead to the optimisation of the catalyst activity.

Various studies have shown that manganese oxide catalysts are able to oxidize CO, however previous studies investigating the use of manganese oxide catalysts for soot, CO and VOC reduction have mostly been conducted at laboratory scale and not under typical practical (real world) conditions. During laboratory testing, the soot or gas mixture has sufficient time to react and sufficient contact is achieved between the catalyst and the soot or gas (Khaskheli et. al. 2022). In a practical application, there will be much less contact time between the catalyst and the flue gas, which may

impact on the efficiency of the catalyst. It is therefore recommended that a range of optimized, potentially active catalysts be tested to improve the oxidation of particulate matter precursors to CO<sub>2</sub>. In addition, it is recommended that further testwork include the analysis of gaseous components such as CO, VOCs and CO<sub>2</sub> to determine the extent of oxidation of the particulate matter precursors.

The testwork showed that an active catalyst can be synthesized onto a mesh catalyst support which can be utilized in domestic fuel burning devices. The potential use of an optimised, cost effective catalyst to reduce domestic fuel burning emissions by oxidising particulate matter precursors would enable the continued use of locally available solid fuel with reduced health and environmental impacts.

## 5. References

- Amann M, Cofala J, Klimont Z, Nagl C, Schieder W (2018) *Measures to address air pollution from small combustion sources*, Report produced under Specific Agreement 11 under Framework Contract ENV.C.3/FRA/2013/00131 of DG-Environment of the European Commission.
- Augustin M, Fenske D, Bardenhagen I, Westphal A, Knipper M, Plaggenborg T, Kolny-Olesiak J and Parisi J (2015) 'Manganese oxide phases and morphologies: A study on calcination temperature and atmospheric dependence', *Beilstein Journal of Nanotechnology*, vol. 6 pp. 47 - 59.
- Benseeba F (2013) *Nanoparticle Technologies, From Lab to Market*, First Edition, Elsevier, ISBN: 9780080919270.
- Cheng M.G, Murphy B, Moon J.W, Lutdka G.M and Cable-Dunlap P.R (2018) 'On the use of high-gradient magnetic force field in capturing airborne particles', *Journal of Aerosol Science*, vol. 120, pp. 22-31.
- Cohen A.J, Brauer M, Burnett R, Ross Anderson H, Frostad J, Estep K, Balakrishnan K, Brunekreef B, Dandona L, Dandona R, Feigin V, Freedman G, Hubbell B, Jobling A, Kan H, Knibbs L, Liu Y, Martin R, Morawska L, Arden Pope III C, Shin H, Straif K, Shaddick G, Thomas M, Van Dingenen R, Van Donkelaar A, Vos T, Murray C.J.L, Forouzanfar M.H (2017) 'Estimates and 25-year trends of the global burden of disease attributable to ambient air pollution: an analysis of data from the Global Burden of Diseases Study 2015', *The Lancet*, vol. 389, pp. 1907–1918.
- Department of Environmental Affairs (2019) *National Environmental Management Air Quality Act 39 of 2004: Strategy to address air pollution in dense low-income settlements*, Government Notice GN666, 14 May 2019.
- Department of Energy (DOE 2012) *A survey of energy-related behaviour and perceptions in South Africa*, Human Sciences Research Council (HSRC)
- Fletcher TH, Ma J, Rigby J, Bown AL and Webb BW (1997) 'Soot in coal combustion systems', *Progress in Energy Combustion Science*, vol. 23, pp. 283-301.
- Forbes PBC (2012) 'Particle emissions from household fires in South Africa', *WIT Transactions on Ecology and the Environment*, vol. 157, pp. 445-456.
- Gao Y, Wang Y, Ciu C, Wang B, Liu W, Liu W and Wang L (2020) 'Amorphous manganese oxide as a highly active catalyst for soot oxidation', *Environmental Science and Pollution Research*, vol. 27, pp. 13448-13500.
- Huang H, Xu Y, Feng Q and Leung DY (2015) 'Low temperature catalytic oxidation of volatile organic compounds: a review', *Catalysis Science and Technology*, vol. 5, pp. 2649-2669.
- Hukkanen A, Kaivosoja T, Sippula O, Jokiniemi J and Tissari J (2012) 'Reduction of gaseous and particulate emissions from small-scale wood combustion with a catalytic combustor', *Atmospheric Environment*, vol. 50, pp. 16 - 23.
- Israel-Akinbo S, Snowball J and Fraser G (2018) 'The energy transition patterns of low-income households in South Africa: An evaluation of energy programme and policy', *Journal of Energy in Southern Africa*, vol. 29, no. 3, pp. 75 - 85.
- Leiman A, Standish B, Boting H, Van Zyl H (2007) 'Reducing the healthcare costs of urban air pollution: The South African experience', *Journal of Environmental Management*, vol. 84, pp. 27–37.
- Li Y, Tan H, Yang XY, Goris B, Verbeeck J, Bals S, Colson P, Cloots R, Van Tendeloo G, and Su BL (2011) 'Well Shaped Mn<sub>3</sub>O<sub>4</sub> Nano-octahedra with Anomalous Magnetic Behavior and Enhanced Photodecomposition Properties', *Nano, Micro, Small*, vol. 7, no.. 4, pp 475–483.

- Lim MT, Phan A, Roddy D and Harvey A (2015) 'Technologies for measurement and mitigation of particulate emissions from domestic combustion of biomass: A review', *Renewable and Sustainable Energy Reviews*, no. 49, pp. 574-584.
- Liu L, Yang Z, Liang H, Yang H, Yang Y (2010) 'Shape-controlled synthesis of manganese oxide nanoplates by a polyol-based precursor route', *Materials Letters*, vol. 64, pp. 891-893.
- Makonese T, Forbes P, Mudau L and Annergarn HJ (2014) 'Aerosol particle morphology of residential coal combustion smoke', *The Clean Air Journal*, vol. 24, no. 2, pp. 24-28.
- Nystrom R (2016) 'Particle emissions from residential wood and biodiesel combustion', Doctoral Thesis, Umea University, Sweden.
- Ozil F, Tschamber V, Haas F and Trouve G (2009) 'Efficiency of catalytic processes for the reduction of CO and VOC emissions from wood combustion in domestic fireplaces', *Fuel Processing Technology*, vol. 90, pp. 1053-1061.
- Perry R and Green DW (1997) *Chemical Engineers Handbook*, 7th Edition, Mcgraw Hill Company Inc.
- Pauw CJ, Murray HM and Howard MA (2022) 'The use of dirty fuels by low-income households on the South African Highveld', *Clean Air Journal*, vol. 32, no. 1, pp. 81-97.
- Rao B.G, Mukerjee D.M and reddy B.M (2017) *Nanostructures for Novel Therapy, Chapter 1: Novel approaches for preparation of nanoparticles*, Elsevier, pp 1-36.
- Spivey JJ (1987) 'Complete Catalytic Oxidation of Volatile Organics', *Industrial Engineering Chemical Research*, vol. 26, pp. 2165-2180.
- Sukhdev A, Challa M, Narayani L, Manjunatha AS, Deepthi PR, Angadi JV, Kumar PM Pasha M (2020) 'Synthesis, phase transformation, and morphology of hausmannite Mn<sub>3</sub>O<sub>4</sub> nanoparticles: photocatalytic and antibacterial investigations', *Heliyon*, vol. 6.
- Torvela T, Tissari J, Sippula O, Kaivosoja T, Leskinen J, Viren A, Lahde A and Jokiniemi J (2014) 'Effect of wood combustion conditions on the morphology of freshly emitted fine particles', *Atmospheric Environment*, vol. 89, pp. 65-76.
- World Health Organization (2014) *WHO guidelines for indoor air quality: household fuel combustion*, WHO Press, World Health Organization, Geneva, Switzerland.
- Xu Z (2014) *Fundamentals of Air Cleaning Technology and Its Application in Cleanrooms*, Springer, Berlin, Heidelberg.
- Yamamoto K, Fujikake F and Matsui K (2013) 'Non-catalytic after-treatment for diesel particulates using carbon fibre filter and experimental validation', *Proceedings of the Combustion Institute*, no. 34, pp. 2865 - 2875.
- Zhang R, Liu C, Zhou G, Sun J, Liu N, Hsu PC, Wang H, Qiu Y, Zhao J, Wu T, Zhao W and Cui Y (2018) 'Morphology and property investigation of primary particulate matter particles from different sources', *Nano Research*, vol. 11, no. 6, pp. 3182-3192.